

THE DEVELOPMENT OF DESIGN REQUIREMENTS AND APPLICATION OF
GUIDED HARD-LAUNCH MUNITIONS ON AERIAL PLATFORMS

BY

Copyright 2016
Lauren Schumacher
All Rights Reserved

Submitted to the graduate degree program in Aerospace Engineering and the
Graduate Faculty of the University of Kansas in partial fulfillment of the
requirements for the degree of Master of Science with Honors.

Dr. Ronald Barrett
Professor, Aerospace Engineering
(Chairperson)

Dr. Jan Roskam
Emeritus Deane E. Ackers Distinguished Professor, Aerospace Engineering
(Committee Member)

Dr. Bozena Pasik-Duncan
Professor, Mathematics
Courtesy Professor, Aerospace Engineering
(Committee Member)

Dr. Willem Anemaat
President, DARcorporation
(Observet Honoratus)

Date Defended: 26 August 2016

The Thesis Committee for Lauren Schumacher certifies that
this is the approved version of the following thesis:

THE DEVELOPMENT OF DESIGN REQUIREMENTS AND APPLICATION OF
GUIDED HARD-LAUNCH MUNITIONS ON AERIAL PLATFORMS

Dr. Ronald Barrett
Professor, Aerospace Engineering
(Chairperson)

Dr. Jan Roskam
Emeritus Deane E. Ackers Distinguished Professor, Aerospace Engineering
(Committee Member)

Dr. Bozenna Pasik-Duncan
Professor, Mathematics
Courtesy Professor, Aerospace Engineering
(Committee Member)

Dr. Willem Anemaat
President, DARcorporation
(Observet Honoratus)

Date approved: 01 September 2016

Abstract

This thesis outlines the potential and need for a paradigm shift that will fundamentally alter the way aerial engagement is carried out in the coming decades. The implementation of guided hard-launch munitions on aerial platforms will effectively allow for greater target versatility while providing a defense system for the aircraft in question. A rearward facing gun barrel equipped with several smaller caliber guided rounds can effectively mitigate air-to-air and surface-to-air missiles from hostile forces, while larger caliber rounds in a traditional forward or side mounted barrel can engage both surface and airborne targets at close and medium-ranges.

This study outlines the concept of operations for various mission types implementing these guided munitions from short-range direct fire encounters to long-range indirect fire. A computational model was then established to outline the design requirements for this particular type of munition family. The aerodynamics, structures, and guidance, navigation and controls were considered for each engagement type. A sample guided projectile concept was then applied to three airframes, the F-35A, AC-130U, and A-10, in order to demonstrate basic capability as a retrofit on existing gunnery systems. The modified system capability was then juxtaposed with existing aerial combat potential.

Acknowledgements

I would like to thank my mother, Linda Schumacher, and my father, John Schumacher for their continual support throughout this endeavor. Their steadfast encouragement has formed the cornerstone of my support network, and without their love and assistance, I would not be where I am today. I also thank my brother, Carl Schumacher, for his support and willingness to offer up distraction should I require a little time away from my work.

I would especially like to thank my committee chair and mentor, Dr. Ronald Barrett, for his support not only throughout my master's work, but also throughout the entirety of my academic endeavors for the past five years. His great breadth of knowledge, willingness to entertain the infeasible, and genuine care that he demonstrates for his students and their points of view has made this research possible.

I would also like to thank Dr. Jan Roskam, Dr. Willem Anemaat, and Dr. Bozenna Pasik-Duncan for their service on this committee. I also offer my sincere thanks to the Madison and Lila Self Graduate Fellowship for their training and financial support throughout this research endeavor.

non per quos sed quomodo

Table of Contents

	<u>Page #</u>
Table of Contents	v
List of Figures	vii
List of Tables	ix
List of Symbols	x
1 Introduction.....	1
1.1 Abbreviated History of U.S. Air-to-Air Combat.....	1
1.1.1 The Early Years	1
1.1.2 Korea	5
1.1.3 Vietnam	10
1.1.4 The Gulf War.....	16
1.1.5 The Yugoslav Wars	19
1.2 Aerial Combat Weapon Systems.....	21
1.2.1 Guns.....	21
1.2.2 Guided Missiles.....	28
1.2.3 Gravity Weapons	33
1.3 U.S. Aerial Engagement Historical Summary	36
1.4 Thesis Motivation and Overview	40
1.5 Historical Guided Hard-Launch Round Programs	41
1.5.1 M712 Copperhead	41
1.5.2 Adaptive Guided Munition Programs.....	43
1.5.3 Extended Range Guided Munition (ERGM).....	44
1.5.4 Extreme Accuracy Tasked Ordnance	44
2 Weapon System Outline	45
2.1 Munitions Design	45
2.2 Weapon System Design and Integration	46
2.3 Concepts of Operations	48
2.3.1 Defense	48
2.3.2 Interdiction.....	51
3 Analytic and Computational Tools	53
3.1 Baseline Geometry	53
3.2 Aerodynamics.....	53
3.2.1 Aerodynamic Forces.....	55
3.2.2 Aerodynamic Moments	61
3.2.3 Equations of Motion	63
3.3 Computational Methods	64
3.4 Model Validation.....	64
3.5 Design Parameters.....	65
3.5.1 Range	65
3.5.2 Lethality.....	70
3.5.3 Control Authority	74
3.5.4 Guidance and Navigation	85
3.5.5 Cost Estimation.....	88

Table of Contents Continued

4 Results..... 90

 4.1 Defensive Capability 91

 4.1.1 Application to the F-35..... 91

 4.1.2 Application to the AC-130 93

 4.2 Offensive Capability 96

 4.2.1 Application to the F-35..... 98

 4.2.2 Application to the AC-130 102

5 Conclusions and Recommendations 105

 5.1 Conclusions 105

 5.2 Recommendations and Future Work..... 106

6 References..... 108

Appendix A: Source Code

Appendix B: F/A-10 Capability..... ..

List of Figures

	<u>Page #</u>
Figure 1.1: Curtiss Model D and a Christofferson Pusher ^[2]	2
Figure 1.2: Sir Frank Whittle and Dr. Hans von Ohain ^{[4], [5]}	3
Figure 1.3: Allied Forces Shooting Down Me-262s ^[6]	4
Figure 1.4: Me-262 and Me-163 ^{[8], [9]}	5
Figure 1.5: MIG-15 Over Korea ^[11]	7
Figure 1.6: F-86 and MIG-15 Comparison ^{[12], [13]}	8
Figure 1.7: F-86s Shoot Down MIG-15s over Korea ^[11]	8
Figure 1.8: (Left to Right) F-86, F-80, F-94, and F-82 ^[14]	9
Figure 1.9: F-4 with External Gun Pod over Vietnam ^[18]	11
Figure 1.10: MIGs Shot Down by Missiles and Gun Fire over Vietnam ^[20]	12
Figure 1.11: F-4 and MIG-21 Comparison ^{[12], [13]}	14
Figure 1.12: Saudi F-5 and two USAF F-15s in Operation Desert Storm ^[26]	17
Figure 1.13: F-18s Shoot Down MIG-21s ^[27]	17
Figure 1.14: F-15 and MIG-29 Comparison ^{[12], [21], [22]}	18
Figure 1.15: F-16 and J-1 Comparison ^[12]	20
Figure 1.16: Sergeant York DIVAD System ^[32]	23
Figure 1.17: Goalkeeper CIWS ^[34]	24
Figure 1.18: Phalanx CIWS ^[36]	25
Figure 1.19: Comparison of Aerial Defenses Between a B-17F and B-52D ^{[37], [39]}	26
Figure 1.20: Little Man and Fat Boy Atomic Bombs ^[58]	34
Figure 1.21: U.S. Aerial Victory Credits Achieved Since 1950 ^{[15], [16], [23], [25]}	37
Figure 1.22: Aerial Victories by Weapon Type ^{[15], [16], [23], [25]}	38
Figure 1.23: Identification Range Trends after 1980 ^[25]	39
Figure 1.24: Engagement Range Trends after 1980 ^[25]	39
Figure 1.25: M712 Copperhead Projectile ^[59]	42
Figure 1.26: Copperhead Projectile Demonstration ^[60]	42
Figure 2.1: 105mm Flechette Projectile "Beehive" ^[66]	46
Figure 2.2: PGU-28/B SAPHEI ^[67]	46
Figure 2.3: Rocket Munition Concept ^[69]	49
Figure 2.4: RF Target Guidance Phases	50
Figure 2.5: RF Target Defense Concept ^[70]	51
Figure 3.1: PGU-28/B versus G7 Standard ^{[71], [67]}	53
Figure 3.2: Coordinate System Convention	54
Figure 3.3: Forces acting on Projectile and Nomenclature	56
Figure 3.4: Zero Angle of Attack Drag Coefficient Approximation ^[71]	60
Figure 3.5: Time of Flight Model Validation ^[67]	65
Figure 3.6: Projectile Density Study when Fired from GAU-8/A	66
Figure 3.7: Sabot Projectile Range Study	67
Figure 3.8: Trajectory and Mach Relation for Extended Ranges	69
Figure 3.9: Projection of Aircraft Through Debris to Estimate R_{miss}	72
Figure 3.10: Normalized Miss Radius from Target Mass Ratio	73
Figure 3.11: Generalized 3D Engagement Scenario	74

List of Figures Continued

Figure 3.12: Idealized 2D Engagement Scenario	75
Figure 3.13: Range Trajectory Generalization (NOT TO SCALE).....	76
Figure 3.14: Maximum Maneuver Capability (NOT TO SCALE) ^[73]	77
Figure 3.15: Vypel R-77 (Adder) ^[74]	79
Figure 3.16: Generalized Tail Guided 20mm Projectile.....	81
Figure 3.17: Comparison of Actuator Performance ^[77]	83
Figure 3.18: PBP Piezoceramic Actuator Example ^[78]	83
Figure 3.19: Ragone Plot of Common Power Sources ^[80]	84
Figure 3.20: Free Space Attenuation	86
Figure 3.21: Atmospheric Absorption ^[84]	87
Figure 3.22: Estimated Upper Bound of Acquisition Cost for Guided Rounds ^{[76], [86]}	89
Figure 4.1: F-35 Sample Guided Projectile	92
Figure 4.2: F-35 Defensive Engagement Cones 2.0s.....	93
Figure 4.3: AC-130 30mm Sample Guided Projectile.....	94
Figure 4.4: AC-130 Defensive Engagement Cones 2.0s	96
Figure 4.5: F-35 Weapons Suite ^[90]	97
Figure 4.6: Sample F-35 Guided Projectile	99
Figure 4.7: F-35 10 Target Mitigation Cost ^{[93], [94]}	100
Figure 4.9: Sample AC-130 Guided Projectile	103
Figure B.1: Sample A-10 Guided Projectile	
Figure B.2: A-10 Defensive Engagement Cones 1.0s	

List of Tables

	<u>Page #</u>
Table 1.1: U.S. Aerial Victories Achieved by Gunnery in Korea ^{[15], [16]}	10
Table 1.2: U.S. Aerial Victories Achieved in Vietnam ^{[16], [23]}	15
Table 1.3: U.S. Aerial Victories Achieved in the Gulf Wars ^[25]	19
Table 1.4: U.S. Aerial Victories Achieved in Yugoslavia ^[25]	21
Table 1.5: Highlights of Various Aerial Gunnery Systems	28
Table 1.6: Highlights of Various SAM Systems	30
Table 1.7: Highlights of Various ASM Systems	31
Table 1.8: Highlights of Various AAM Systems	33
Table 1.9: U.S. Historic Nuclear Bombs	36
Table 2.1: Sample Projectiles for Various Targets	45
Table 3.1: Sample Gunnery Systems with Sabot Rounds	69
Table 3.2: Missiles Used in Scaling Laws	71
Table 3.3: Acceleration Required for Sabot Projectiles	78
Table 3.4: R-77 Salient Characteristics	80
Table 3.5: Potential Savings Per Su-35 Mitigation ^[86]	89
Table 4.1: F-35 Guided Projectile Characteristics	92
Table 4.2: AC-130 Guided Projectile Characteristics	95
Table B.1: A-10 Guided Projectile Characteristics (Defensive Maneuver)	

List of Symbols

Symbol	Definition	Units
AR	Aspect Ratio	~
C	Coefficient	~
d	Caliber/Diameter	mm
F	Force	N
g	Acceleration Due to Gravity	m/s ²
H	Total Angular Velocity	N.m ² /s
I	Moment of Inertia	kg-m ²
K	Factor	~
l	length	m
m	Mass	kg
M	Mach	~
M	Moment	N.m ²
MR	Mass Ratio	~
n	Acceleration	g's
p	Angular Rotation Rate	rad/s
q	Transverse Angular Velocity	rad/s
\bar{q}	Dynamic Pressure	Pa
R	Range	m
R	Radius	m
t	Time	s
V	Velocity	m/s
Ψ	Volume	m ³
x	Body x-axis	~
\hat{x}	Unit Vector along x	~
y	Body y-axis	~
Greek Symbol	Definition	Units
α	Angle of Attack	rad
δ	Deflection Angle	rad
β	Yaw Angle	rad
η	Efficiency Factor	~
ρ	Density	kg/m ³
Subscript	Definition	
b	Body	
c	Canard	
cross	Crosswind	
F	Fin	
l	Spin	
L	Lift	
N	Normal	
ref	Reference	
t	Tail	

List of Symbols Continued

Acronym	Definition
AAA	Anti-Aircraft Artillery
AAM	Air-to-Air Missile
AEW&C	Airborne Early Warning & Control
AIM	Air Intercept Missile
AMRAAM	Advanced Medium-Range Air-to-Air Missile
AP	Armor Piercing
APDS	Armor Piercing Discarding Sabot
APFSDS	Armor Piercing Fin Stabilized Discarding Sabot
ASM	Air-to-Surface Missile
BLAM	Barrel Launched Adaptive Munition
BVR	Beyond Visual Range
CAP	Combat Air Patrol
CAS	Close Air Support
CFIT	Controlled Flight Into Terrain
CG	Center of Gravity
CIWS	Close In Weapon System
CLOS	Command to Line of Sight
CP	Center of Pressure
DARPA	Defense Advanced Research Projects Agency
DIVAD	Division Air Defense
EFP	Explosively Formed Penetrator
ERGM	Extended Range Guided Munition
EXACTO	Extreme Accuracy Tasked Ordnance
GP	General Purpose
HE	High Explosive
HEAT	High Explosive Anti-Tank
HITT	Hypervelocity Interceptor Test Technology
HVAR	High Velocity Air Rockets
IADS	Integrated Air Defense System
ICBM	Intercontinental Ballistic Missile
IIR	Imaging Infrared
IR	Infrared
LFLAR	Light Fighter Lethality Adaptive Round
PZT	Lead Zirconate Titanate
RAP	Rocket Assisted Projectiles
REAM	Range-Extended Adaptive Munition
RF	Radio Frequency
RHAW	Radar Homing and Warning
SAPHEI	Semi-Armor Piercing High Explosive Incendiary
SARH	Semi-Active Radar Homing
SAM	Surface-to-Air Missile
SCAR	Spike-Controlled Adaptive Round
SCREAM	Shipborne-Countermeasure Range-Extended Adaptive Munition

List of Symbols Continued

SEADS	Suppression of Enemy Air Defenses
SLBM	Submarine-Launched Ballistic Missile
SRAM	Short Range Attack Missile
SSM	Surface-to-Surface Missile
USAF	United States Air Force
VHF	Very High Frequency

1 Introduction

The purpose of this study is to inform both the decision makers of this nation and the technical community about an aerial weapon system technology that has the potential to fundamentally alter the way aircraft are designed and utilized in the modern air combat theatre: causing a paradigm shift in aerial engagement.

After a century of manned flight, the role of aircraft in combat has become further diversified and has altered the rules of aerial engagement. Aerial gunnery, once crucial to any fighter platform, has seen decreased utilization as the United States Air Force (USAF) moves to a combat model with increased beyond visual range (BVR) engagement. The utility of aerial gunnery in the 21st century has now been brought into question. In this section, the historical perspective behind jet based aerial combat is outlined to both provide a basis for aerial engagement scenarios and to demonstrate the capabilities required for the next generation of aircraft weapon systems.

1.1 Abbreviated History of U.S. Air-to-Air Combat

The survey of jet based aerial gunnery provided in the following sections was limited to U.S. official aerial victories by jet aircraft since their integration in to the U.S. armed forces in the 20th century. While air-to-ground sorties were also significant, the vast number of missions flown and lack of adequate documentation for the scope of this study has limited the quantitative investigation to air-to-air engagements exclusively.

1.1.1 The Early Years

According to Harry Woodman, aviation historian, the first aerial engagement occurred in 1913 in the midst of the Mexican Revolution [1]. The conflict occurred between the famed Dean

Ivan Lamb and Phil Rader, both early aviators and friends hired on opposing sides of the conflict. Lamb was flying a Curtiss Model D (Figure 1.1) when he was instructed to shoot down Phil Rader if he encountered him while airborne. Rader, flying a Christofferson Pusher, had been repeatedly dropping handheld bombs from elevations too great to be countered by rifle fire from the ground. [2] Lamb recalled the fabled encounter:

[Rader] then drew a pistol and fired downward below my machine.

For a second my heart stopped beating as I drew my own gun, but before starting action it occurred to me that he had not actually aimed at me, but beneath. Following his example, I fired twice, and he suddenly tilted his plane my heart jumped into my throat, thinking that by accident he had been hit. He straightened out again and copied my example by firing two shots. We then fired spaced shots until our guns were empty... [2]

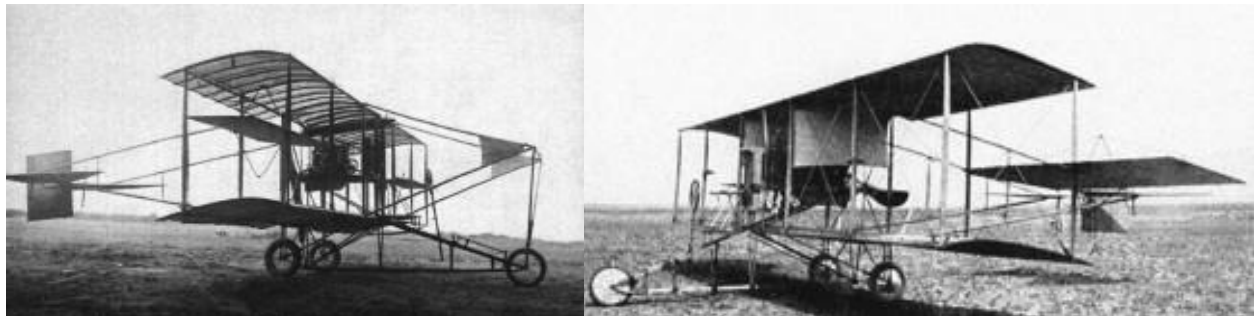


Figure 1.1: Curtiss Model D and a Christofferson Pusher^[2]

Although neither pilot had been reportedly aiming to kill, the story lives on in infamy as the first aerial “dogfight.” This form of rudimentary dogfighting would continue into the beginning of WWI. According to French aviation historian David Méchin, the first aerial kill of this conflict was reportedly between a Russian Morane and Austrian Albatros. Russian pilot Pyotr Nesterov took out the enemy aircraft with his Morane by ramming the aircraft, resulting in

the death of both aircrews. The first official aerial victory however, marked a key change in the way dogfighting was carried out. On October 5, 1914, Sgt. Frantz, a French pilot, and gunner Louis Quénault used a French Voison biplane to take down a German Aviatik biplane. The French plane however, had an 8 mm machine gun fixed to the nose. Reportedly, the passenger in the German aircraft had taken out a rifle to shoot when Quénault fired a few rounds into the Aviatik. The pilot was killed by the bullets fired; the observer died in the subsequent crash [1]. Fixed aircraft guns would increase in popularity until by WWII, they were the standard on any fighter. The beginning of jet based aerial combat would not begin until the latter half of WWII however.

Sir Frank Whittle (Britain) and Dr. Hans von Ohain (Germany) (Figure 1.2) brought about the beginning of the jet age at the onset of WWII. The results of their work, the Allied Gloster Meteor and Axis Messerschmitt 262, became operational in the latter portion of this conflict in limited numbers. While the Meteor was used primarily for air defense over Britain, the German jet platforms entered into the combat arena with potent capabilities. [3]

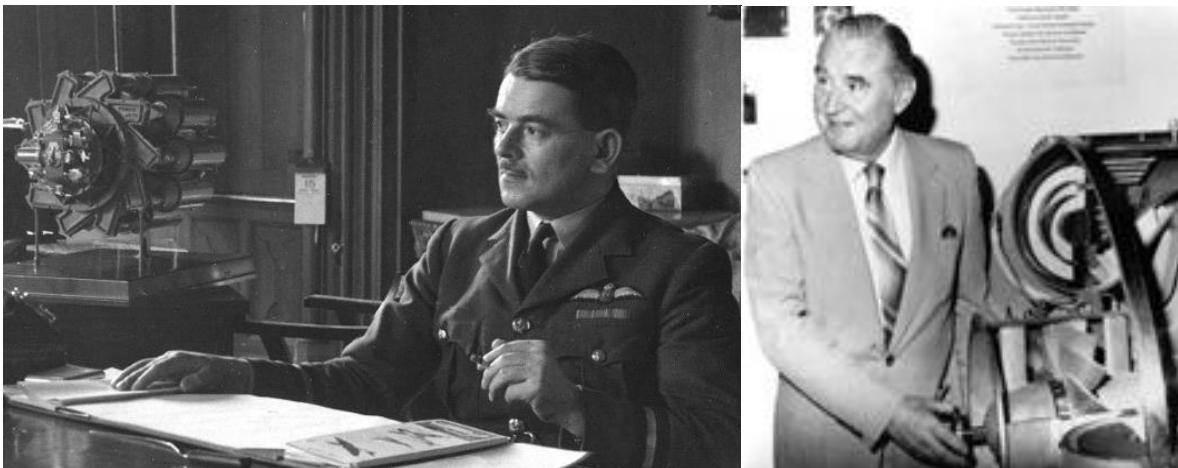


Figure 1.2: Sir Frank Whittle and Dr. Hans von Ohain^{[4], [5]}

The Me-262 and rocket propelled Me-163 Komet, shown in Figure 1.4, were introduced too late to change the eventual outcome of WWII, but still managed to wreak havoc on allied bombers and fighters alike. One bomber pilot described an encounter with the Komet:

...when this little thing came straight up at us, so fast no one had time to call it in. It passed between my plane and the leader, firing all the way, then ran out of fuel and dove straight down through the same gap, guns blazing, bullets flying all around. No one laid a glove on it. When it was gone, I saw the copilot of the lead plane wave a big white handkerchief up and down in his window. Total unconditional surrender! That was how we all felt. [3]



Figure 1.3: Allied Forces Shooting Down Me-262s^[6]

The U.S. then joined in the jet race by beginning initial development on the Bell XP-59B during WWII. The project was later transferred to Lockheed where the P-80 Shooting Star (future F-80) was developed. This aircraft was the first U.S. fighter to exceed 500 mph during initial testing in 1944. The P-80 was not operationally prepared for entry into WWII, but would

feature in the upcoming Korean War. [7] The advantage jet-speed lent to the aerial gunnery platform could no longer be denied.

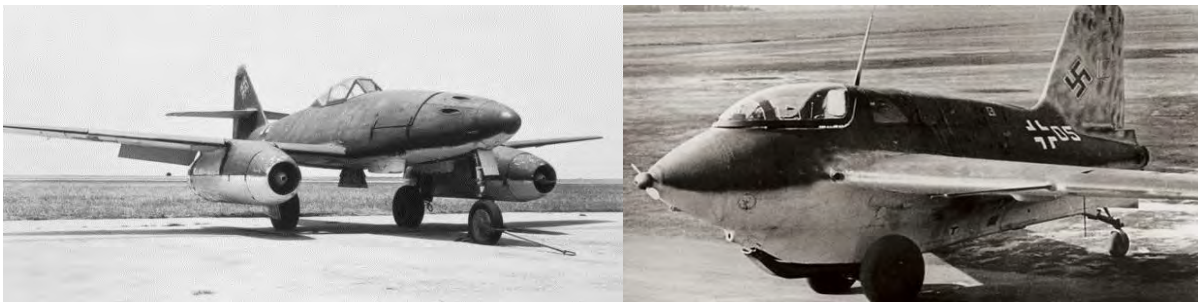


Figure 1.4: Me-262 and Me-163^{[8], [9]}

1.1.2 Korea

The true beginning of jet based aerial combat in the U.S. began with the onset of the Korean War in June 1950. Although the F-80 had been developed during the final portion of WWII, the first U.S. jet fighter proved itself up to the initial air challenge found in Korea. Outmatching the WWII era conventional fighters, the F-80 proved the value of jet fighters with the achievement of the first U.S. jet-based aerial victory on June 27: downing a Soviet Yak-9 and several Il-10s. The F-80 also achieved another first in June when it performed the first jet-based reconnaissance sortie for the United States. Early in its service in Korea, the F-80 served as a strike fighter, orbiting a target area to engage hostile aircraft and then finishing up a mission by strafing targets on the ground with .50 caliber rounds. The aircraft developed an impressive reputation as a strafing platform. Equipped with 6 machine guns, the F-80, meeting minimal challenges in the air, proved more than a match for stationary and moving targets. Hit-and-run tactics enabled by the airframe's superior speed made it invaluable during the first portion of the conflict in Korea. In addition to the employment of the .50-cal for air-to-ground strikes, the F-80 was also equipped with up to 16 5-inch high-velocity air rockets (HVAR) that were used to

engage Soviet tanks. The nearly unrivaled air-superiority enjoyed by the F-80 and older F-51s was to be short lived however. [10]

November 1 brought an unexpected challenge to the USAF in Korea. A squadron of 6 F-51 Mustangs was engaged by an unidentified swept-wing jet fighter. Later, these new aerial combatants were identified as Soviet MIG-15s. The commonly used Mustangs were far outclassed by the speed at which the MIGs could intercept, engage, and depart the scene. The first all-jet aerial engagement occurred just after this incident on November 7th with the MIG-15s interception of a group of F-80 aircraft providing cover for a strike mission. Although it was readily apparent that the newer MIG-15s outclassed the aging F-80s in nearly every way, the lack of pilot experience in the MIG-15s kept the engagement from becoming a turkey shoot. The first MIG-15 was shot down during this encounter by F-80 pilot Lt. Russell J. Brown. Now technologically outmatched, the appearance of the MIG-15s pushed the U.S. to introduce the next generation of jet fighters: the F-84 Thunderjet and F-86 Sabre. As the war progressed, the F-80 still found utility in armed reconnaissance (RF-80) and strike missions alongside the F-84s in what was known as a “Circle 10” mission. [10]



Figure 1.5: MIG-15 Over Korea^[11]

The Thunderjets were first tested against the MIG-15 in January of 1951 when a bridge bombing strike group carried out by two flights of the F-84 was intercepted by a group of MIGs. Although a single F-84 was lost, Lt. Col. William E. Bertam became the first F-84 pilot to achieve a MIG-15 kill. As subsequent encounters continued, it was apparent that the F-84 was still too slow to present an adequate answer to the challenge brought by the MIG-15s. At altitudes of less than 20,000 ft, the F-84 could out turn a MIG, but the MIGs still had the upper hand in overall speed and acceleration. The F-86 Sabre however (Figure 1.6), met with more consistent success when pitted against the MIG-15s. Again, at lower altitudes, the F-86 was shown to slightly outperform the Soviet MIGs, yet the MIGs retained an advantage in climb and zoom characteristics at higher altitudes. The Sabre was equipped with 6 .50-caliber machine guns but was limited in its patrol runs by its fuel consumption. To achieve enough airspeed when engaging a MIG, the Sabre was required to patrol above $M = 0.85$. At this speed, the F-86 could only patrol for a maximum of 20 minutes before requiring a refuel. [10] Despite its limited

operation time, the F-86A and subsequent models proved to be a critical asset for the maintenance of air superiority during the Korean War.

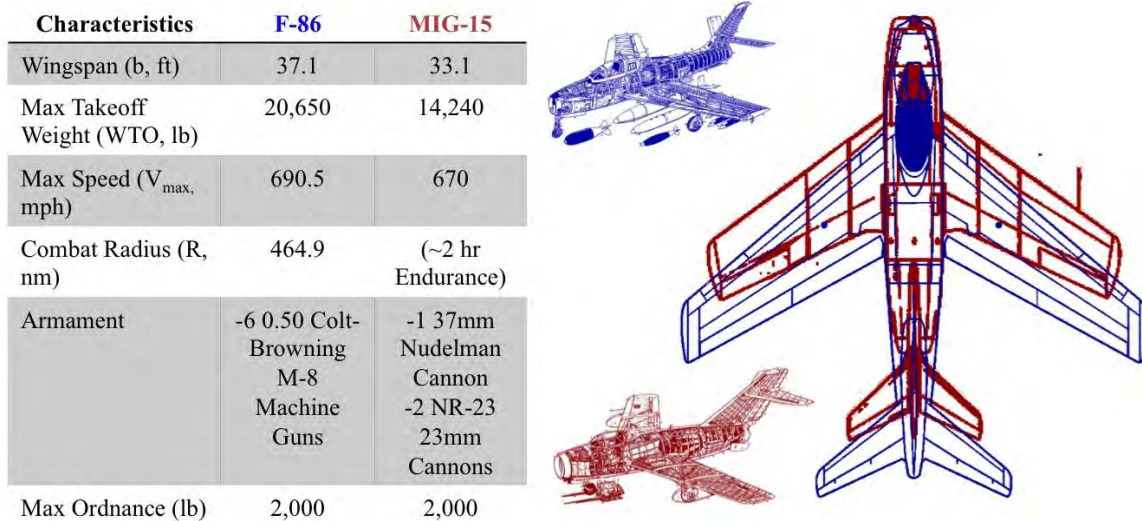


Figure 1.6: F-86 and MIG-15 Comparison^{[12], [13]}



Figure 1.7: F-86s Shoot Down MIG-15s over Korea^[11]

Three other jet platforms were introduced during the Korean War (though none quite lived up to the reputation of the F-86 Sabre). The F-94 Starfire (Figure 1.8) was first introduced in Korea in December of 1951 as a platform for all-weather air defense, a niche previously inhabited by the F-82 Twin Mustang. The Starfire was initially limited to local air defense. As

the war progressed however, it was used (with very limited success) as a night interceptor and as a barrier patrol for bombers. The Navy and Marines introduced the other two jet fighter platforms: the F9F Panther and F3D-2 Skyknight. The Panther had the distinction of being the first successful jet-fighter platform for carrier operations. During the war in Korea, the F9F was often used in tandem with F4U Corsairs and AD Skyraiders to carry out fighter-bomber strikes against troops and supplies. The Marines first received the F3D-2 Skyknight as an all-weather, night jet fighter platform to replace F7F Tigercats. In this role, the Skyknight proved its worth by becoming the first aircraft to achieve a night jet vs. jet kill on November 8, 1952 after shooting down a possible MIG-15 [10].









Figure 1.8: (Left to Right) F-86, F-80, F-94, and F-82^[14]

Although active US engagement over Korea ended on what could best be described as a stalemate and the division of the country, the significance of jet based aerial combat was fully realized during this engagement. As this conflict predated the use of guided missiles on the jet platforms discussed previously, most aerial victories in this war were achieved with .50-caliber rounds. A summary of the official U.S. aerial victories is included below in Table 1.1. Note, probable kills were denoted as a 0.5 kill. While the aerial engagements over Korea were carried

out with gunnery alone, some aerial victories may be attributed to maneuvering tactics, etc. These are not broken out in Table 1.1.

Table 1.1: U.S. Aerial Victories Achieved by Gunnery in Korea^{[15], [16]}

Aircraft	Target	IL-10 -12	L-7 -9	PO-2	T-2	YAK-3 -9 -11 -15	Propeller no ID	MIG-15	Jet no ID	Total
F-80		5	-	-	-	9	-	6	-	20
F-84		-	-	-	-	1	-	10	-	11
F-86		2	6	-	9	1	-	834	-	852
F-94		-	-	-	-	-	2	1	1	4
F3D-2		-	-	1	-	1	-	4	-	6
F9F		-	-	-	-	2	-	5	-	7
Total		7	6	1	9	14	2	860	1	900

1.1.3 Vietnam

The Vietnam War represented a turning point for the way aerial combat was performed. During this engagement, air-to-air combat was primarily carried out with missiles rather than hard-launched munitions. Various engagement scenarios still encouraged the use of aerial gunnery however, as will be described in the overview of the air war provided in this section.

The air war in Vietnam began on March 2, 1965 as the first tactical strikes were initiated as part of operation Rolling Thunder. Early objectives for the air war according to Secretary of Defense Robert McNamara, aimed to “reduce the flow and/or increase the cost of infiltration of men and supplies from North Vietnam to South Vietnam.” [17] The first air-to-air engagement of the war occurred on April 3 as MIG-17s closed on a Navy strike unit and subsequent group of

F-105 Thunderchiefs. The MIG-17s, though ill trained in this first portion of the Korean War, had tighter turning capabilities than the 20mm-armed Thunderchiefs. When matched against the F-4 Phantom II (Figure 1.9) however, the MIG-17s no longer enjoyed this particular advantage. U.S. aerial forces also had to contend with the growing capability of the air-defense system in North Vietnam. Strike forces encountered AAA and SAM routinely on missions. The SA-2 in particular posed a great challenge to any strike missions undertaken and would have to be addressed in the coming years [17].



Figure 1.9: F-4 with External Gun Pod over Vietnam^[18]

In the beginning of 1966, the F-100F was brought to Thailand as a means of countering the SA-2 threats. This aerial platform included a radar homing and warning (RHAW) system which enabled pilots locate the radar guidance signals used by the SA-2s following a launch. Once a location was marked, the F-105s could then target the area and nullify that particular threat. The F-100Fs would eventually be replaced with the upgraded F-105Fs several months later.

The U.S. aerial forces soon faced a new threat with the deployment of the Soviet MIG-21 in April of 1966. Early attempts by the MIG-21s to hamper the strike forces were not highly

successful at this time however, perhaps due to a lack of pilot experience. An F-4C CAP downed the first MIG-21 on April 26th [17]. The Navy also became engaged in the air war during this timeframe with the first kill of a MIG-17 by a F-8 Crusader on June 12 and a MIG-21 kill on October 9th. The Crusaders were assigned to the Essex class attack carriers while the larger carriers sported the F-4 Phantom IIs. Though carrier landings proved a challenge for the F-8s, they remained an asset in the conflict over Vietnam. [19] By this time, the MIG-21s had fully realized their potential when forced to engage the U.S. strike forces. In particular, the Soviet platform could effectively outmaneuver the majority of air-to-air missiles employed by the U.S. forces at this time: the AIM-7 Sparrow and AIM-9 Sidewinder. Once engaged, the MIG-21s would enter a rapid turning descent that the missiles at the time could not match. In response to this frightening development, the F-4s, equipped only with missiles, demanded a modification that would allow an external 20-mm gun pod to be installed on their aircraft. This modification was then deployed in May 1967. [17]



Figure 1.10: MIGs Shot Down by Missiles and Gun Fire over Vietnam^[20]

During this timeframe, changing aerial tactics were employed by the MIG-21s to devastating effect. A flight of the MIGs would fly towards a U.S. force at extremely low altitude to escape notice by radar. After passing through the U.S. force from below, the MIG-21s would then rapidly climb with afterburner to well above the U.S. aircraft and then dive at supersonic speeds towards the force. In a single pass, they fired ATOLL IR seeking missiles, and would either continue through the formation or climb out again before scattering and fleeing back to their respective bases in a true hit-and-run. These new tactics, coupled with more experienced pilots, changed the balance for the U.S. forces. Between mid-1967 and early 1968, MIG aerial victories exceeded those achieved by the U.S. The increased implementation of advance warning systems such as the EC-121M in late 1967 and the combined efforts of the Air Force and Navy for improved command and control allowed the U.S. fighters to once again take the lead in aerial victories by 1972. [17]

Characteristics	F-4	MIG-21
Wingspan (b, ft)	38.4	25
Max Takeoff Weight (WTO, lb)	54,600	16,700
Max Speed (V_{max} , Mach)	2.16	2
Combat Radius (R, nm)	782	326
Armament	-6 Sparrow III -or 4 Sidewiner + 2 underwing mounts	-1 30 mm cannon -2 Atoll missiles
Max Ordnance (lb)	16,000	~

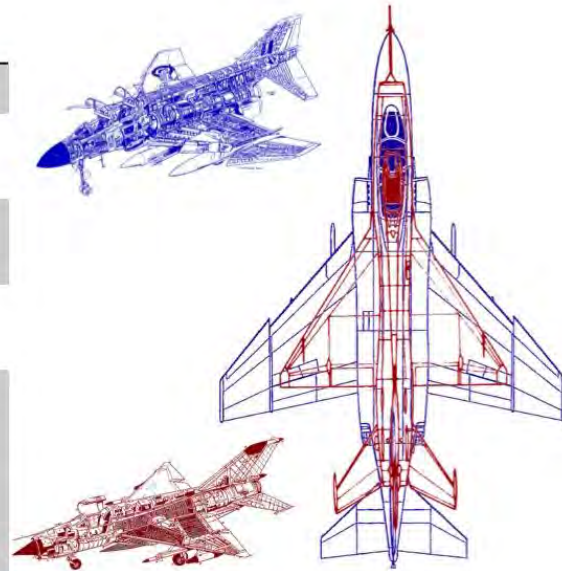






Figure 1.11: F-4 and MIG-21 Comparison^{[12], [13]}

In December of 1972, the Air Force brought in the F-111 Aardvark and A-7 Corsair II. As part of operation Linebacker II, the F-4 and A-7 would engage in strike missions during the day, while the F-111 and B-52s would operate at night. The F-105s and F-4s continued the mission to search and destroy any SAM sights detected, while the F-111s primarily targeted airfields. During the multifarious aerial operations of Linebacker II, even the B-52 tail gunners scored 2 aerial victories. In less than 10 days, North Vietnam signed the ceasefire and agreed to resume negotiations in Paris in January. The US involvement in Vietnam would officially cease in August 1973. [17]

Table 1.2: U.S. Aerial Victories Achieved in Vietnam^{[16], [23]}

Weapon	Target	An-2	MIG-17	MIG-19	MIG-21	Total
B-52D		-	-	-	2	2
Guns		-	-	-	2	2
F-105		-	30	-	-	30
Guns		-	27	-	-	27
AIM-9		-	2	-	-	2
AIM-9+Guns		-	1	-	-	1
F-4		1	43.5	9.25	73	126.75
Guns		-	7	1	7	15
AIM-4		-	4.5	-	1	5.5
AIM-7		1	9.5	4	39.5	54
AIM-9		-	20.5	3	22.5	46
AIM-9+Guns		-	-	-	1	1
Maneuver		-	2	1.25	2	5.25
F-8		-	12.5	-	3.5	16
Guns		-	0.5	-	-	0.5
Guns+Zuni Rockets		-	1	-	-	1
AIM-9		-	9	-	3.5	12.5
AIM-9+Guns		-	2	-	-	2
Totals		1	86	9.25	79	174.75

As shown in Table 1.2, Vietnam proved the turning point for aerial gunnery with the majority of aerial victory claims resulting from the use of missiles. The difference in engagement tactics between the F-105 and slightly newer F-4 can be seen here as well. While the F-105 was equipped with both a 20mm cannon and AIM-9s, the Thunderchief pilots favored the cannon in aerial engagements. The F-4 Phantom IIs however, perhaps as they started from an exclusively

missile platform, still favored missiles even after a 20mm cannon was installed at their behest. F-8 Crusaders were slightly older than either of these platforms and had both the 20-mm cannon and AIM-7 missiles, but greatly favored the missiles for aerial engagement. The diverse preferences across these platforms that were introduced at roughly the same time highlight how the Vietnam conflict served as a pivot for aircraft weaponry.

1.1.4 The Gulf War

The air campaign in the Gulf War began on January 17, 1991 during Operation Desert Storm. This effort followed the previous Operation Desert Shield in response to the Iraqi invasion of Kuwait in August 1990. By this time, the Coalition forces had assembled close to 1,800 aircraft from 12 different countries to participate in the four-phase air campaign. Phase I, a strategic air campaign, would target “centers of gravity” such as the Iraqi National Command Authority, Iraq’s chemical/biological/nuclear centers, and the republican Guard Forces Command. Phase II would focus on maintenance of air superiority in the region, while Phase III, Battlefield Preparation, used aircraft to target ground forces. Phase IV, the Ground Offensive Campaign, would not only focus on the destruction of communication lines and Republican Guard, but also to liberate Kuwait while providing close air support (CAS) to ground forces [25].



Figure 1.12: Saudi F-5 and two USAF F-15s in Operation Desert Storm^[26]

Air-to-air engagements during this conflict were largely successful. By the end of Operation Desert Storm, 33 hostile fixed wing aircraft had been shot down by Coalition aircraft while a single loss was incurred [24]. U.S. air presence was maintained well after the end of active engagement in the region with Operation Southern Watch—providing a continuing Coalition air presence over southern Iraq, and Operation Provide Comfort—aiding in the humanitarian effort and the suppression of enemy air defenses (SEADS). [25]



Figure 1.13: F-18s Shoot Down MIG-21s^[27]

Unlike the previous U.S. aerial engagements, gunnery only accounted for two air-to-air kills during the Gulf conflict. The other 38 kills were obtained by missiles, maneuvering tactics

(pilot ejection, failed defensive maneuvering resulting in CFIT, and failed defensive tactics at loss of a flight leader), and 1 was the result of an F-15 dropping a GBU-10 through a helicopter rotor. The two kills attributed to guns were achieved by A-10 Warthog pilots. Robert Swain Jr. achieved the first on February 6, 1991. Swain closed on an unidentified rotorcraft to 5000 ft and after verifying that no friendlies were expected in the area, fired several bursts before the last 100 found their mark and brought down the aircraft. While returning to base, the rotorcraft's status friendly or hostile aircraft was brought into question, but later reports confirmed that all friendlies were accounted for and the helicopter was listed as a Bo-105. This engagement was the first air-to-air victory for the A-10. Todd Sheehy obtained the second A-10 aerial victory on February 15, 1991. While on a strike mission, Sheehy was called to check out a low and slow radar contact. Sheehy obtained a visual on the Mi-8 helicopter and made two strafing passes amidst AAA fire before achieving the kill. This engagement was also the last reported aerial gun kill by U.S. forces. [25]

Characteristics	F-15	MIG-29
Wingspan (b, ft)	42.8	33.6
Max Takeoff Weight (WTO, lb)	68,000	36,375
Max Speed (V_{max} , Mach)	2.5+	2.2
Max Range (R, nm)	1,000	430
Armament	-1 M61A1 20 mm cannon (940 rounds) -AIM-120, AIM-9, AIM-7	-1 30 mm cannon (150 rounds) -6 air-to-air missiles of types R-60, R-27R, R-77
Max Ordnance (lb)	23,600	8,820

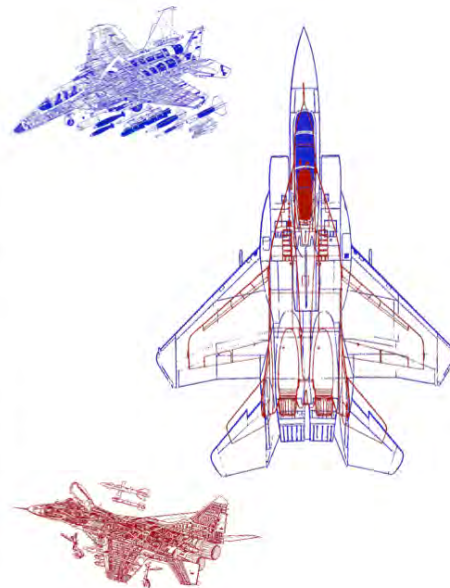






Figure 1.14: F-15 and MIG-29 Comparison^{[12], [21], [22]}

Table 1.3: U.S. Aerial Victories Achieved in the Gulf Wars^[25]

Target		Helicopter	IL-76	PC-9	MIG -21 -23 -25 -29	Su -7 - 22 -25	F-1	Total
Weapon								
A-10		2	-	-	-	-	-	2
Guns		2	-	-	-	-	-	2
F-14		1	-	-	-	-	-	1
AIM-9		1	-	-	-	-	-	1
F-15		3	1	1	17	7	6	35
AIM-7		2	1	-	12	3	5	23
AIM-9		-	-	-	4	4	-	8
Maneuver		-	-	1	1	-	1	3
GBU-10		1	-	-	-	-	-	1
F/A-18		-	-	-	2	-	-	2
AIM-7		-	-	-	1	-	-	1
AIM-9		-	-	-	1	-	-	1
Totals		6	1	1	19	7	6	40

1.1.5 The Yugoslav Wars

In 1992 Bosnia seceded from Yugoslavia, increasing hostilities in an already tense region. U.S. armed forces became involved alongside 20 other coalition nations in both naval and aerial efforts over Bosnia. The primary role of navy aircraft in this conflict was the enforcement of the “no-fly-zones” over this region. [28] On these missions, the F-16 achieved 6 aerial victories with missiles alone, holding true to the decreased utilization of gunnery in aerial engagements. Bob Wright however, who claimed 3 J-1 Jastreb kills on February 28 in his F-16C, explained that while he did want to use guns to take out the last of three J-1s, he sighted a residential area in the background and switched back to an AIM-9 for the kill. The majority of

the engagements in this theater were close enough for the implementation of aerial gunnery (~4000 ft), though pilots still favored the AIM-9 and AIM-120 missiles. [25]

Characteristics	F-16	J-1
Wingspan (b, ft)	32.8	38.3
Max Takeoff Weight (WTO, lb)	42,300	11,243
Max Speed (V _{max} , Mach)	2+	510 mph (19,680 ft)
Maximum Range (R, nm)	2,100	820
Armament	-M61A1 20mm with 515 rounds -9 hardpoint attachments	-3 .50 Colt-Browning machine guns -8 underwing attachments

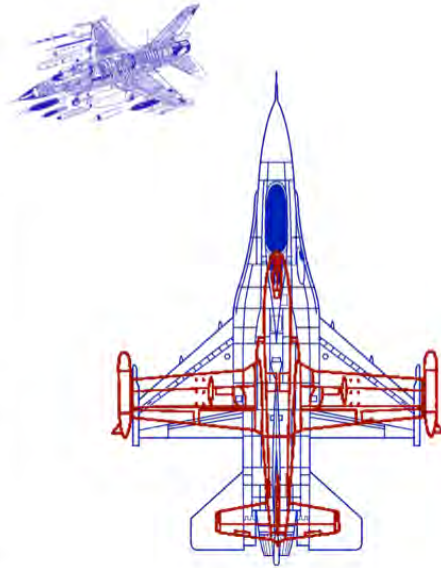




Figure 1.15: F-16 and J-1 Comparison^[12]

Tensions continued to escalate in the region, and on March 24, 1999 NATO officially launched Operation Allied Force. Air strikes were authorized at the beginning of the year in response to Serbian President Slobodan Milosevic’s troop movement into Kosovo [29]. The initial strikes were implemented by cruise missiles targeting the electrical grid and military airfields. Strike aircraft were then sent in to target the integrated air defense system (IADS) components. Nearly half of the U.S. air-to-air victories for this portion of the conflict were achieved in that first night and 2 MIG-29 kills were achieved by F-15Cs. [30] Air-to-air engagement was not common throughout the remainder of this primarily strike-oriented campaign, and only 3 additional U.S. aerial victories were achieved by F-15s and F-16s against MIG-29s. Overall, engagement distances increased greatly, and only a single engagement (conducted by an F-16) occurred at short range. [25]

Table 1.4: U.S. Aerial Victories Achieved in Yugoslavia^[25]

Weapon	Target	J-1	MIG-23	MIG-25	MIG-29	Total
F-15 		-	-	-	4	4
AIM-120		-	-	-	4	4
F-16 		4	1	1	1	7
AIM-9		3	-	-	-	3
AIM-120		1	1	1	1	4
Totals		4	1	1	5	11

1.2 Aerial Combat Weapon Systems

A brief introduction to several types of aerial combat weapon systems is provided in this section. Within each system type, a brief historical overview is provided along with highlights of the systems currently fielded by the U.S.

1.2.1 Guns

1.2.1.1 Aerial Defense Artillery

A brief overview of a few historical and modern aerial defense artillery systems is given in this section to highlight the defensive capability of systems against hostile aircraft and lend historical grounding to the field of guided gunnery.

Sergeant York Division Air Defense (DIVAD)

In 1978, the Sergeant York Division Air Defense (DIVAD) gun system was initiated. This program was established to satisfy a deficiency in the U.S. gun defense capabilities against low flying enemy aircraft. This system was to follow in the footsteps of the Soviet ZSU-23-4 anti-aircraft gun. The ZSU-23-4 was comprised of four radar-directed automated cannons that

(along with systems similar to the ZSU-23-4) proved highly effective against hostile aircraft. The DIVAD program had 7 years bring a system into production with the following characteristics:

- A target acquisition time of not less than 8 seconds required from identification or following entry into engagement range;
- A target engagement range of 4 km;
- Gun to allow for 180 degrees rotation;
- All weather, day/night, system;
- Sufficiently mobile to endure combat environment.

The contract was awarded in May 1981 to Ford Aerospace and Communications Corporation. The design selected included proven components from a variety of existing systems such as: radars from the F-16, M-48A5 tank chassis, and twin Bofors 40-mm guns. As the program progressed through the testing phases however, numerous deficiencies in contract fulfillment, test plans and execution, and weapon system capability, led to the demise and cancellation of this program. The DIVAD procurement was cancelled in August 1985 for a multitude of reasons. The official cancellation was brought about due to the ineffective engagement range of 4km (as Soviet helicopter standoff ranges at the time were 6km), as well as cost concerns. The radar system also had difficulty identifying targets in the presence of ground clutter (such as terrain irregularities), severely limiting battlefield potential. Three main reasons are given in Reference [31] for the program failure: inadequate specifications given at the initiation of the program, contract terms that highly favored schedule over necessary technological decision making, and overall inadequate testing that was performed too late in the acquisition of the system. [31]



Figure 1.16: Sergeant York DIVAD System ^[32]

Although the Sergeant York DIVAD gun system did not reach operational status, this system is included for comparison as it was a U.S. program that utilized autonomously aimed (radar based) twin guns. The program also highlights an interesting case study of the importance of adequate system requirements early in the design phase.

Goalkeeper CIWS

The Goalkeeper CIWS (close in weapon system) is a fully autonomous system used for ship-based defense. This system, initially conceived by the Thales Netherlands branch, is designed to detect and mitigate threats posed to ships by aircraft, surface vessels, and highly maneuverable missiles. [33]



Figure 1.17: Goalkeeper CIWS^[34]

The gun incorporated on the Goalkeeper system is the 7-barrel GAU-8/A also fielded on the A-10 (see Section 1.2.1.2), and is capable of firing 30mm rounds at a rate of 4200rps. An I-band and K-band radar system is integrated into the system for target tracking, and automated optronic tracking is also achievable. The system has a maximum of 1190 rounds and may take standard TP, HEI, or missile-piercing discarding-sabot (MPDS) and frangible MPDS (FMPDS) to ensure the destruction of missiles. [33]

Phalanx CIWS

The Phalanx CIWS is the United States version of the Dutch Goalkeeper. This system is designed to detect and engage anti-ship threats including missiles, aircraft, and other littoral threats. Production on this system began in 1978 and it is currently in service. The system incorporates the M61A1 Gatling Gun discussed in Section 1.2.1.2. The gunnery system is capable of firing 20mm rounds at a rate of 4,500rpm for aircraft and missile threats, though firing rates are reduced on this platform to 3,000rpm. More recent variants have also integrated an electro optic sensor to engage other aerial threats such as UAS, helicopters, etc. as well as surface craft. The system weighs 13,600lb and has a maximum capacity of 1,550 rounds. [35]



Figure 1.18: Phalanx CIWS^[36]

1.2.1.2 Aerial Gunnery Systems

Aircraft gunnery systems have evolved dramatically from the hand-held rifles such as those carried by Lamb and Rader (see Section 1.1.1) to the systems used today such as the M61 Vulcan 20mm cannon and GAU-8 30mm system. Throughout the entirety of the history of aerial gunnery however, the focus has been placed on direct fire support missions alone, with pilots firing directly at, or just leading the intended target.

The earliest aerial engagements were carried out using handheld guns prior to WWI when aircraft were primarily used for reconnaissance purposes. As time progressed, aerial gunnery developed to encompass variable gun mounts on aircraft during WWI. While highly effective, many of these systems required a separate gunner to aim the barrel independent of the aircraft. The first true “fixed” gun mount system was implemented in 1915. The fixed gun mount was enabled by the development of timing technology that would allow the gun to fire along the body axis of the aircraft without shooting off the propeller blades on a tractor type aircraft. By the time WWII had begun, aerial gunnery systems for aircraft included several fixed guns. The U.S.

fighters of the time were generally equipped with 6 12.7mm machine guns, while for British fighters, standard gunnery armament was 4 20mm guns. Bombers typically employed a variety of systems including power-aimed guns of 20mm and 23mm caliber. Following the end of WWII and the beginning of the jet aircraft revolution, advancements were also made in aerial gunnery. Increasing number of rounds fired per minute and gun reliability corresponded with fewer guns installed on aircraft. [37] This transition can be seen by juxtaposing the defensive fields of fire of the B-17 (WWII) with that of the B-52D as shown in Figure 1.19. The B-17 incorporated .50 caliber guns in the following locations: the tail turret (2), waist guns (1 per beam), ball turret (2), the dorsal hatch, dorsal turret (2), nose guns (2), and finally a single .30 caliber in the lateral nose gun. The B-52D however, incorporated just a single variant of the M61 Vulcan in the tail. [37]

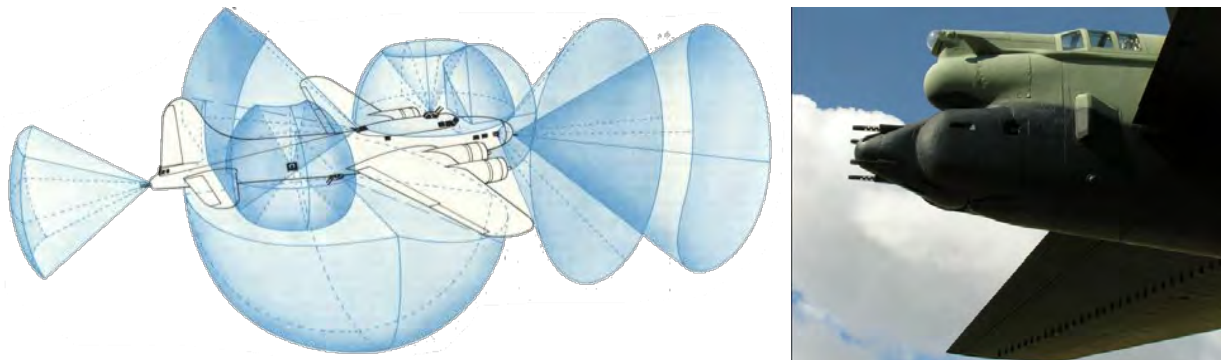


Figure 1.19: Comparison of Aerial Defenses Between a B-17F and B-52D^{[37], [39]}

Several systems of note have emerged for use on modern aerial jet platforms. The German Mauser BK27 is a single-barrel, 27mm cannon that utilizes a revolving 5-chamber cylinder to achieve high rates of fire. This system was originally designed for use on the Panavia Tornado, but would later find applications on aircraft such as the the JAS 39 Gripen and Eurofighter Typhoon. The unique caliber used by this system has caused some concern over commonality between other gun systems that use the more common 30mm or 20-25mm rounds. [37] Similar to the BK-27, the French GIAT/Nexter 30M791 gun fires 30mm rounds using a

single barrel. Ammunition feed is achieved using links that are removed prior to chamber loading, and the ammunition feed may be taken from either the left or right sides. The firing rate may be selected as either bursts of 0.5 or 1 seconds, or continuous fire. One type of ammunition for this system, a HE/AP/I, may be fired and remain inactive for the first 66 ft after firing. This gun was originally developed for the Dassault Rafale. [37] In the United States, the General Electric M61 Vulcan and its derivatives have seen great utility. The Vulcan, originally designed in the 1950s, is a multi-barrel system based upon the studies of Dr. Gatling a century before. The gun has 6 barrels that are connected to a rotating breech rotor, allowing the system to achieve firing rates between 4,000 and 6,000 rounds per minute. Early designs attempted to use a standard link feed, but the extreme rate of fire caused numerous problems in link disposal and reliability. A linkless feed was designed as a result and is implemented on the current systems. Early applications of this system and derivatives included guns on the F-104 Starfighter, F-105 Thunderchief, F-4 Phantom and B-58 Hustler. Later aerial platforms would include the B-52, F-14, F-15, and F-16. [37] Table 1.5 highlights several aerial gunnery systems and their salient characteristics for comparison.

Table 1.5: Highlights of Various Aerial Gunnery Systems

System	Caliber (mm)	Muzzle Velocity (m/s)	Rate of Fire (rpm)	Gun Weight (lb)	Aerial Platform
30M 791 ^[37]	30	1,025	300/600/1,500/ 2,500	243	Dassault Rafale Tornado, JAS-39, Typhoon, Alpha Jet
BK-27 ^[37]	27	1,025	1,000/1,700	221	
GAU-8/A Avenger ^{[37], [38]}	30	1,066	2,100/4,200	620	A-10
GAU-12/U Equalizer ^[37]	25	1,100	3,600-4,200	276	AV-8B
GAU-22/A ^[40]	25	1,036- 1,085	3,300	230	F-35A (internal), F-35B/C (pods)
GSh-301 ^[41]	30	860	1,500-1,800	101	MIG-29, Su-27, Su-30, Su-33, Su- 34, Su-35
M61 Vulcan ^[37] M102	20	1,036	4,000/6,000/ 6,600	265	F-104, F-105, B- 58*, B-52*, F-14, F-15, F-16, F-18, F-22
Howitzer ^{**[42]}	105	494	10	900	AC-130

*Denotes a variant used for bomber tail turrets.

**Field Artillery Variant

1.2.2 Guided Missiles

A brief overview of the early development of several varieties of missiles used by or against aerial vehicles is presented in this section. Focus is given primarily to those systems fielded by the United States and Russia. Surface-to-surface missiles (SSM) are not, therefore, considered in this section. The term “missile” is taken to mean any guided, powered projectile fired with the purpose of removing a specified threat. By this definition, the glide bombs developed as early as WWI are considered instead to be gravity weapons and are noted in Section 1.2.3.

1.2.2.1 Surface-to-Air

The evolution of land-based surface-to-air missiles (SAMs) began during WWII with the German experimentation on a Rheinmetall-Borsig design “Hecht” prior to 1941. Several other SAM development programs followed in rapid succession, though none reached operational status prior to the end of hostilities. The majority of these systems were guided to target with radio command to line of sight (CLOS) systems. Japan also experimented with early SAM concepts: Funryu 2 and Funryu 4. The Funryu 4 was propelled by a Japanese variant of the Me-163 liquid fueled rocket, and included a radar command guidance system (though it was likely assisted by a pilot on the ground). It was not until after the war that the rest of the world began development on surface based SAM systems. [43]

Sea launched SAMs also arose out of the WWII conflict with efforts by the British Royal Navy as a means of defense against aircraft at low altitude in 1939. Preliminary designs allowed for radio guidance, but no serious designs were put forth until after the Kamikaze threat peaked in 1944. No systems became operational prior to the mid 1950s however. [43] Several SAM systems of note along with their salient characteristics are shown in Table 1.6.

Table 1.6: Highlights of Various SAM Systems

System	Length (ft)	Weight (lb)	Maximum Speed (Mach)	Range (mi)	Guidance/Seeker
Aster 15 ^[44]	13.8	683	3	18.6	active RF
Aster 30 ^[44]	16.1	992	4.5	62	active RF
Mistral Albi ^[47]	6.1	43	2+	4	IR
Guideline (SA-2) ^{[43], [45]}	35.2	5,070	~3.5	31	separate radar with UHF link
Gainful (SA-6) ^[43]	20.3	1,213	2.8	37	separate radar with I-band link
9D32 Streal (SA-7) ^[43]	4.4	20	1.5	6.25	IR
RIM-174 ERAM ^[51]	21.5	3,300	3.5	230	ING, active/semi active RF
FIM-92 Stinger ^{[43], [46]}	5	22.3	2.2	3	IR
MIM-104 Patriot ^{[43], [52]}	17	2,200	3.9	43	external radar/semi active RF

1.2.2.2 Air-to-Surface

Like surface to air missiles, early advances in tactical air to surface missiles (ASMs) occurred during WWII. Excluding the extensive research into glide-bombs during this timeframe, the first ASM designs by Germany and Japan were modeled after more conventional aircraft. Dr. Voepl of Henschel performed the groundwork on what would have become the first guided supersonic missile, the Zitteroschen, in 1944. Development on this system was never completed, though wind tunnel tests were performed up to Mach 1.5. Siegfried Holzbauer’s “composite aircraft” concept would evolve into the Mistel family of ASMs. The Mistel system comprised of a converted aircraft carrying a sizeable warhead and contact fuse that was suspended beneath a traditionally piloted aircraft. Once the target was within range, the “missile” was dropped and steered by a radio command link to its destination. The Mistel 1 did see combat, though the vast majority of the systems did not become operational before the end of

hostilities. By 1942, Japan was also experimenting with ASM design. The Funryu 1 concept, though never fielded, was to be a conventional airplane type configuration to be used as an anti-ship system. The I-GO-1 series was also developed during this timeframe as a family of radio guided warheads capable of 80 seconds of rocket-powered flight. The United States and Sweden would not begin development of these systems until after the war. [43]

Strategic ASMs were designed not to target areas with greater precision, but to allow strikes against defended targets that might not otherwise be reached safely with conventional aircraft. The majority of the strategic ASMs carried nuclear warheads, and before advancements in nuclear technology allowed the size of these warheads to shrink, it was not uncommon for a bomber to only carry one or two of these massive missiles. Later programs such as the famed thermonuclear Hound Dog and SRAM (Short Range Attack Missile) were capable of achieving ranges of over 100 miles for the latter, and 700 miles for the former using inertial guidance systems. [43] Several ASM systems of note are provided in Table 1.7.

Table 1.7: Highlights of Various ASM Systems

System	Length (ft)	Weight (lb)	Maximum Speed (Mach)	Range (mi)	Guidance/Seeker
AGM-84A Harpoon ^[53]	12.6	1,145	0.75	57	radar altimeter/active radar homing
AGM-88 HARM ^[53]	13.7	807	2+	10	GPS/INS/passive radar
AGM-114 Hellfire ^{[53], [48]}	5.3	99	1.17	5.6	semi active laser
AS-14 Kedge ^{[53], [49]}	14.8	1,323	~2	12.4	semi-active laser
AS-15 Kent ^[53]	23	3,307	0.9	746	Tercom IGS
HOT ^[53]	4.2	55	~0.7	2.5	wire CLOS
Exocet ^[53]	15.4	1,444	0.93	43.5	INS/active radar homing

1.2.2.3 Air-to-Air

Unsurprisingly, the first air-to-air missiles (AAM) were designed and developed during the technology boom generated during WWII. The first AAM developed and produced was the German HS 298. Though the program was shut down after 1944, the HS 298 saw use in active combat on the Ju-88, Ju-388, and Fw-190 aerial platforms. The missile had an inverted H-tail with fixed vertical fins and elevators, and also had conventional swept wings complete with ailerons. The 55lb warhead was steered with a Kehl/Colmar radio command link and plans for a proximity fuse and wire-guided version were started prior to the program cancellation. The X-4 was an even further developed AAM program out of Germany. This missile had a fixed cruciform wing with roll tabs, a cruciform tail with control surfaces, and was guided to target by the aircraft pilot through a Düsseldorf/Detmold command link. Over 1000 X-4s were produced, though none reportedly made it to active combat units prior to the end of the war. [43]

The majority of the AAM developed outside of Germany occurred after WWII. The U.S. began the development of the first non-German flight-tested AAM after WWII in 1947 with the XAAM-A-1 Firebird. Similar to the famed Ryan Firebee, the Firebird was guided with a radio command link, and semi-active radar homing (SARH) was attempted after the introduction of the missile in 1950. The U.S. also operated the first guided AAM with the AIM-4 Falcon series. This missile boasted a radar-based fire-control system. Later models would carry improved SARH systems as well as IR seeking variants. [43] Several AAM systems of note are outlined in Table 1.8.

Table 1.8: Highlights of Various AAM Systems

System	Length (ft)	Weight (lb)	Maximum Speed (Mach)	Range (mi)	Guidance/Seeker
AIM-7F Sparrow ^[53]	12	503	4	62	SARH
AIM-9 Sidewinder ^[53]	9.4	193	2.5	12	IR
AIM-120A AMRAAM ^{[53], [50]}	11.8	335	~4	~30	INS/terminal active radar
AIM-54 Pheonix ^[53]	13.2	985	5+	124	active radar
Meteor BVRAAM ^[54]	12.1	419	~	~	INS/active radar
MICA RF ^[53]	10.2	243	4	31	INS/active radar
R-77 Vypel ^{[55], [56]}	3.6	175	4	50	INS,RF/terminal active radar

1.2.3 Gravity Weapons

1.2.3.1 Unguided Bombs

Unguided gravity weapons predate powered aircraft flight by more than half a century. According to Reference [57], the first gravity weapons to be used were delivered from some of the first unmanned aerial vehicles, balloons, in the Austrian siege of Venice in 1849. With the event of powered aircraft flight, bombs quickly gained popularity if not in effectiveness. The majority of these early weapons were in fact, weapons taken from traditional infantry based combat (such as artillery rounds and grenades). During the first world war, strategic bombing tactics emerged from multiple nations with bombs ranging from just a couple pounds to a couple thousand pounds. Reference [57] notes that these weapons achieved very limited success due not only to inadequate bomber range and capacity, but also because of anti-aircraft defenses. During WWII, bombs saw much greater utility and were used against both soft and hardened targets.

The size of some of the gravity weapons designed for use against large hard targets increased dramatically to include weapon systems up to 22,000 lb. [57]

Following WWII, the development of more accurate gravity weapons came to the fore and would eventually evolve into the precision guided munitions (PGM) used today. Conventional gravity weapons are still used and being developed, though the introduction of PGM has resulted in the new designator “dumb bombs” for these general purpose (GP) bombs. In the United States, the Mark series GP bombs have come to the fore ranging from 250 to 2,000lb. [57]

1.2.3.2 Atomic and Nuclear Bombs

Nuclear weapon development originated with the work of the Manhattan Project on fission bombs during WWII. The first of these weapons to be deployed in combat, “Little Boy,” was dropped on Hiroshima on August 6, 1945 to devastating effect. The second, “Fat Man” was then dropped on Nagasaki on August 9, 1945. While the decision to drop these weapons on Japan lead to the end of the war, the use of these weapons also sparked an unprecedented nuclear arms race between the United States and the Soviet Union in what would become the Cold War.

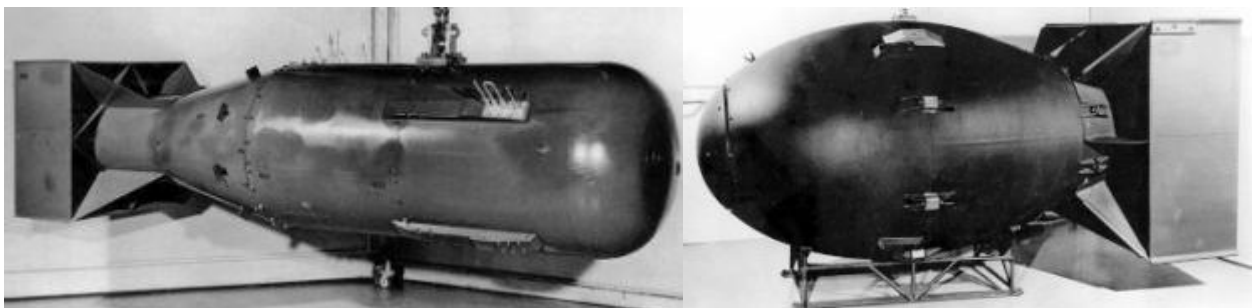


Figure 1.20: Little Man and Fat Boy Atomic Bombs^[58]

Following the demonstration of the capabilities of the atomic bomb in WWII, the U.S. continued the development of these weapon systems to increase the efficiency (and decrease the

size) of these weapons. The first thermonuclear designs (a fusion or hydrogen bomb) were developed in 1953. During this timeframe, nuclear capability was designed to be deployed on strategic bomber platforms such as the B-36, B-47, and B-52 airframes. By the 1960s however, due to the bomber's vulnerability on the ground, the continuous airborne alert system was developed. Due to activities in the Soviet Union and the large cost associated with new strategic bomber platforms, intercontinental ballistic missiles (ICBMs) and submarine-launched ballistic missiles (SLBMs) came to the fore in the 1960s. Development of nuclear-capable bomber platforms continued through the 1990s with more modern designs such as the B-2 Spirit. [57]

The Soviet Union developed its first nuclear weapon in 1949, and this weapon was largely based on the WWII *Fat Man* design. Additional development of these nuclear bombs continued through the 1950s and the first Soviet thermonuclear weapon was tested in 1955. Like the U.S. initial development of nuclear capability, the focus was on deployment on strategic bomber platforms. Unlike the U.S. however, the Soviet Union did not have the advantage of numerous platforms developed for use throughout WWII. Instead, the Tu-95 Bear and 3M Bison were fielded as strategic platforms in 1956. By the end of the 1950s however, the Soviet Union instead turned its focus to ICBMs and SLBMs. Development on strategic bombers did not entirely cease however, and prior to the dissolution of the Soviet Union in 1991, more modern bombers such as the Tu-160 Blackjack had been developed. [57]

Table 1.9 highlights several historic nuclear gravity weapons developed by the United States.

Table 1.9: U.S. Historic Nuclear Bombs

Weapon System	Yield (Kilotons)	Main Bomber Platforms
<i>Little Boy</i> ^[57]	15	B-29
<i>Fat Man</i> ^[57]	~20	B-29
B28 ^[37]	70-1,450	B-52
B53 ^[37]	9,000	B-47, B-52, B-58
B61 ^[37]	10-500	B-52, B-1B
B83 ^[37]	~1,000	B-52, B-1B, F-111A

1.2.3.3 Precision Guided Bombs

Similar to many of the weapon systems discussed in this section, the development of precision guided munitions (PGMs) began with research performed during WWI and WWII. The guided bomb is a subset of this type of munition. The first operational example of a guided bomb fielded was the Azon bomb, a radio controlled bomb implemented in the U.S. Army Air Corps prior to the end of 1944. In the 1960s further development into alternative guidance systems emerged to include laser-guided bombs (LGBs) and television guidance systems. More modern systems developed in the 1990s include satellite-guided weapons, the most popular of which is the Joint Direct Attack Munition (JDAM). This system uses a standard GP bomb such as the Mark series and attaches a guidance kit to the tail to enable accurate targeting. [57]

1.3 U.S. Aerial Engagement Historical Summary

To generate quantitative historical trends for jet based air-to-air combat, official U.S. armed forces victory credits were collected. In addition to the type of aircraft making the kill and the target, the type of weapons used and the engagement environment (such as elevation, airspeed, range, etc.) were recorded where available. From these data, the following charts were established. Note, probable kills are attributed as 0.5 credits and verified damage claims are attributed as 0.25 credits.

An overview of jet aerial victories by aircraft type is presented in Figure 1.21. From this figure, it is readily apparent that the majority of all U.S. jet based aerial victories were achieved by the F-86 Sabre during the conflict in Korea (see Section 1.1.2). Two other items of note are the small number of kills achieved by B-52s and A-10s. These encounters are described in Section 1.1.

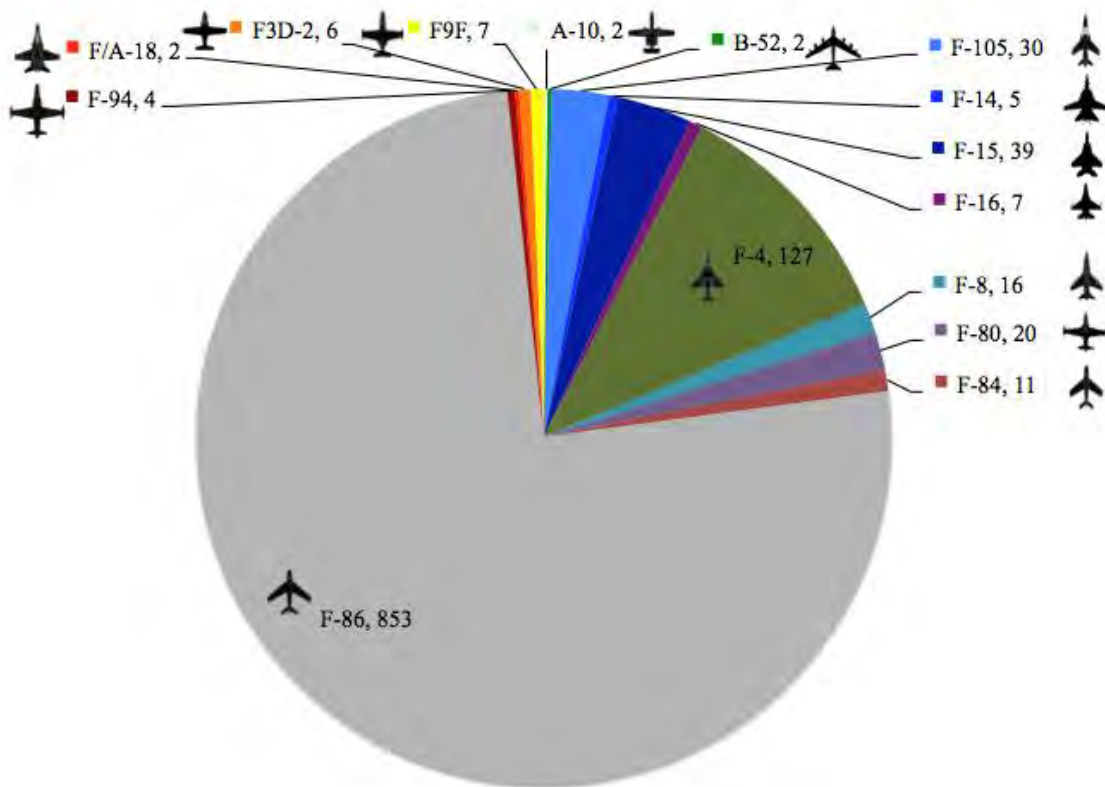


Figure 1.21: U.S. Aerial Victory Credits Achieved Since 1950^{[15], [16], [23], [25]}

Figure 1.22 was compiled to show the evolution of aerial weapons with time. Again, the large number of victories achieved during the Korean War dominates the victories achieved with gunnery. As time progresses, the number of kills achieved by missiles increases dramatically. After the 1960s, gunnery accounted for 35% of all victories recorded. Another important trend that can be gleaned from this chart is the overall decrease in air-to-air victories as time progresses. Early jet engagement scenarios, including short-range dogfighting with limited

capability to sense enemy aircraft at distances beyond visual range, corresponded with increased number of aircraft in the engagements. Later advances in radar and integrated command and control systems as well as increased standoff ranges for weapon systems correspond with fewer aerial victories achieved. This is also an indication of the changing role of aircraft in a given conflict scenario as fewer air-to-air engagements are noted with increasing time.

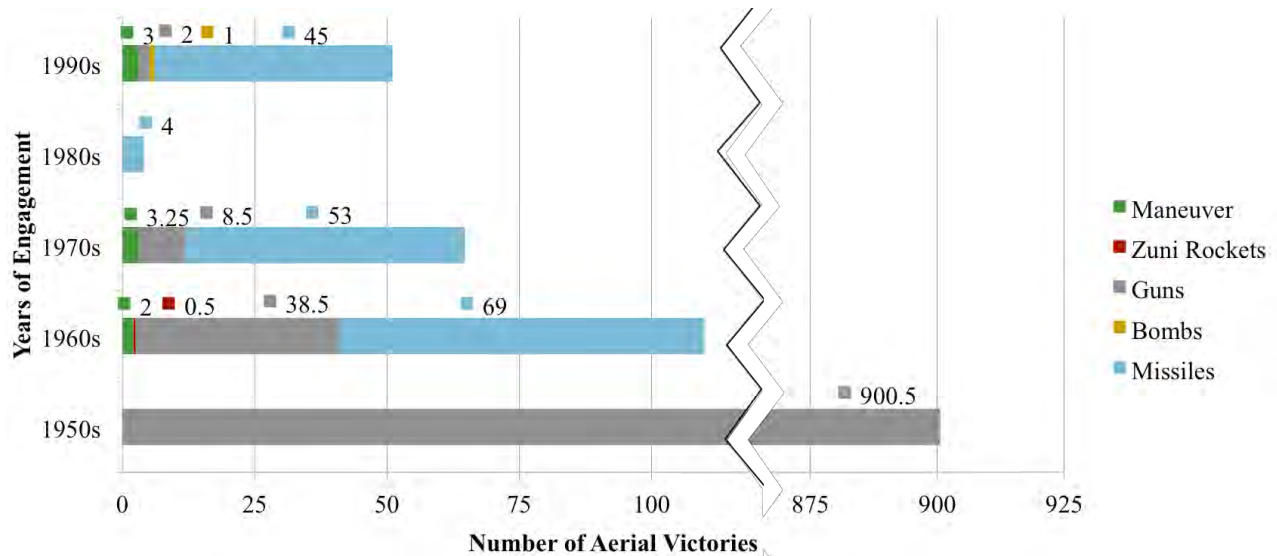


Figure 1.22: Aerial Victories by Weapon Type^{[15], [16], [23], [25]}

Figure 1.23 and Figure 1.24 again demonstrate the changing role of aircraft in engagements in the last 40 years. With the introduction and integration of airborne early warning and control (AEW&C) aircraft and advancements in radar, the ranges for positive identification of hostile aircraft have greatly increased. As a direct result, the capability and demand for increased engagement ranges has pushed the envelope of weapon systems design to nearly exclusively missile-based platforms. This push towards BVR engagement has in turn promoted the development of increasingly stealth conscious aircraft with increased standoff ranges for engagement. Increasingly “smart” missiles that allow for fire-and-forget engagement from stealth fighters have become the new standard when devising aerial engagement scenarios.

Increased airframe design and maintenance costs and expendable weapon system costs have driven the price of aerial fighters ever higher to satisfy these engagement needs.

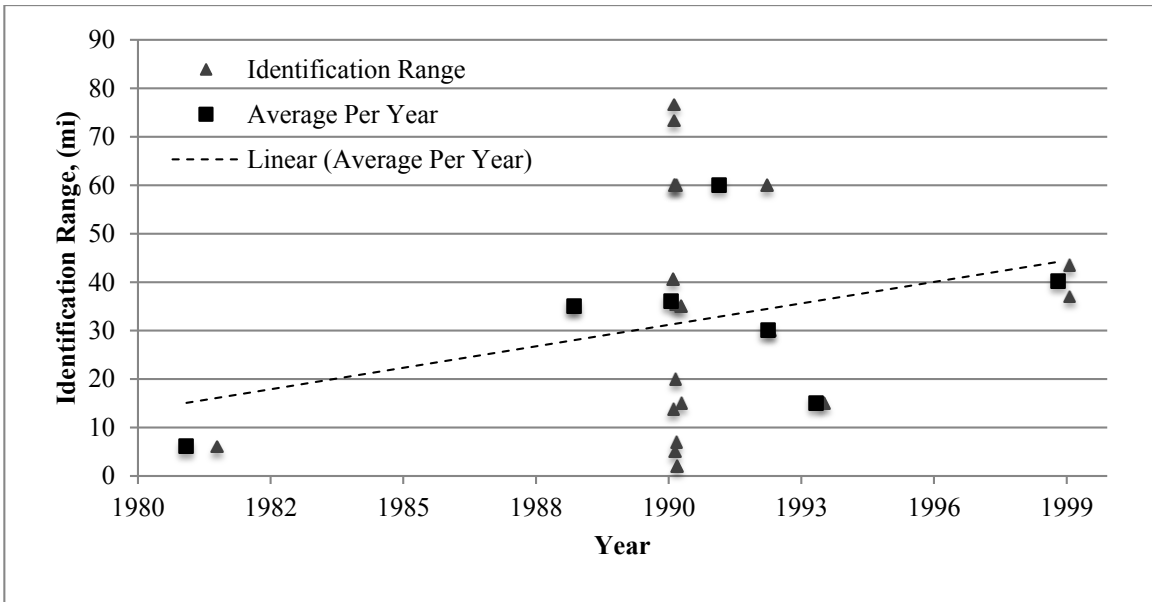


Figure 1.23: Identification Range Trends after 1980^[25]

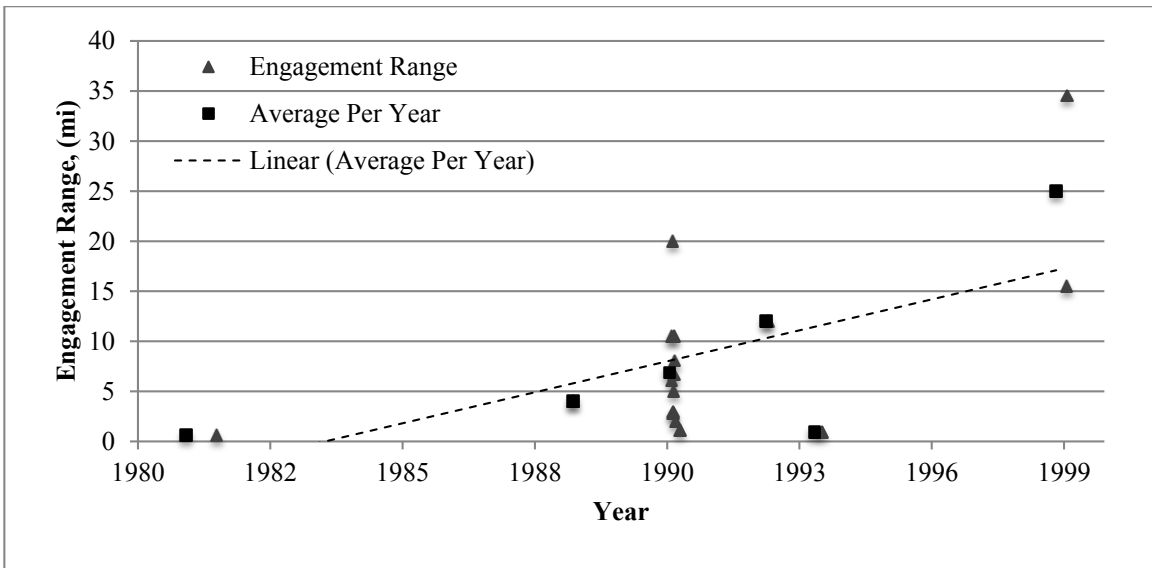


Figure 1.24: Engagement Range Trends after 1980^[25]

1.4 Thesis Motivation and Overview

As demonstrated in this section, aerial fighter platforms have continually moved away from hard-launched munitions with time. Missiles have become the center of air-to-air engagements due to increased targeting accuracy over standard unguided hard-launch alternatives as well as the increased engagement distances they support. Increased engagement distances have been required to support the efforts of the U.S. armed forces to move to BVR combat, precluding the need for traditional dogfight at close range. While missiles do support all of these requirements, their large size (due to the necessity of an on-board, often inefficient, propulsion system) limits their maneuvering capability once launched. Their size also necessitates large internal weapons bays, or if stealth is not a requirement, external hardpoints on the fighter platforms they serve. This thesis serves as a conceptual study to demonstrate the potential of using hard-launched rounds that employ a variety of missile-like guidance and navigation and control techniques for target engagement.

The range of engagement with the employment of guided hard-launch munitions is highly versatile: ranging from several meters to over 100 statute miles. Multiple rounds fired from a single barrel may be used to achieve a high kill probability based upon target type. At close range, standard direct line of fire techniques would be used to guide these munitions while extended ranges necessitate the employment of an indirect guided semi-ballistic trajectory.

Setting aside preconceptions of hard-launch munitions as aerial offensive weapons, it may be noted that these rounds also offer a unique opportunity for aircraft defense. Due to their increased turning capability and smaller size, guided hard-launch munitions provide an opportunity for defensive overmatch superiority on any aerial platform. An aft or forward mounted gun capable of firing smaller caliber guided rounds can support this defensive

requirement. These rounds, launched at high Mach, can effectively outmaneuver inbound surface-to-air or air-to-air missiles (SAM or AAM) or hostile aircraft, and can mitigate these threats with either proximity fuse detonation or kinetic kills. A family of guided munitions may be developed to engage targets equipped with IR, passive RF, and active RF seekers by chambering the rounds specific to the target type.

The application of guided hard-launch munitions on aerial platforms will fundamentally alter the way aerial engagement occurs in the coming decades. Increased targeting versatility and range will preclude the need for missiles in fundamental close and medium range aerial engagement scenarios. Precision air support for ground forces can be provided for at extended range engagement distances. The defensive overmatch potential of these rounds facilitates the acquisition of combat superiority over virtually any force in the air or on the ground. Because of the increased defensive capability of these aerial platforms, stealth requirements may also be relaxed. The risk is greatly decreased for sorties into hostile territory with advanced air defense systems, and the overall versatility of engagement of the aerial platform is greatly enhanced.

1.5 Historical Guided Hard-Launch Round Programs

An overview of several historic guided hard-launch munitions programs is provided in this section along with general performance characteristics.

1.5.1 M712 Copperhead

The Copperhead program was initiated in the 1970s as a “smart” weapon. This 155mm ground based guided munition has a launch weight of approximately 140lb and a maximum range of 12.4 miles [43]. The munition is designed for indirect fire against both stationary and moving hard targets (tanks, armored vehicles, etc.) and is designed to launch from the M109A1/A2/A3, M114A2, and M198 platforms [59].

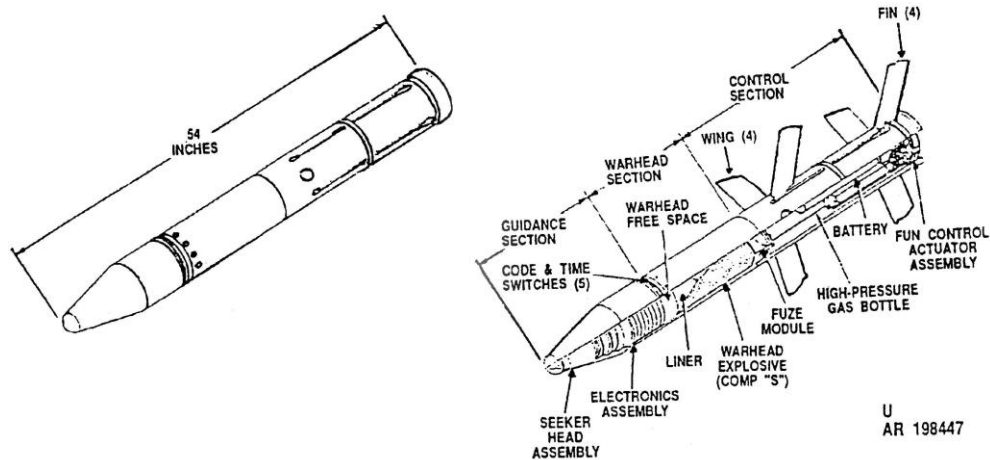


Figure 1.25: M712 Copperhead Projectile^[59]

The aft section of this projectile is designed with a rotating obturator that reduces the spin of the projectile when fired to approximately 10rps. At this angular velocity, the fins are deployed upon leaving the barrel. The munition then proceeds in either a high trajectory ballistic mode or a lower trajectory glide mode towards an established target. At the midpoint of the trajectory, the wings are deployed and active guidance to target begins. [59] The target is illuminated by a laser from an external source and the seeker assembly located in the nose of the projectile then guides the munition to target [43].



Figure 1.26: Copperhead Projectile Demonstration^[60]

1.5.2 Adaptive Guided Munition Programs

The Barrel Launched Adaptive Munition (BLAM) is a conical, guided hard-launch munition developed in 1995. This round utilizes adaptive materials (specifically PZT) to serve as actuators for the guided round. Rather than achieving control authority with the use of conventional fins and canards, the BLAM consists of a forward and aft section connected by a ball joint. The nose of the munition is then pivoted about this joint with the use of the PZT tendons that connect the two sections. The proof of concept model and testing has been completed for this system. [61]

The Hypervelocity Interceptor Test Technology (HITT) was a demonstrator program that focused on a hypersonic interceptor vehicle actuator design. This program ran from 1998 to 2000 and demonstrated that the adaptive actuators were the “quickest fully proportional flight control mechanisms ever built.” [62]

In 1998, the Range-Extended Adaptive Munition (REAM) program was initiated as a small caliber guided round in support of an Army sniper mission. The technology was proven out after design, build, and subsequent testing. Following this program, the Shipborne-Countermeasure Range-Extended Adaptive Munition (SCREAM) was developed as a continuation of the REAM project. In this program, small caliber cannon shells and bullets were designed with adaptive actuators for use against sea-skimming missiles. This program reached Phase II in the Small Business Innovation Research program. The results of the research from these programs were then implemented in the Light Fighter Lethality Adaptive Round (LFLAR) to study subsonic rounds using adaptive flight control mechanisms. [62]

In 2000, the Spike-Controlled Adaptive Round (SCAR) was presented to DARPA as a means of guidance for supersonic projectiles using low control authority. The initial proposal was rejected, but a subsequent proposal received funding [62].

1.5.3 Extended Range Guided Munition (ERGM)

The Extended Range Guided Munition (ERGM) is a 5in diameter guided projectile designed to engage targets between 13 and 54nmi. The 61in long projectile is rocket-assisted once first fired and has a conventional configuration including a set of deployable tail fins and actuated canards. The system relies upon both GPS and INS to guide to target following launch. The tail fins deploy immediately following the launch and the rocket motor boosts the projectile to altitude. The canards then deploy and the GPS system is activated. The program had met with some limited successes alongside numerous technical difficulties prior to its cancellation. [63]

1.5.4 Extreme Accuracy Tasked Ordnance

The Extreme Accuracy Tasked Ordnance (EXACTO) program is an initiative put forth by DARPA for a guided, small caliber sniper bullet. The goal of the program is to advance technologies that would allow for increased sniper effectiveness by increasing the standoff distances and reducing the engagement time. Successful live fire tests had been performed as of 2015, though much of the round design and actuation methods have not been released to the public. [64]

2 Weapon System Outline

This section outlines overall projectile design characteristics, the design of the projectiles themselves, and the concept of operations for this family of guided projectiles. The concept of operations varies based on the type of target and engagement environment.

2.1 Munitions Design

The design of this family of guided projectiles centers around two main factors: the engagement range and target type. While the range of the munition varies largely as a function of firing system, caliber, density, and altitude, the target type will dictate the overall type of munition used. For lightly armored targets, the projectile may act as a means of transport for some form of high explosive. More heavily armored targets will instead call for either a type of shaped charge or kinetic kill system that does not rely solely upon explosives at terminal impact.

[65]

Table 2.1: Sample Projectiles for Various Targets

Target Type	Projectiles
<i>Aerial (Light Armor)</i>	High Explosive (HE) Frangible Flechette
<i>Mobile Ground (Light Armor)</i>	High Explosive (HE) Flechette
<i>Mobile/Stationary Heavily Armored</i>	High Explosive Anti-Tank (HEAT) Explosively Formed Penetrator (EFP) Armor Piercing (AP, APFSDS, APDS)

Frangible and flechette rounds are considered for aerial targets (and mobile targets) as these projectiles are designed to release smaller fragments of metal at high velocity upon detonation. Specifically, these rounds may be used to construct a cone of debris when fired at high Mach to improve the probability of a hit. Flechettes have been historically implemented as

anti-personnel rounds like the 105mm “Beehive” used in the Vietnam War (Figure 2.1). This design allows for several, high velocity metallic darts to be released at high Mach around a particular area target.

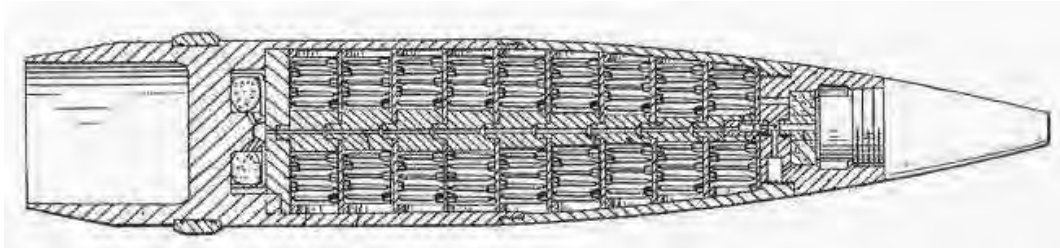


Figure 2.1: 105mm Flechette Projectile "Beehive"^[66]

The PGU-28/B used for the baseline geometry in this study is a Semi-Armor Piercing High Explosive Incendiary (SAPHEI) round. This round is designed to first penetrate the target and then detonate the high explosive; damage is caused by the high velocity fragments generated by the detonation. [67]

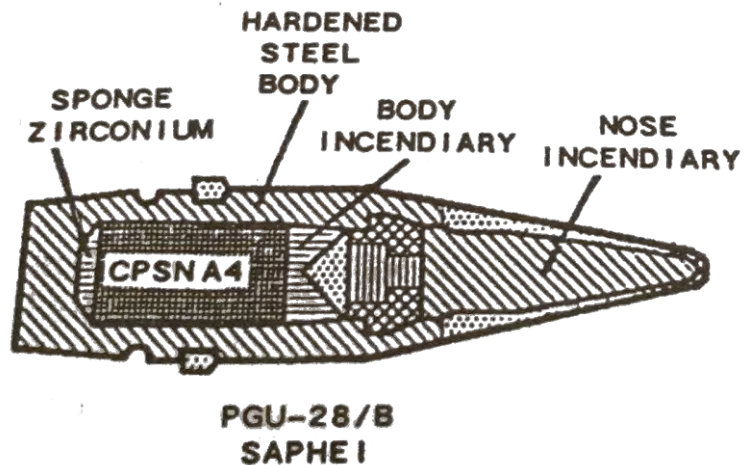


Figure 2.2: PGU-28/B SAPHEI^[67]

2.2 Weapon System Design and Integration

The effectiveness of the overall weapon system implementing guided hard-launch munitions is greatly dependent upon the proper gun integration with the airframe. While existing

gun systems such as the M61 Vulcan and GAU-8/A Avenger may be used to fire these projectiles with obturating bands to despin the projectiles, the performance of the gun may be greatly improved by incorporating a smooth bore design. The rifling standard to the majority of modern aerial gunnery imparts a spin to a projectile to stabilize it, but this rifling not only allows high pressure gasses to escape from behind the bullet, but also uses a significant portion of the firing energy to impart a spin. This leads to a decrease in the overall muzzle velocity of the projectile. A smooth bore muzzle is thus recommended for a future gunnery system design study.

Another important consideration in gun system integration is the location of the barrel and exhaust gasses. As good design practice, these parts of the gun system should be located away and behind any aircraft engine inlets to avoid exhaust and debris ingestion.

As will be further discussed in this study, the number of projectiles required to achieve a high probability of kill for this guided rounds allows for fewer rounds fired per minute. The Gatling style aerial autocannon may then be simplified to a single-barrel weapon system. This simplification will reduce the gun system weight and allow for the potential decrease in airframe weight. The volume required to support the gun system may then also be decreased to allow for more room for additional rounds or other equipment.

The muzzle velocities for this family of projectiles may be further increased by extending the length of the gun barrel. For a specific gun system, the muzzle velocity is roughly linearly dependent upon the muzzle length [68]. An increase in gun barrel length will lead to challenges in implementing these weapons in existing systems, though future airframe development can include longer barrels that are oriented to both the front and back of the aircraft.

In this study, it is assumed that the guided projectiles are fired from existing gun systems onboard US aircraft. Namely, the rounds include obturators to nullify the effect of rifling and do

not include extended length barrels. This assumption will provide a conservative estimate on the projectile capabilities due to the lower muzzle velocities incurred. Larger established systems such as the M102 Howitzer on the AC-130 would likely not see great benefits from a gun system redesign (as this is a single barrel weapon), and all rounds made for this system would include the obturator.

2.3 Concepts of Operations

2.3.1 Defense

The use of guided hard-launch munitions against missile threats is broken out into two categories based upon the type of guidance employed by the target: infrared and radar. An outline of the use of guided munitions against each of these types of targets is given in this section.

2.3.1.1 IR Homing Targets

IR homing missiles pose a unique threat to aircraft in that these weapon systems focus on the IR (heat) signature of the target aircraft. Countermeasures such as flares may be used to attempt to draw the missile off target, though these methods are not always effective. Hard-launch munitions may be used in place of traditional countermeasures to not only draw an IR seeking missile off target, but also to negate the threat entirely.

To effectively draw an IR homing missile off of the target aircraft, the missile seeker must be presented with a stronger thermal signature to lock onto. The missile may be redirected to lock onto the hard-launch munition directly by lining the munition with foil strips to effectively make the entire munition a pyrophoric flare. Upon launch from a rearward or forward barrel, the munition comes into contact with air and automatically ignites the strips on the

exterior of the munition. The bullet, now a directed flare, would then travel at high velocity towards the IR seeking missile. The missile would then ideally lock onto this new target, simplifying the terminal guidance of the bullet to achieve a proximity detonation that would disable the missile. As the munition now serves as the missile target, guidance would no longer be required and the munition is simply a high velocity directed flare.



Figure 2.3: Rocket Munition Concept⁶⁹¹

A second means of countering an IR homing missile is to equip the hard launch munition with an under-expanded rocket propulsion system. With an under-expanded propulsion system, the munition would generate shear layer boundaries well outside of the nozzle; this generates a large IR signature to present as a decoy to the missile seeker. The rocket propulsion system would also have the added benefit of increasing the closing velocity between the munition and

missile when fired from the aft section of an aircraft. As before, with the munition now serving as the decoy missile target, guidance would no longer be necessary to achieve a proximity or kinetic detonation to disable the missile.

2.3.1.2 RF Homing Targets

When engaging RF homing targets (either active or passive), the munition guidance problem is broken into two separate phases: gross target maneuvering and terminal guidance. In the first phase, the munition is set along a trajectory to intercept and fly up the flight path of the inbound missile. This gross maneuver will be a high-g, low-bandwidth maneuver that will size the control surfaces of the munition. The second guidance phase involves fine pointing while flying up the flight path of the missile. This low-g, high-bandwidth maneuvering is required to account for high frequency flight modes in the munition and missile (short-period/nutation) as well as atmospheric gusting that will be present at any altitude or flight condition.

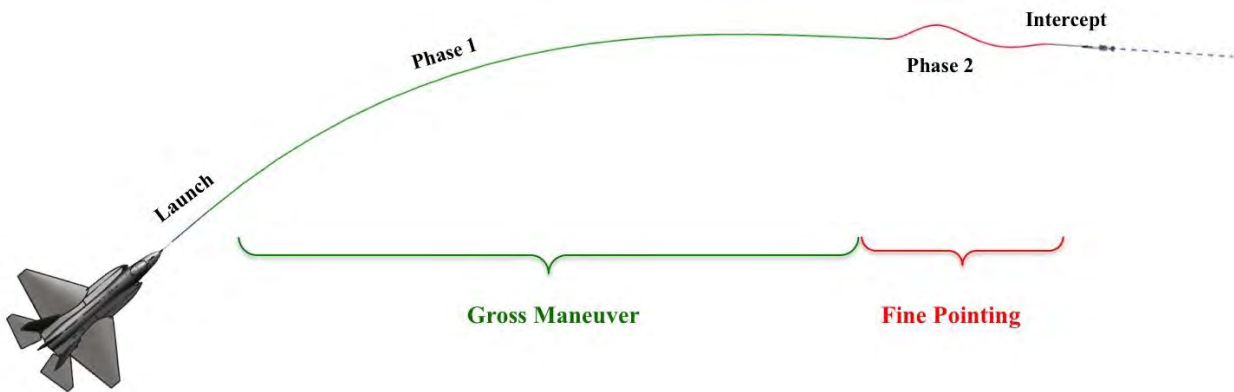


Figure 2.4: RF Target Guidance Phases

Commands will be sent over a VHF command link from the aircraft to the munition to simplify the complexity and cost of the munitions. For an active RF seeking missile, the aircraft would lock onto the seeking signal of the missile and then direct the munition along this path. Passive seeking RF missiles (using an external radar for guidance) would be engaged simply by

tracking the RF signature of the missile itself from the aircraft. In each scenario, both gross maneuvering and fine pointing guidance would be required to achieve a close proximity detonation to disable the missile.



Figure 2.5: RF Target Defense Concept^[70]

2.3.2 Interdiction

2.3.2.1 Air-to-Air Combat

In aerial combat, the guided munitions would be implemented in a manner similar to engagements with RF seeking missiles (as discussed in Section 2.3.1.2). Guidance would be achieved in two stages with commands sent from the aircraft over a VHF command link. Several guided munitions would be required to achieve a kill for most aircraft. The number of rounds required to achieve a required percent kill probability would be fired and guided to target along

the flight trajectory of the target aircraft. For beyond visual range combat, the munitions would be fired along a semi-ballistic trajectory and then guided to target.

2.3.2.2 Air-to-Ground Combat

To engage ground targets, a different type of round may be required. For heavily armored targets, guided explosively formed penetrators would be used to engage targets after an indirect fire trajectory. Several rounds may be required to achieve a required percent kill probability for a specific target. The aircraft would guide the rounds over a VHF command link, or at extended ranges, a GPS guidance system may be implemented.

3 Analytic and Computational Tools

In this section, the tools used to analyze the projectile capabilities are outlined. The theoretical approaches used as well as the computational models are described in detail.

3.1 Baseline Geometry

For the purposes of this study, a projectile geometry similar to the configuration of the PGU-28 (currently used by U.S. fixed wing aircraft) is used as a baseline. The G7 standard geometry was thus assumed and scaled for all projectiles in this study.

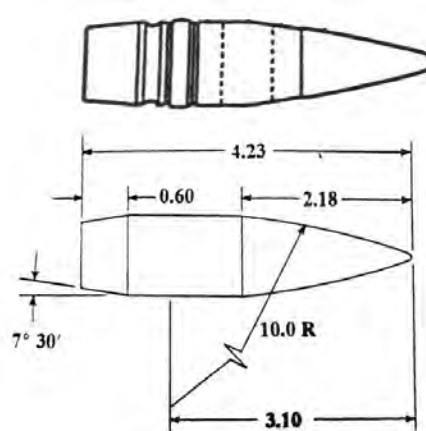


Figure 3.1: PGU-28/B versus G7 Standard^{[71], [67]}

3.2 Aerodynamics

Two standard coordinate systems were used in this analysis: body-fixed and earth-fixed. Each of these coordinate systems and the positive moment directions are denoted in Figure 3.2.

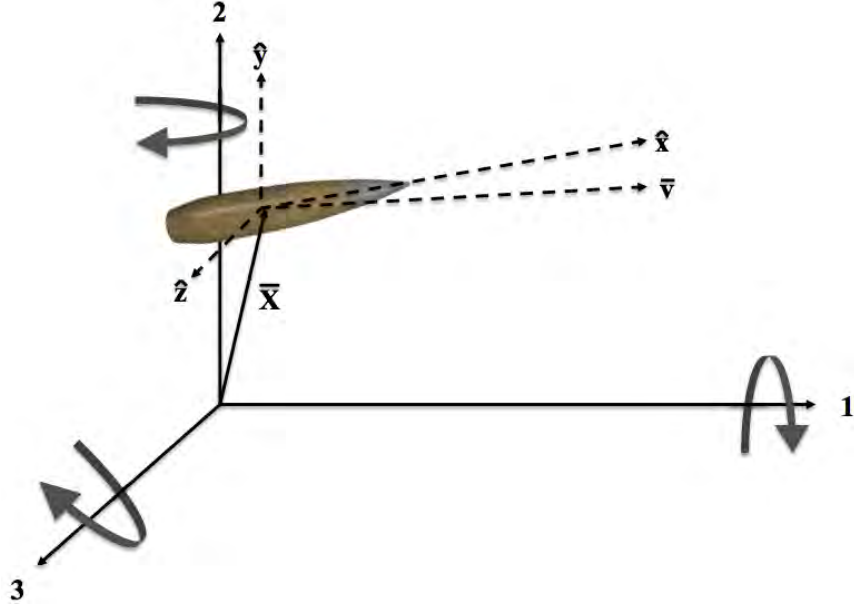


Figure 3.2: Coordinate System Convention

The aerodynamic model was solved in the global coordinate system using the methods found in Reference [71]. The general equations of motion may be derived with the application of Newton's Second Law to the projectile displayed in Figure 3.2. Surface and volume integrals are denoted with S and Ψ respectively.

$$\frac{d}{dt} \int_{\Psi} \rho_{body} \frac{d\bar{X}}{dt} d\Psi = \int_S \bar{F} ds + \int_{\Psi} \rho_{body} \bar{g} d\Psi \quad (\text{Eq. 3.1})$$

$$\frac{d}{dt} \int_{\Psi} \bar{X} \times \rho_{body} \frac{d\bar{X}}{dt} d\Psi = \int_S \bar{X} \times \bar{F} ds + \int_{\Psi} \bar{X} \times \rho_{body} \bar{g} d\Psi \quad (\text{Eq. 3.2})$$

The total forces and moments acting on the projectile are rewritten for clarity. The time differential of the position vector is rewritten as velocity \bar{V} , and the time differential of the total angular momentum of the body is denoted as \bar{H} . Assuming that the mass of the projectile is constant in time, the following equations of motion are obtained.

$$\mathbf{m} \frac{d\bar{\mathbf{v}}}{dt} = \mathbf{m}\bar{\mathbf{g}} + \bar{\mathbf{F}}_{aerodynamic} \quad (\text{Eq. 3.3})$$

$$\frac{d\bar{\mathbf{H}}}{dt} = \bar{\mathbf{M}}_{aerodynamic} \quad (\text{Eq. 3.4})$$

As the projectile is assumed to be axisymmetric about the axis of rotation ($\hat{\mathbf{x}}$), the perpendicular moments of inertia are equal and the total vector angular momentum may be written:

$$\bar{\mathbf{H}} = I_x \mathbf{p} \hat{\mathbf{x}} + I_y \left(\hat{\mathbf{x}} \times \frac{d\hat{\mathbf{x}}}{dt} \right) \quad (\text{Eq. 3.5})$$

The transverse angular velocities (P, Q, and R) are represented by $\frac{d\hat{\mathbf{x}}}{dt}$. Dividing both sides of the equation by the perpendicular moment of inertia and taking the derivative with respect to time, the differential vector equation governing the angular motion of the projectile may be expressed.

$$\frac{d\bar{\mathbf{h}}}{dt} = \left(\frac{I_x}{I_y} \right) \mathbf{p} \frac{d\hat{\mathbf{x}}}{dt} + \left(\frac{I_x}{I_y} \right) \left(\frac{d\mathbf{p}}{dt} \right) \hat{\mathbf{x}} + \left(\hat{\mathbf{x}} \times \frac{d^2\hat{\mathbf{x}}}{dt^2} \right) \quad (\text{Eq. 3.6})$$

3.2.1 Aerodynamic Forces

In addition to the external forces noted in this section, a gravitational force is also experienced by the round and is included in the final equilibrium equations. For this conceptual study, it is assumed that all projectiles are de-spun and no internal propulsion is inherent to the projectile. The mass of the projectile is assumed constant along the flight path.

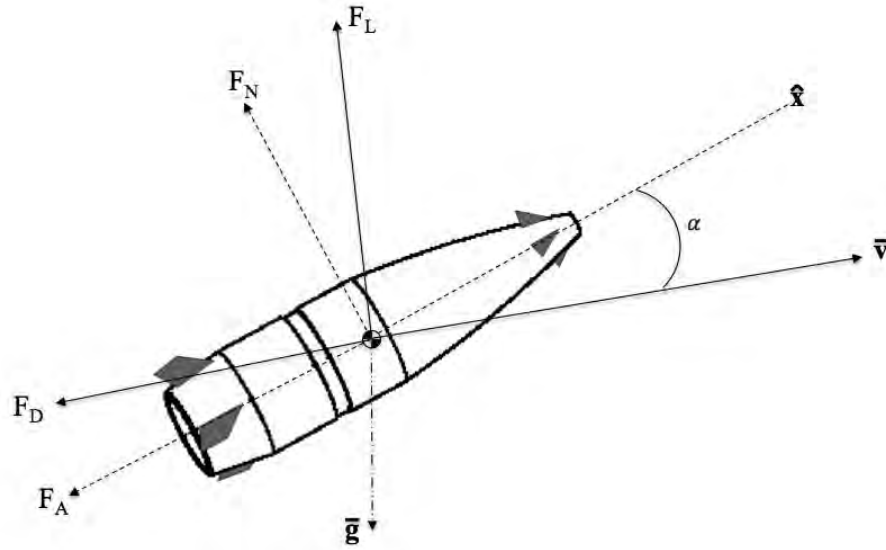


Figure 3.3: Forces acting on Projectile and Nomenclature

3.2.1.1 Lift Force

The total lift force acting on the projectile in the global coordinate system, positive along the 2-axis, was generated using the component build up method. The total lift force may be expressed as:

$$\bar{F}_L = -\frac{1}{2}\rho SC_{L\alpha}[\bar{V} \times (\hat{x} \times \bar{V})] \quad (\text{Eq. 3.7})$$

Rewriting the vector cross product terms using vector algebra, the simplified lift force expression may be written.

$$\bar{F}_L = \frac{1}{2}\rho SC_{L\alpha}[V^2\hat{x} - (\bar{V} \cdot \hat{x})\bar{V}] \quad (\text{Eq. 3.8})$$

Where:

ρ – Density at altitude

V – Magnitude of velocity with respect to freestream

\hat{x} – Unit vector along body x-axis

\bar{V} – Velocity vector with respect to freestream

Projectile Body

The normal force acting on the projectile body was approximated as a function of Mach and geometry. For supersonic Mach, the normal force coefficient was found using Reference [72] for cylindrical bodies. Note, this reference focuses primarily upon blunt bodies with a higher fineness ratio, though this method is still used as an approximation for this study. Subsonic body normal force coefficient was approximated with the Sierra International .308” bullet as slender body theory is less applicable at low fineness ratios due to nose bluntness effects [72]. The normal force coefficient on the body may be expressed as follows.

$$C_N = C_{N_{\alpha body}}(\alpha) + \eta C_{Dc} \left(\frac{L}{S}\right) \sin^2(\alpha) \quad (\text{Eq. 3.9})$$

The second term in this expression accounts for the increase in crossflow drag generated by the portion of the projectile body exposed to the wind at increasing angles of attack. This effect is more pronounced for blunt bodies with small nose radius to diameter ratio [72]. As such, this term is neglected for the projectiles studied assuming the geometry shown in Figure 3.1 and small angles of attack.

Fins and Canards

For supersonic and transonic speeds, the normal force contributed by the lifting surfaces was generated by interpolating the plots given in Reference [72]. It is assumed for this study that the thickness to chord ratio of all surfaces is 0.1. At subsonic speeds, the normal force coefficient of a surface is given by Reference [72]:

$$C_{N_{\alpha surface}} = AR \left(\frac{2\pi}{2 + [AR^2(\beta^2 + \tan(\Lambda_c/2)) + 4]^{\frac{1}{2}}} \right) \quad (\text{Eq. 3.10})$$

Total

The normal force coefficients for the body, tail, and canards were tabulated separately in the body coordinate system, transposed into the global coordinate system, and then combined as a function of the reference areas for each of these components as described in Reference [71].

$$\begin{aligned} C_N = & C_{N_{\alpha_{body}}} \alpha + C_{N_{\alpha_t}} \alpha K_f \eta_t (K_{f(b)} + K_{b(f)}) \eta_{t(b)} \dots \\ & + C_{N_{\alpha_c}} \alpha K_c \eta_c (K_{c(b)} + K_{b(c)}) \eta_{c(b)} + \eta C_{D_{cross}} \frac{A_p}{S_{ref}} \sin^2 \alpha \end{aligned} \quad (\text{Eq. 3.11})$$

Where:

C_N – Normal Force Coefficient

α – Angle of Attack (relative to freestream)

$K_{i(j)}$ – Fin/body interference factors (i on j)

η – Ratio of reference areas (S)

For small angles of attack, the cross flow component is assumed to be negligible, thus the last term may be ignored. Note, for actuated control surfaces, this equation will still hold with the exception that the effective angle of attack is now the sum of the freestream alpha and the control surface deflection.

The normal force coefficient as a function of alpha is approximated by dividing C_N by alpha to obtain C_{N_α} . This is then rotated back into the global coordinate space to generate C_{L_α} , as shown in Equation 3.8.

Center of Pressure

The center of pressure (CP) is a spatial location on the projectile through which the aerodynamic force vectors generated by pressure may be assumed to act. The displacement of this point from the center of gravity (CG) of the projectile will yield an overturning moment as

discussed in the subsequent sections. At subsonic speeds, the center of pressure of the projectile body is assumed to be a function of geometry alone and is approximated using Reference [72]. This same reference was also used to approximate the center of pressure of the projectile body for supersonic and transonic speeds, where the location of the CP is a function of both Mach and geometry. The center of pressure of the fins may be approximated as at half of the mean geometric chord for supersonic speeds, and one quarter of the mean geometric chord at subsonic speeds. At subsonic speeds, the center of pressure of the projectile body is approximated based on the center of pressure of the Sierra .308” bullet found in Reference [71].

3.2.1.2 Drag Force

Body

The drag coefficient of the projectile body may be broken down into a zero lift component (C_{D0}), and a nonlinear term dependent upon the total angle between the velocity vector and the body x axis, α_t [71].

$$C_D = C_{D0} + C_{D\alpha} \alpha_t^2 \quad (\text{Eq. 3.12})$$

$$\alpha_t = \sqrt{(\sin^2 \alpha \cos^2 \beta + \sin^2 \beta)} \quad (\text{Eq. 3.13})$$

Where:

C_D = drag coefficient

α_t = total angle of attack

α = angle of attack

β = yaw angle

For the purposes of this conceptual study, the C_{D0} of the projectile body is modeled after the drag curves of the 20mm PGU-28 round shown in Figure 3.1. This drag model is juxtaposed

with other projectiles of note: the 105mm M1 round, and 7.82mm 168 Grain Sierra International bullet.

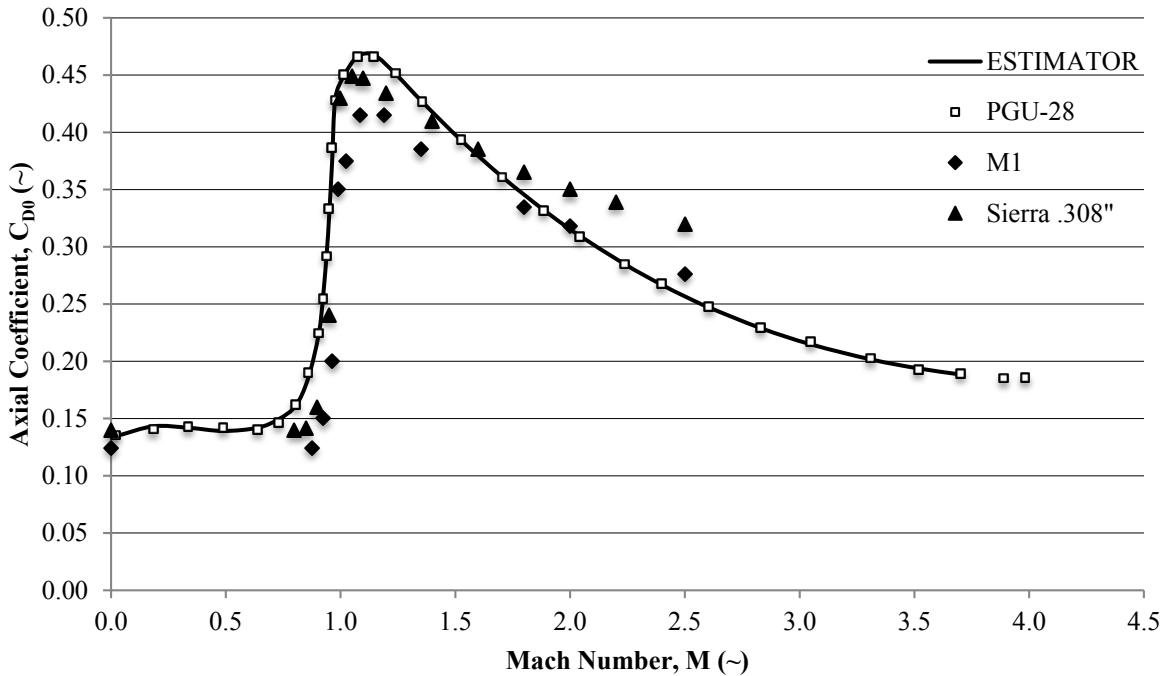


Figure 3.4: Zero Angle of Attack Drag Coefficient Approximation^[71]

The nonlinear drag coefficient term was approximated from the data given in Reference [71] for the Sierra .308” round.

Fins and Canards

For the preliminary analysis performed in this study, the drag increment caused by the addition of fins or canards on the projectile at zero angle of attack was assumed to be zero with linearized supersonic flow theory. While this is not physical, an increment in drag was generated with an angle of attack by translating the lift force generated by the fins into its components along the body axes. The total drag force experienced by the projectile may then be expressed as follows:

$$\mathbf{F}_D = -\frac{1}{2}\rho S C_D \bar{V}V \quad (\text{Eq. 3.14})$$

3.2.1.3 Pitch Damping Force

According to Reference [71], the pitch damping force is generally much smaller than the force acting in the normal direction on a projectile. This force is thus neglected in this study, though the pitch damping moment will be included for dynamic stability.

3.2.1.4 Magnus Force

As noted previously, the projectiles in this conceptual study are despun. As such, the force generated by the pressure differential on the sides of a spinning projectile, the magnus force, is assumed to be negligible.

3.2.2 Aerodynamic Moments

3.2.2.1 Spin Damping Moment

For the purposes of this study, guided projectiles are not spin stabilized. Instead, combinations of movable fins and or canards are used to both guide and stabilize the rounds. As such, it is assumed that all rounds are despun with the use of an obturator. For verification against known time of flight and trajectory models, the spin damping moment coefficient (C_{lp}) of spin-stabilized projectiles is modeled after the .308 Sierra International Bullet data found in Reference [71].

3.2.2.2 Pitch Damping Moment

The pitch damping moment derivative (C_{Mq}) is generated by two separate phenomena: the total transverse angular velocity, q_t , and the time rate of change of total angle of attack, $\dot{\alpha}$. A positive coefficient tends to increase the pitch angle (unsteady), therefore it is desired for this

coefficient to be negative for stability. The pitch damping moment coefficient for this study is estimated from the .308 Sierra International Bullet in Reference [71]. The total pitch damping moment is given in Equation 3.15.

$$\mathbf{M}_q = \frac{1}{2} \rho V S d^2 C_{M_q} \left(\hat{\mathbf{x}} \times \frac{d\hat{\mathbf{x}}}{dt} \right) \quad (\text{Eq. 3.15})$$

3.2.2.3 Pitching and Yawing Moment

The total pitching moment of the projectile is approximated using the component build up method that parallels the methodology used to determine the coefficient of lift. Each lifting component will generate a moment about a reference on the projectile unless the lifting vector is acting through the reference. The pitching moment, for example, is caused by the lift from the tail, canard, and body and their respective displacements from the center of gravity. The moment generated by a component is the product of the lifting force and the distance from the center of gravity. Each of these moment components are then summed as outlined in Reference [72]. The pitching moment coefficient about the center of gravity is given in Equation 3.16.

$$\begin{aligned} C_{M_{CG}} = & C_{N_{\alpha_{body}}} \alpha * l_{body} + C_{N_{\alpha_t}} \alpha K_f \eta_t (K_{f(b)} + K_{b(f)}) \eta_{t(b)} * l_t + \\ & C_{N_{\alpha_c}} \alpha K_c \eta_c (K_{c(b)} + K_{b(c)}) \eta_{c(b)} * l_c \end{aligned} \quad (\text{Eq. 3.16})$$

It is important to note that the sign of the distance term (l) determines if a positive or negative pitching moment is encountered. This distance term is measured positive from the center of gravity location to the center of pressure. Thus, a standard tail configuration yields a negative l and negative pitching moment coefficient. To have a stable response, the pitching moment coefficient should be negative. The total pitching moment is given in the equation below.

$$\mathbf{M}_{\alpha_{CG}} = \frac{1}{2} \rho S d V C_M (\bar{\mathbf{V}} \times \hat{\mathbf{x}}) \quad (\text{Eq. 3.17})$$

This methodology may also be used to determine the yawing moment of the projectile. As the fins and canards on the body are assumed to represent a radially symmetric, 4-surface system, the yawing moment coefficient magnitude is identical to the pitching moment coefficient and the total yawing moment may be expressed in the following equation.

$$\mathbf{N}_{\beta_{CG}} = \frac{1}{2} \rho S d C_M (\bar{\mathbf{V}} \times (\bar{\mathbf{V}} \times \hat{\mathbf{x}})) \quad (\text{Eq. 3.18})$$

3.2.2.4 Rolling Moment

The rolling moment caused by fin deflection may be calculated similarly to the pitch and yawing moment with one exception. The effective moment arm, instead of representing the distance between the surface AC and the CG of the projectile along the body x-axis, is now defined as the distance between the aerodynamic center deflection surface and the body centerline (assuming a symmetric projectile).

3.2.2.5 Magnus Moment

As stated previously, rounds in this study are despun and fin/canard stabilized. As such, the magnus moment may be neglected in this study.

3.2.3 Equations of Motion

Solving for the free-body diagram of the projectile, the equations of motion may be generated by combining the non-negligible forces and moments described in the previous sections.

$$\frac{d\bar{\mathbf{V}}}{dt} = -\frac{\rho V S C_D}{2m} \bar{\mathbf{V}} + \frac{\rho S C_{L\alpha}}{2m} (V^2 \hat{\mathbf{x}} - (\bar{\mathbf{V}} \cdot \hat{\mathbf{x}}) \bar{\mathbf{V}}) + \bar{\mathbf{g}} \quad (\text{Eq. 3.19})$$

$$\frac{d\bar{\mathbf{h}}}{dt} = \frac{\rho V S d^2 C_{lp}}{2I_y} (\bar{\mathbf{h}} \cdot \hat{\mathbf{x}}) \hat{\mathbf{x}} + \frac{\rho V^2 S d \delta_F C_{l\delta}}{2I_y} \hat{\mathbf{x}} + \frac{\rho V S d C_{M\alpha}}{2I_y} (\bar{\mathbf{V}} \times \hat{\mathbf{x}}) \dots$$

$$+ \frac{\rho V S d^2 C_{Mq}}{2I_y} (\bar{\mathbf{h}} - (\bar{\mathbf{h}} \cdot \hat{\mathbf{x}})\hat{\mathbf{x}}) \quad (\text{Eq. 3.20})$$

3.3 Computational Methods

Equations 3.19 and 3.20 represent the six-degree of freedom model of the exterior ballistics flight of the projectile. These six equations were solved simultaneously using MATLAB for a fixed time interval using the classical fourth-order Runge-Kutta solving scheme as denoted below.

for $\dot{\mathbf{y}} = \mathbf{f}(t, \mathbf{y})$ with $\mathbf{y}(t_0) = \mathbf{y}_0$ and step size h at iteration n :

$$\mathbf{k}_1 = \mathbf{f}(t_n, \mathbf{y}_n);$$

$$\mathbf{k}_2 = \mathbf{f}\left(t_n + \frac{h}{2}, \mathbf{y}_n + \frac{h}{2}\mathbf{k}_1\right);$$

$$\mathbf{k}_3 = \mathbf{f}\left(t_n + \frac{h}{2}, \mathbf{y}_n + \frac{h}{2}\mathbf{k}_2\right);$$

$$\mathbf{k}_4 = \mathbf{f}(t_n + h, \mathbf{y}_n + h\mathbf{k}_3);$$

$$t_{n+1} = t_n + h;$$

$$\mathbf{y}_{n+1} = \mathbf{y}_n + \frac{h}{6}(\mathbf{k}_1 + 2\mathbf{k}_2 + 2\mathbf{k}_3 + \mathbf{k}_4) \quad (\text{Eq. 3.21})$$

The new state at each time step was estimated such that the force and moment coefficients as well as state variables were updated for each time in the solver. The full program is attached in Appendix A: Source Code.

3.4 Model Validation

In order to validate the aerodynamic and computational model, the time of flight (TOF) per range data is compared to Reference [67]. The aerodynamic drag coefficient is also juxtaposed with that of the PGU-28 in Figure 3.4. As demonstrated, the computational range and time of flight data for this projectile matches that obtained from experimental data.

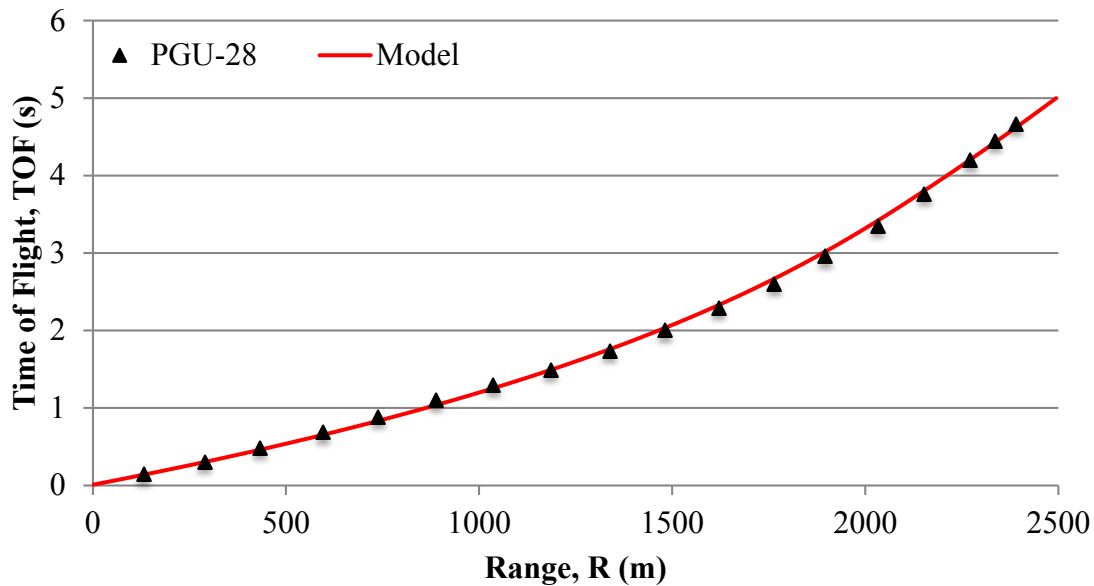


Figure 3.5: Time of Flight Model Validation^[67]

3.5 Design Parameters

The overall design parameters necessary and achievable by a generalized family of guided hard-launch munitions when applied to aerial platforms is discussed in this Section. Design parameters such as the range, lethality, control authority, guidance navigation and controls, and cost estimations are outlined.

3.5.1 Range

The maximum range for the baseline projectile geometry (excluding fins and canards) was determined using a variety of calibers. The simulated trajectories were determined using the computational methods described above for each of these calibers at an elevation of 15,000m, elevation angle of 45 degrees, and firing energy of a GAU-8/A gun system. The muzzle velocity for each round was determined by calculating the kinetic energy of the standard 30mm round used by the GAU-8/A fired at 1010m/s, and then solving for the muzzle velocity of a round of a certain size using the same kinetic energy as shown below. It is assumed that there is zero relative airspeed; projectiles are fired from a stationary point in space.

$$V_{muzzle} = \sqrt{\frac{2}{m} E_{gun}} \quad (\text{Eq. 3.22})$$

$$E_{gun} = \frac{1}{2} m V_{muzzle}^2$$

The ranges and impact Mach numbers of each of the rounds are compared in Figure 3.6. Note, the material (and by extension, density) of each of these rounds was also adjusted and substituted into Eq. 3.22 to study the effects of different materials on the maximum range of a projectile. The ranges and velocities shown are included to show general trends in caliber and density only. Actual maximum ranges will be determined based upon the projectile configuration (including movable surfaces), aerial platform, and gun system used. Although it is not physically possible to fire some of these rounds from the GAU-8/A system, the muzzle energy was maintained across the rounds studied to discount the variation in range due to the firing system.

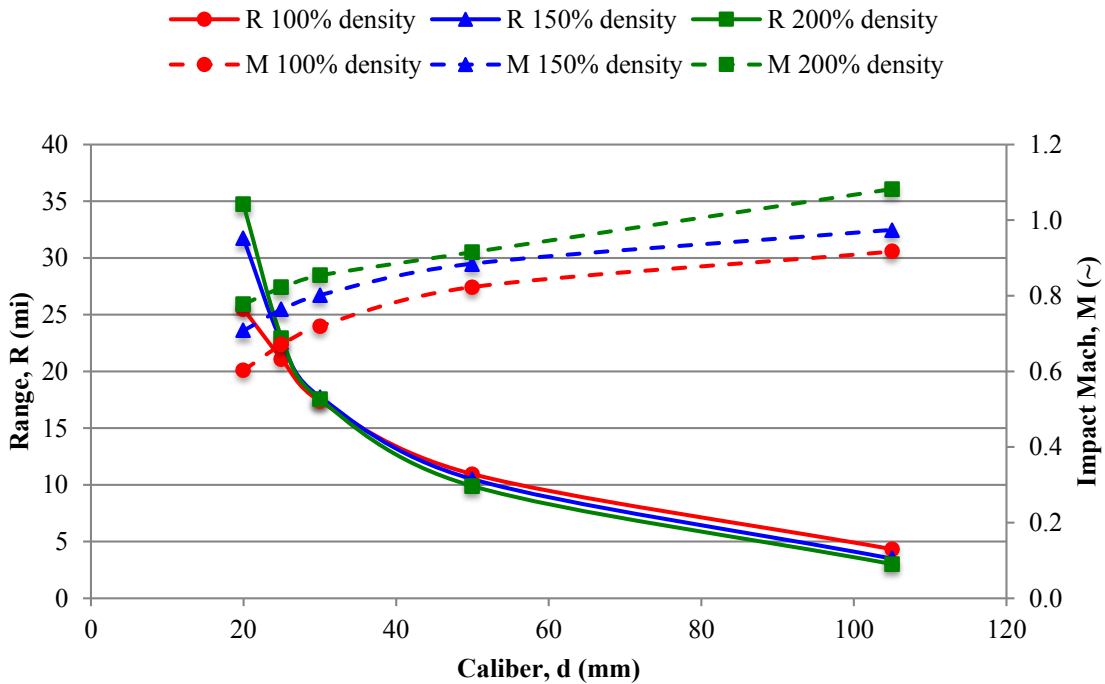


Figure 3.6: Projectile Density Study when Fired from GAU-8/A

As demonstrated in Figure 3.6, the standard hard-launch munition may only be used in medium range engagements. To increase the range of these projectiles and allow for clearance of control surfaces inside the gun muzzle, each of these rounds will include a sabot. By decreasing the diameter of the rounds, the same energy is imparted to a round of smaller mass and diameter, greatly increasing the muzzle velocity and range of the projectile. Increasing the density of these rounds to incorporate tungsten flechettes (for use against aerial targets) does have a slightly negative impact on the overall range of the projectile, but may greatly increase the lethality of the rounds. The generalized effects of decreasing the diameter of the projectile launched from a given barrel size is demonstrated in Figure 3.7 for three systems: the M61 Vulcan, the GAU-8/A (implemented on the A-10), and the M102 Howitzer (used on the AC-130). These simulations were conducted in standard atmosphere at elevations of 1,500m and 15,000m and an initial muzzle angle of 45 degrees.

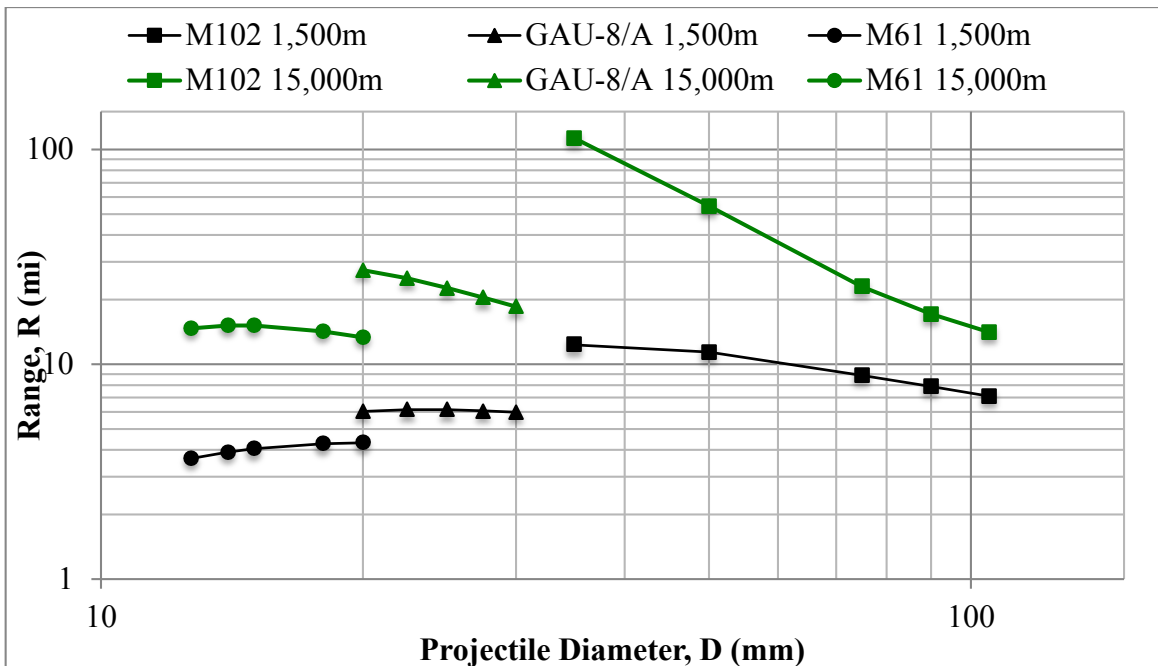


Figure 3.7: Sabot Projectile Range Study

Figure 3.7 yields an interesting result. For large projectiles (such as the 105mm mortar rounds fired from the M102), it would appear that the relation between the sabot size and the range of the projectile is approximately linear. When observing the trends for smaller gunnery systems such as the 30mm GAU-8 and 20mm M61, it is clear that the relation between the projectile diameter and range is nearly quadratic with a defined maximum. The current maximum for each system studied, defining the optimal projectile size design for range at these conditions, appears to occur between 10mm and 25mm. As anticipated, with increasing altitude, the overall range of the projectiles increases due to the rarified atmosphere. However, it would also appear that the curves shift to the left as well. In order to increase the range of these munitions, aircraft must engage targets at a high altitude. The author wishes to note that this simulation does not include hypersonic aerodynamics, which is encountered in many of the highly sabot rounds in this study. These simulations are also conducted to demonstrate general trends only as the projectile configuration (including stabilization) will greatly impact the range of the projectile.

Example systems using sabot rounds and high-density projectiles are given below for several existing US armed forces platforms. As before, each of these simulations do not include control surfaces and use only the G7 geometry to generate a baseline for range potential; these simulations thus represent a maximum case scenario. Each simulation was fired at 15,000 m with an elevation angle of 45 degrees and 150% density. Note, for larger caliber munitions, this result may not be physical due to airframe limitations.

Table 3.1: Sample Gunnery Systems with Sabot Rounds

Weapon System	Standard Caliber / Sabot Caliber (mm)	Maximum Range (mi)	Muzzle Velocity / Impact Velocity (M)
<i>M61 Vulcan</i> ^[37]	20 / 12.7	20.6	5.62 / 0.577
<i>GAU-8/A Avenger</i> ^[37]	30 / 20	35.2	5.39 / 0.708
<i>M102 Howitzer</i> ^[42]	105 / 50	50.2	3.97 / 0.884

Additional increases in range may be achieved by varying the geometry of the rounds or with the addition of a propulsion system: effectively creating a family of rocket assisted projectiles (RAP). For extended ranges, some form of limited propulsion system may be investigated to maintain a high degree of control authority at low flight speeds encountered at the apogee of the projectile and at the terminal guidance phase. A sample Mach profile for a long range projectile is given to demonstrate how the velocity of the projectile varies along a standard ballistic flight path. The projectile tested is fired from a M102 Howitzer.

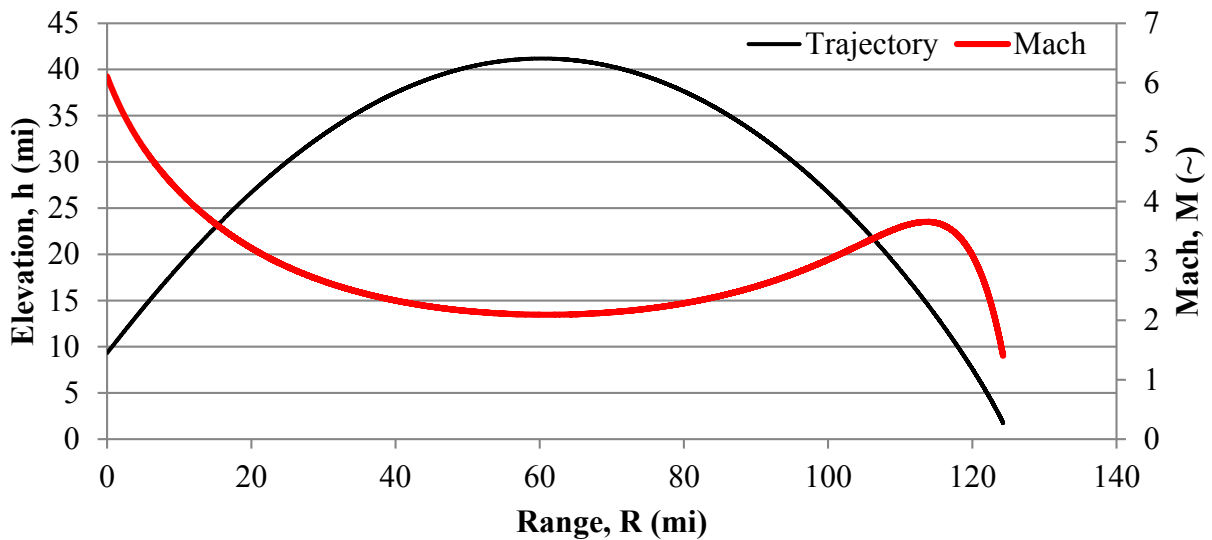


Figure 3.8: Trajectory and Mach Relation for Extended Ranges

The reader is asked to note that the observations given in this section are to be viewed as a baseline trend for projectiles. As may be noted in Section 3.2, hypersonic aerodynamics are not

incorporated into the computational model though the muzzle velocities of the sabot rounds merit further study into this flight regime.

3.5.2 Lethality

To determine the lethality of the projectiles, two kill scenarios were considered: a kinetic kill where projectiles directly impact the target, and a distance kill where a proximity fuse detonates the projectile at some distance from the target.

3.5.2.1 Kinetic Kill

The required number of projectiles to negate a particular threat is based upon the probability of kill for a PGU-28 series munition. As outlined in the concepts of operation, when engaging a target, the round is designed to fly up the flight path of the target, resulting in a front impact. For a PGU-28, the probability of a kill given a hit from the front for a single round engaging a target with wet wings, light armor, and redundant flight controls is 0.10 [67]. It is then assumed that the lethality of the projectile increases with decreasing target size (mass). The probability of a kill given a hit for a particular target is then scaled to the relative mass of the engaging projectile and intended target. It is also assumed that there is no fundamental difference in engagement effectiveness between a missile and an aircraft when normalized for mass. For the purposes of this study, it is assumed that the 0.1 P_k corresponds to the PGU-28 targeting a loaded Su-35 (~25,000kg). The number of projectiles to achieve a certain kill probability (P_k) may then be expressed as shown in Eq. 3.23. The probability of a kill given a hit for the projectile against a particular type of target is expressed in Eq. 3.24. Note, if the $P_{k, \text{projectile}}$ is greater than 1, this result is not physical, but represents a very high kill probability when given a hit.

$$N = \frac{\ln(1-P_{k,desired})}{\ln(1-P_{k,projectile})} \quad (\text{Eq. 3.23})$$

$$P_{k,projectile} = 0.1 * \left(\frac{25,000kg}{m_{target}} \right) \left(\frac{m_{projectile}}{0.1kg} \right) \quad (\text{Eq. 3.24})$$

Using the above expressions, it may be concluded that a single projectile, given a hit, is able to negate the threat of most missiles. This estimate may also be conservative given that when engaging a missile from the front, the target is the radome: without which the missile is rendered completely ineffective. When engaging aircraft, the loss of the radome may decrease the combat potential of the airframe, but not mitigate the entire threat.

3.5.2.2 Lethal Radius

Although aerial gunnery has traditionally been used to achieve kinetic kills exclusively, to engage more diverse targets (including missiles), a direct kinetic kill may not always be achievable. Instead, proximity fuse detonation may be used to negate a threat at some specified miss radius caused by errors in targeting (i.e. atmospheric gust, etc.). For this conceptual study, the miss radius for a given projectile and target was determined by scaling the explosive potential of standard air-to-air missiles and the mass of both the target and interceptor.

Table 3.2: Missiles Used in Scaling Laws

System	Warhead Mass (kg)	Range (km)	Guidance/Seeker	Calculated R _{miss} (m)
AIM-7 Sparrow ^[53]	40.0	100	SARH	1.23
AIM-120A AMRAAM ^[53]	51.8	48	INS/terminal active radar	1.35
R-77 (AA-12 Adder) ^[55]	22.5	80	INS/terminal active radar	0.16

The three missiles used to determine the miss radius scaling laws are juxtaposed in Table 3.2. For each missile, it is assumed that the mass of the warhead contains 85% explosive and 15% metallic shrapnel. The Gurney method (Reference [65]) is then used to approximate the

initial velocity of the metal fragments upon warhead detonation. The velocity of the fragments is outlined in Eq. 3.25 assuming a cylindrical denotation pattern. The Gurney velocity of the explosive used is 2830m/s (similar to RDX).

$$V_{fragment} = \sqrt{2E} \left(\frac{m_{metal}}{m_{charge}} + \frac{1}{2} \right)^{-\frac{1}{2}} \quad (\text{Eq. 3.25})$$

Assuming each of the missile warheads contain the same ratio of explosive to shrapnel, the initial velocity of the fragments is approximately 3,441m/s. With a forward travel velocity of Mach 4 at an elevation of 4,000m, the detonation cone of debris generated by the warhead may be calculated at a given instant in time for each missile. Several of these cross sections are shown in Figure 3.9.

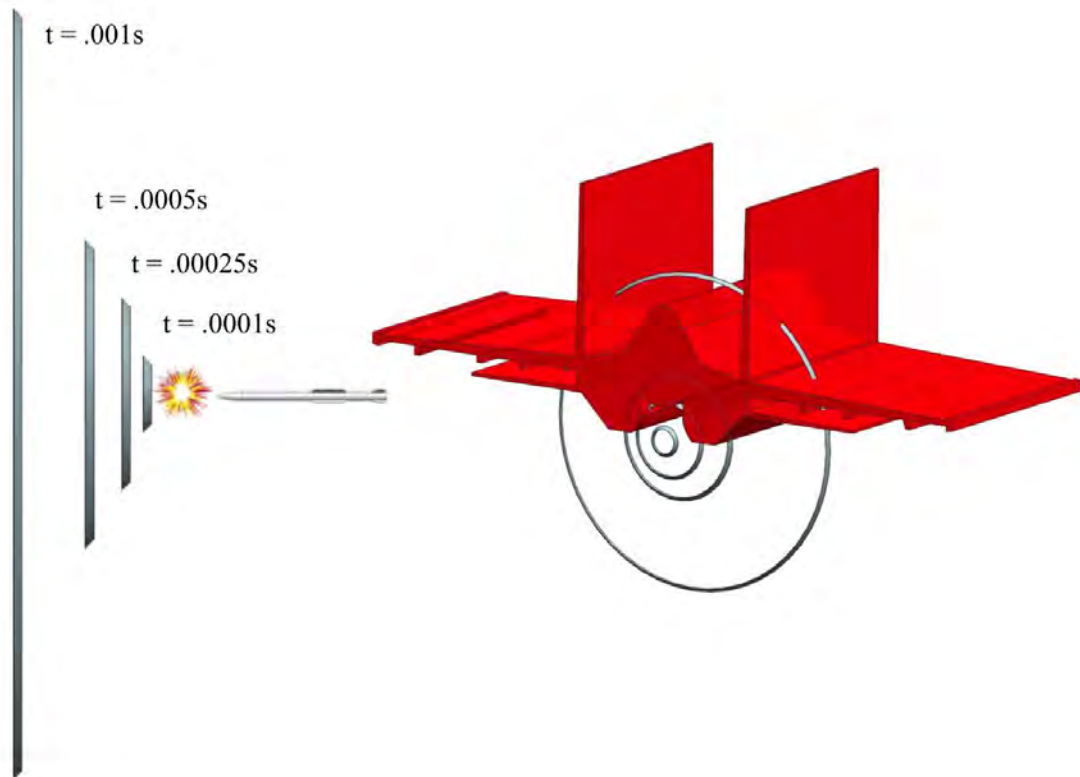


Figure 3.9: Projection of Aircraft Through Debris to Estimate R_{miss}

The metallic fragments dispersed in the explosive disk at a given instant in time are assumed to be comprised of fragments similar in size and composition to the PGU-28 projectile.

These fragments are also assumed to be distributed equally throughout the area of the explosive disk after 0.00025 seconds. The cross section of an aerial target may then be projected through these disks at varying distances from the point of detonation to determine the maximum miss radius to achieve a 95% P_k as shown in Figure 3.10. As previously mentioned, the cross section of a Su-35 was used as a standard target aircraft for this study. By using Eq. 3.23 and 3.24, the number of impacts for a PGU-28 type munition against a Su-35 must exceed 28 to achieve the desired probability of kill. The R_{miss} generated for each aircraft are given in Table 3.2. The miss radius is then normalized with the hydraulic diameter of the target and the results are compared against the ratio of target mass to warhead mass in Figure 3.10.

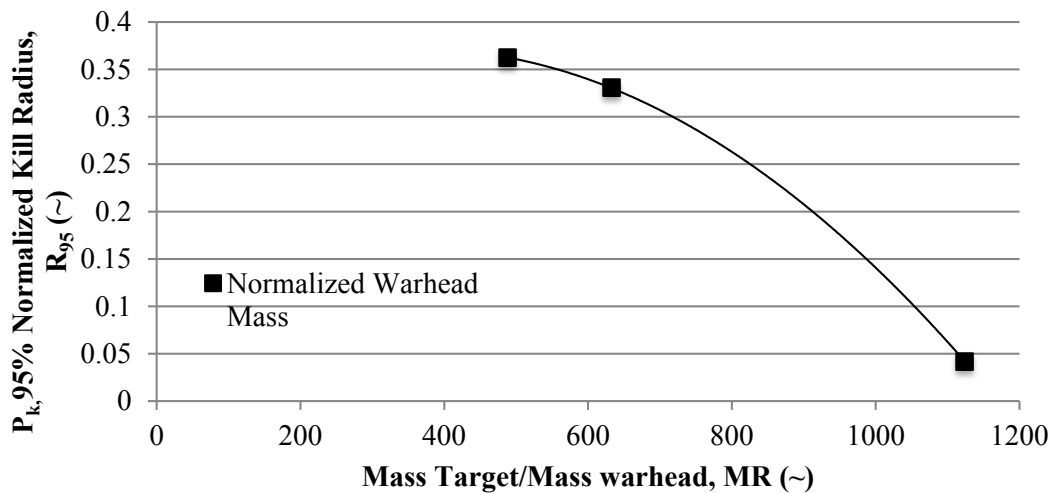


Figure 3.10: Normalized Miss Radius from Target Mass Ratio

The approximate relation between normalized miss radius and target mass ratio is given in Eq. 3.25.

$$R_{95} = -5.71E - 7 * MR^2 + 0.000416 * MR + 0.295 \quad (\text{Eq. 3.26})$$

For example, to mitigate an empty R-77 missile with a 20mm round similar to the PGU-28 ($MR = 433.5$, $R_{95} = 0.36$), the miss radius is approximately 7cm. As previously noted, this

represents a conservative estimate for the maximum miss radius for a given projectile and target. From this relation, it is also observed that for a MR greater than approximately 1170, it is no longer possible to achieve a P_k of 95% with any amount of miss radius. In this case, the only way to achieve a probability of a kill to this standard is to engage in a kinetic kill scenario (likely with multiple rounds).

3.5.3 Control Authority

To outline the control requirements for these projectiles, the intercept path between the projectile and intended target must be well defined. In a general scenario, the aircraft, projectile, and target are simplified to point masses, each with a velocity vector oriented in 3D space as demonstrated in Figure 3.11. The projectile will initially have a velocity vector parallel to the aircraft in order to represent a forward or aft mounted gun barrel.

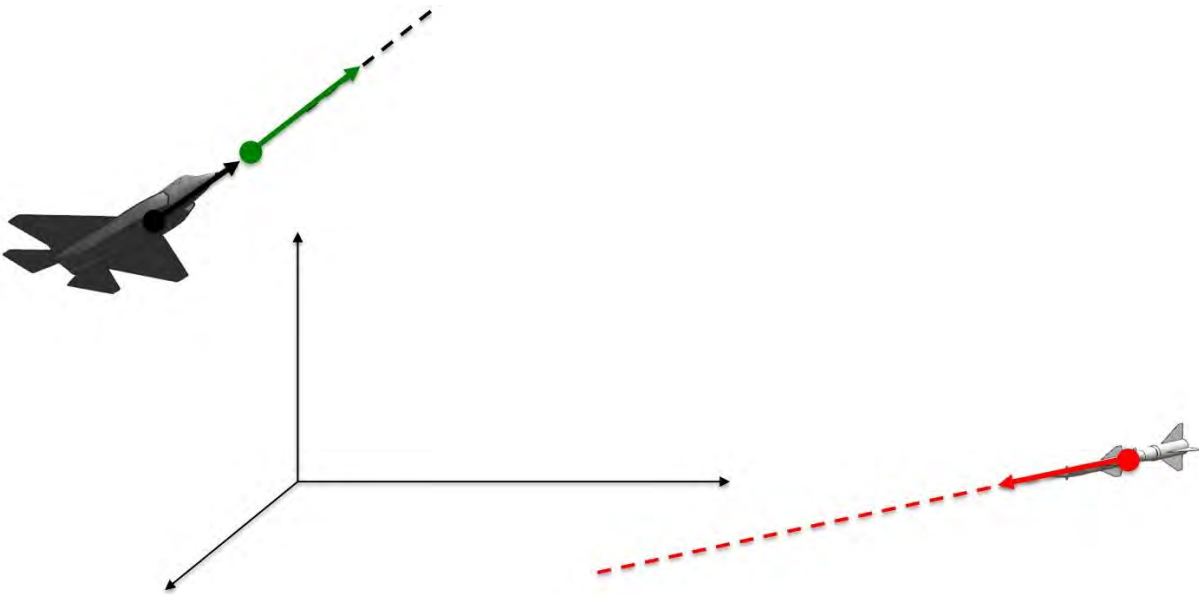


Figure 3.11: Generalized 3D Engagement Scenario

By definition, in an ideal engagement scenario (neglecting errors and atmospheric effects), to intercept the aircraft, the velocity vector of the target and the aircraft must intersect at some instant in time and space. Assuming the target is using proportional navigation to intercept

the aircraft and the aircraft does not employ evasive maneuvers, the angle between the aircraft and target is constant. The intersection point and velocity vectors of the aircraft and target may then be used to define an engagement plane along which all maneuvers may be completed to engage the target. This result is demonstrated in Figure 3.12, and is used to simplify this three-dimensional engagement into a two-dimensional guidance problem on the intercept plane (shown in purple). This simplification is then used to outline the maneuverability and control requirements for this family of guided projectiles.

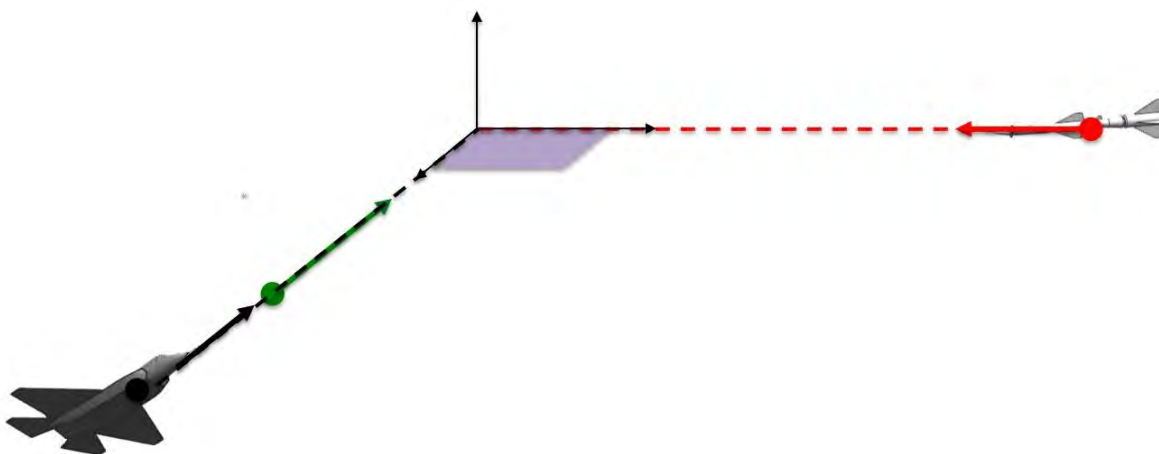


Figure 3.12: Idealized 2D Engagement Scenario

3.5.3.1 Phase I Control

Phase I flight control requirements are governed by the engagement scenario maneuver requirements. These combat scenarios must incorporate maximum g maneuver environments that are representative of the diversity of the air combat theatre. The three categories of air combat trajectories, long, medium, and short range, are demonstrated in Figure 3.13. Note, these engagement scenarios will have a diverse target base, though the range and overall control authority required will be similar.

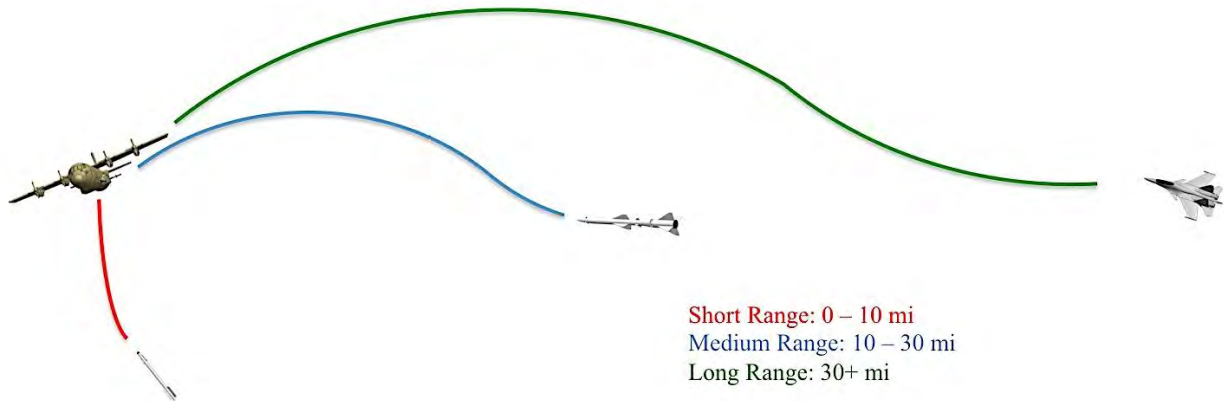


Figure 3.13: Range Trajectory Generalization (NOT TO SCALE)

In both the medium and long-range scenarios, projectiles will have longer maneuver times, and turn radii will be much larger. Consequently, these scenarios do not represent the limiting case Phase I control authority required. Instead, the small turning radii encountered in many short range aerial engagements will dictate the required g turning capability of this family of munitions. The Phase I control authority is governed by short-range engagements with missiles, aircraft, and ground targets. As demonstrated in Figure 1.24, traditional short-range air-to-air combat is becoming obsolete with the advancement of detection technologies. Ground targets, both stationary and mobile, are engaged at lower closing velocities, and will therefore also not dictate the limiting case maneuverability.

A low altitude engagement with a SAM is thus selected as the limiting case engagement maneuver. Specifically, an aircraft flying at an altitude of approximately 2,100m (7,000ft) to avoid AAA fire was set to intercept a general SAM after a four and a half second time of flight. This time was selected to allow the missile to pass through the boost acceleration phase and into a cruise velocity of Mach 4. Assuming the missile is fired at sea level, has zero initial airspeed, and experiences constant acceleration, the intercept path of the aircraft and missile may then be

roughly approximated as a right triangle as shown in Figure 3.14. The turning angle required prior to the five-second-detonation time may then be tabulated as approximately 50.7 deg.

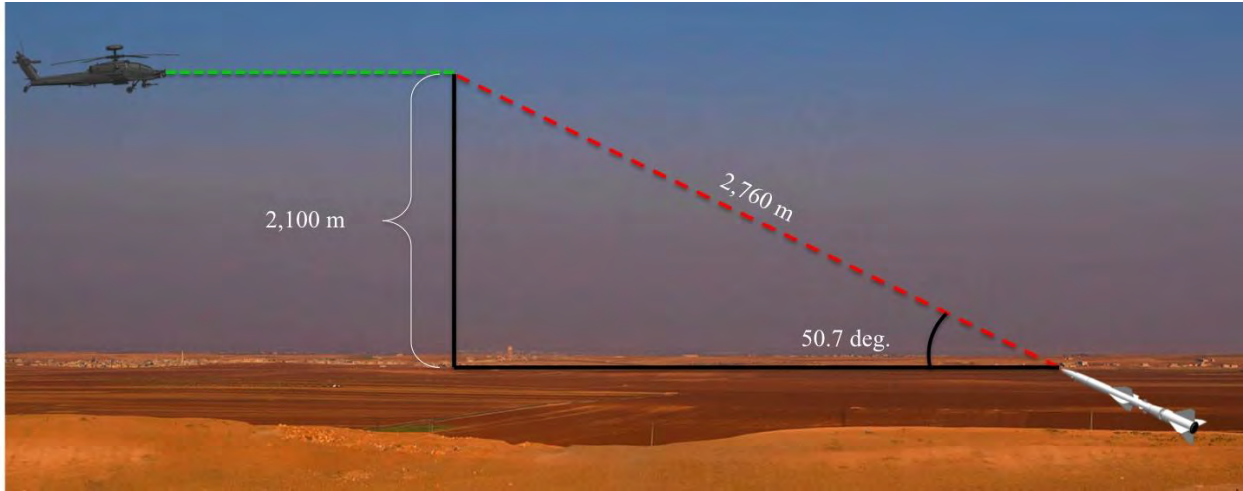


Figure 3.14: Maximum Maneuver Capability (NOT TO SCALE)^[73]

The acceleration required to achieve the turning angle may then be tabulated as a function of the velocity of the projectile. For this first design iteration, the effects of gravity and drag are neglected and a constant speed circular arc trajectory was assumed for the 2D intercept path. The tangential acceleration for a constant speed circular arc is given as:

$$a = g * n = \frac{v^2}{R}$$

$$R = \frac{v^2}{g * n} \quad (\text{Eq. 3.27})$$

The total angle turned may then be determined from:

$$\theta = \omega * t = \frac{d\theta}{dt} * t = \frac{v}{R} * t \quad (\text{Eq. 3.28}).$$

Combining Eq. 3.27 and Eq. 3.28, the total number of g's required, n, is defined by:

$$n = \frac{\theta v}{t g} \quad (\text{Eq. 3.29}).$$

Equation 3.29 demonstrates that the acceleration commanded by this family of projectiles is proportional to the velocity of the projectile. The acceleration required for the gunnery systems

previously noted in Table 3.1 are given in Table 3.3 assuming the aerial platform is traveling at 270 m/s.

Table 3.3: Acceleration Required for Sabot Projectiles

Weapon System	Standard Caliber / Sabot Caliber (mm)	Muzzle Velocity / Impact Velocity (M)	Acceleration Required (g's)
<i>M61 Vulcan</i> ^[37]	20 / 12.7	9.22 / 0.581	44.8
<i>GAU-8/A Avenger</i> ^[37]	30 / 20	8.20 / 0.716	40.4
<i>M102 Howitzer</i> ^[42]	105 / 50	6.10 / 1.40	31.3

3.5.3.2 Phase II Control

The control authority required to satisfy the Phase II flight trajectory of a given projectile is governed primarily by the short period mode of the projectile and target. In order to damp out these effects, the bandwidth of the actuators must be greater than the frequency of the disturbances. The short period mode of the projectile in various flight regimes will ultimately size the bandwidth of the actuators required as the projectile is designed to be much smaller than the target, and an example estimation of the short period frequency is provided for a 20mm tail guided projectile. As an interceptor, the bandwidth must also be larger than the short period frequency of the target in order to increase the probability of a hit. Oscillations in target position due to atmospheric gusts may also size the bandwidth required as well as the required targeting accuracy. In this conceptual study, the estimated short period frequency of a standard target (R-77 AAM) is used to represent a baseline for target oscillation frequency. This baseline is compared against estimated frequency of the sample projectile in order to determine the required actuator bandwidth.

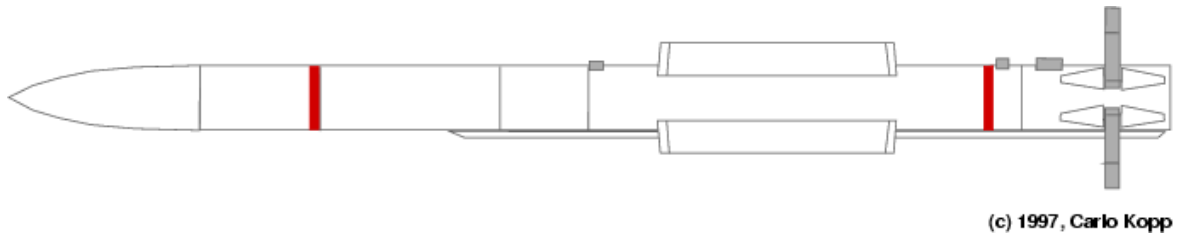


Figure 3.15: Vympel R-77 (Adder)^[74]

To estimate the dynamic behavior of a missile similar to the R-77 the geometry was analyzed and the stability coefficients approximated for a cruising flight regime. The missile geometry approximated from images of the R-77 is summarized in Table 3.4. The configuration was broken into three major components: the radome, navigation/warhead, and the propulsion section. The approximate density of each of these components was used to determine the center of gravity (CG) of this missile assuming half of the propellant has been burned and expelled. Siemens NX CAST software was used to approximate the volume of each of these components, measure approximate geometry, and approximate the moments of inertia of the missile. The weight of the radome is assumed to be negligible compared to the other components. The stability coefficients were determined from the methods outlined in Section 3.2. As this missile incorporates a grid fin tail, it is assumed that perfect flow turning is achieved through this surface.

Table 3.4: R-77 Salient Characteristics

Parameter	Value	Units
<i>Loaded Mass (W)</i>	175	kg
<i>Total Length (L)</i>	3.60	m
<i>Diameter (D)</i>	0.2	m
<i>Reference Area (S)</i>	0.157	m ²
<i>Nose Length (L_{nose})</i>	0.558	m
<i>Navigation/Warhead Density</i>	8060	kg/m ³
<i>Propulsion Section Density (full)</i>	2450	kg/m ³
<i>CG location (from nose)</i>	2.14	m
<i>Strake Area (S_s) x 4</i>	0.580	m ²
<i>Fin Area (S_{fin})</i>	0.0350	m ²

The frequency of the nutation (short period mode) may then be approximated using the methods found in Reference [75]. Namely, the approximation was obtained as shown in Eq. 3.30.

$$\omega_{sp} = \sqrt{\frac{Z_{\alpha} M_q}{V} - M_{\alpha}} \quad (\text{Eq. 3.30})$$

$$Z_{\alpha} = -\frac{\bar{q}S(C_{L\alpha} + C_D)}{m}$$

$$M_q = \frac{\bar{q}S\bar{c}^2 C_{mq}}{2I_y V}$$

$$M_{\alpha} = \frac{\bar{q}S\bar{c}^2 C_{m\alpha}}{2I_y V}$$

Using Eq. 3.30, the short period frequency of the R-77 missile is approximately 0.772Hz. To outmaneuver this target, the response of the projectile must be higher than this frequency.

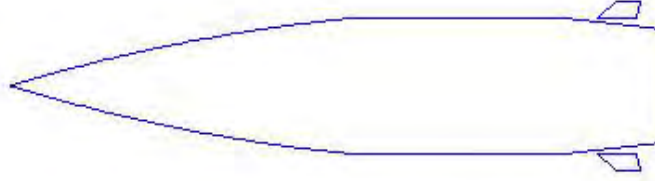


Figure 3.16: Generalized Tail Guided 20mm Projectile

The generalized tail guided 20mm projectile shown in Figure 3.16 was then analyzed using the same method. The short period of this round was approximately 10.6 Hz, more than an order of magnitude greater. This dynamic mode will thus determine the actuator design parameters. As mentioned in Reference [76], good design practice dictates that corner frequencies for these actuators should be approximately four times the frequency of the highest dynamic mode. This would then indicate that the actuator corner frequency must be approximately 40Hz.

3.5.3.3 Control System Outline

Although an aircraft design approach has been used primarily for this preliminary conceptual study, component design is very different for smaller guided aerial vehicles. The minimization of aircraft weight factors heavily into traditional airframe design. In this projectile study, increased density was beneficial: allowing for the increase in impact speed in medium and long-range engagements. Instead, volume is the primary design driver for this class of aerial vehicles. The structural properties of each of the components must also be carefully considered in order to select a design that can withstand the high launch forces encountered in interior ballistics.

Structural Requirements

Accelerations encountered in interior ballistics must be considered before selecting any design components. Setback, setforward, balloting, and ringing accelerations dictate the structural design. Of these load conditions, setback accelerations encountered from the moment of fire as the round accelerates through the length of the barrel are the greatest. Reference [76] lists a general approximation for the peak acceleration experienced and outlines the various causes of these accelerations. Hard-launch munitions may experience peak accelerations of over 15,000g's.

$$a_{peak} \cong 1.45V_{muzzle}^2/2L_{barrel} \quad \text{(Eq. 3.31)}$$

Actuator Type

To satisfy the volume constraints in projectile design, the actuator type must have a low power specific volume, low specific power consumption (to minimize the battery size), and a high corner frequency to satisfy the requirements listed in Section 3.5.3.2. As these rounds operate primarily in the supersonic and high subsonic flight regime, control surface deflections will typically be small: on the order of a few degrees. Adaptive materials provide a means of satisfying each of these requirements. Piezoceramic actuators in particular, satisfy these requirements for high bandwidth, small deflection capability at low power-specific volume and power consumption levels. For the purposes of this conceptual study, the generalized results obtained from the 20mm guided projectile applied to the F-35 (Section 4.1.1) was used as a baseline design requirement: approximate 3 deg. point-to-point deflection at 44Hz.

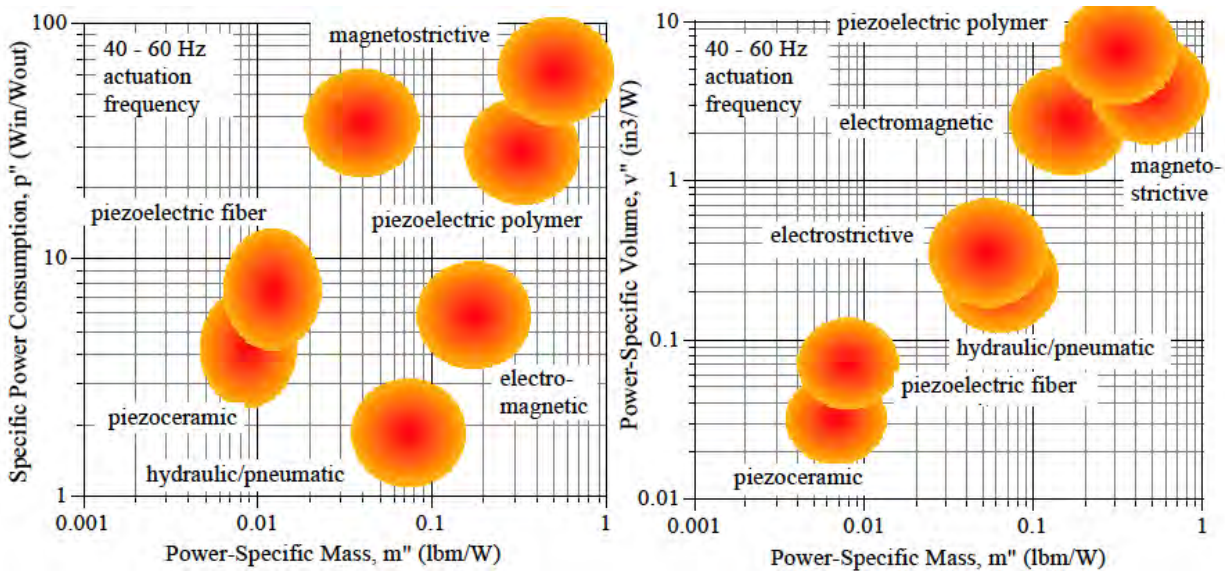


Figure 3.17: Comparison of Actuator Performance^[77]

A post-buckled precompressed (PBP) piezoceramic actuator as detailed in Reference [78] may be implemented to increase the stroke distance and mechanical work when compared with standard piezoceramic actuators. An example PBP type actuator applied to a movable surface is shown in Figure 3.18.



Figure 3.18: PBP Piezoceramic Actuator Example^[78]

Power Supply

The design of a power supply onboard a guided hard-launch munition is directly tied to the type of mission these projectiles undergo. Guidance, navigation, and controls equipment is designed to decrease the volume and energy required. Despite these precautions, the type of mission (including actuation in both the Phase I and Phase II guidance sections) will require a high specific power as mission flight time will range from a few seconds to just a couple of

minutes. Additionally, storage life and structural ruggedness must be factored into the selection of the power supply as, although the system will only go through a single discharge cycle, controlled environment storage life may be up to 20 years and then the round must undergo several thousand g's during firing [76]. In this conceptual study, two forms of power supply are outlined.

A traditional battery powered system may be implemented on these projectiles. Due to the structural conditions and high specific power required, thermal batteries may prove to be a favorable design selection. A thermal battery contains a solid, non-conducting electrolyte that minimizes discharge during periods of extended storage. The battery is activated by increasing the temperature above the melting point of the electrolyte, allowing the material to conduct. This process then allows for a single battery discharge at a high specific power. These batteries may be easily miniaturized and due to the solid-state electrolyte, are very rugged in design. For this reason, these batteries have been considered for use on guided missiles. [79]

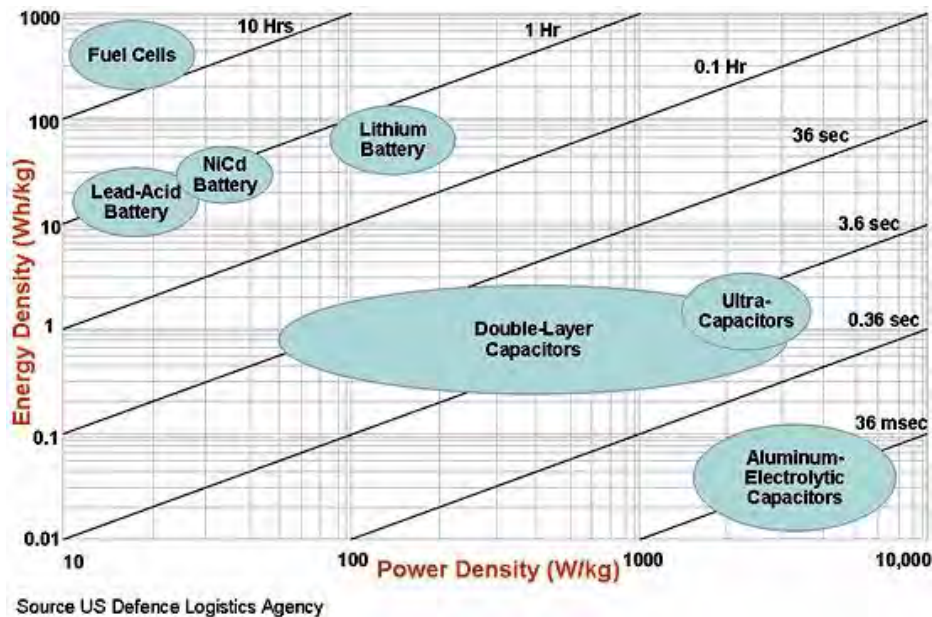


Figure 3.19: Ragone Plot of Common Power Sources^[80]

A second means of providing power to the various systems within the guided projectile is by the use of a capacitor. Unlike a battery that must be charged well in advance of a mission flight, a capacitor may be charged as part of an arming process just prior to firing a bullet or as part of a pre-flight procedure. Capacitors also generally have higher specific power than batteries, and for applications involving flight times less than a minute (close range engagements), may provide a lower volume solution. The shelf life of these components may extend over a decade in controlled conditions, and leakage current growth may be controlled by re-aging the components (by applying a specified voltage and current for a period of time). [81] Specifically, a double layer type capacitor as depicted in Figure 3.19, operates with a high power density at discharge times that match both short and medium-range engagement projectile flight times. One type of double layer capacitor, a Capattery, in addition to long life may operate under extreme temperatures (-55° to 85°C) and is designed to withstand high shock loads [82].

3.5.4 Guidance and Navigation

To reduce the cost and complexity of the munitions, simple forms of guidance and navigation are implemented within the projectiles, and more complex components, such as transmitters, are housed within the aircraft. Unlike the majority of modern aerial missiles, homing capability is not included, and the projectiles are designed to rely entirely on communication from the airframe.

The size of the projectile will dictate the length of the antenna that can be implemented. This will in turn dictate the transmission frequency. Signal strength will also be affected by free space attenuation and atmospheric absorption. The amount of signal loss is also dominated by the transmission frequency. The free space attenuation loss (in dB) is outlined in Reference [83],

and the attenuation as a function of frequency and range is demonstrated in Equation 3.32 and Figure 3.20.

$$FSPL(dB) = 20 \log_{10} \left(\frac{4\pi R}{\lambda} \right) \quad (\text{Eq. 3.32})$$

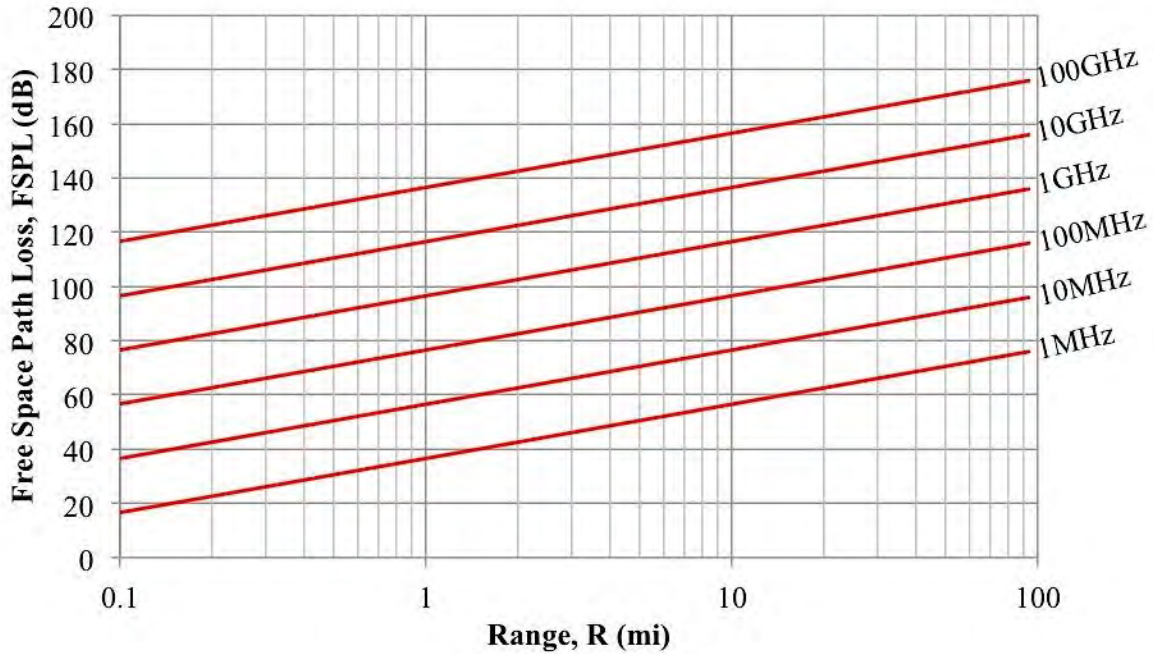


Figure 3.20: Free Space Attenuation

Losses due to atmospheric absorption are also dependent upon the signal frequency, atmospheric conditions, and range. As these projectiles are designed for use in all-weather conditions, the losses during poor weather conditions must be considered. Figure 3.21 shows losses due to common atmospheric conditions. For the purposes of this study, long-range engagements in heavy clouds are considered.

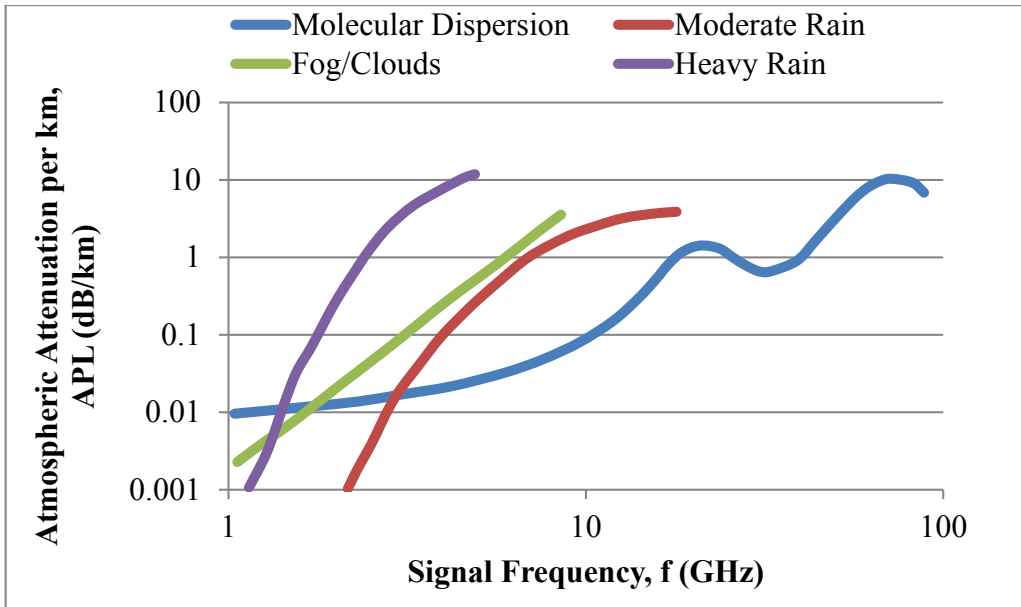


Figure 3.21: Atmospheric Absorption^[84]

The physical dimensions of the receiving antenna on the projectile will also dictate the selection of transmission frequencies. As a rule of good design practice, in order to ensure the antenna is tuned for the frequency of transmission, the size of the array must be approximately half of the signal wavelength [85]. For example, if it is assumed that the antenna spans the diameter of the projectile, the frequency of the transmitted signal for a 20mm round at an engagement range of 50 miles may be determined. The wavelength of the signal is thus 40mm, and the command signal would be at ~750MHz. Under these conditions, the free space attenuation would be 128dB and assuming 50% cloudy conditions, the atmospheric attenuation would be 28.18dB. If it was possible to bring the frequency down to 250MHz, the losses would be 119dB and 0.6dB. To counteract these signal losses, high gain transmitters and receivers may be implemented as well as corner reflectors on the projectile to focus the incoming signal.

To accurately guide the projectile along a certain trajectory, the orientation of the projectile with respect to the target must be well established. A polarized signal will thus be used to determine the vertical and horizontal orientation of the projectile at a given instant in time.

Note, when using this method, the angle with respect to the vertical or horizontal plane may be established, but there is uncertainty in the orientation (+180deg or -180 deg). This uncertainty may be eradicated with a brief dither command (or series of commands) after the round has left the barrel. Once the brief control surface deflection is enacted, the exact orientation of the projectile will be known. With a known, commanded low spin rate, the orientation of the projectile may be determined at a given instant based upon this early commanded response.

While increasing the frequency of the signal increases the range resolution, accuracy, and decreases the size of the antenna required onboard the projectile, signal dissipation effects become more pronounced. The physical size of the antenna onboard the projectile will dictate the frequencies required, though efforts may be made to decrease the frequency used in order to counteract attenuation effects during medium and long-range engagements. Extended range engagements, employing higher caliber munitions, may also be guided with GPS.

3.5.5 Cost Estimation

A rough order of magnitude shipset cost of these guided hard-launch munitions may be obtained from Reference [76]. This reference compares the cost difference between the current conventional rounds used by the US armed forces and the projected cost of a large caliber guided round that underwent detailed design: the Mk171 ERGM (Section 1.5.3). The authors concluded guided hard-launch munitions costs are one to two orders of magnitude higher than those of comparable caliber conventional rounds. The upper bound of acquisition cost data used in Reference [76] was updated to reflect the 2016-dollar, and these data were then magnified (by two orders of magnitude) to reflect the upper cost bound for guided projectiles in Figure 3.22.

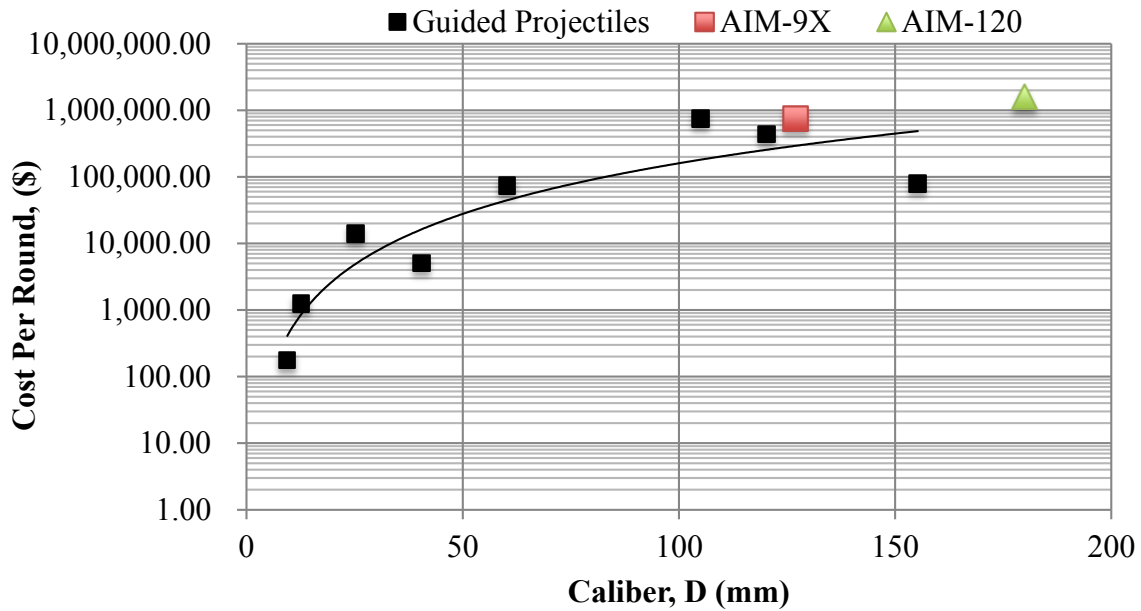


Figure 3.22: Estimated Upper Bound of Acquisition Cost for Guided Rounds^{[76], [86]}

From these data, assuming the cost of the guided projectile is two orders of magnitude higher, a general guided 20mm round would be approximately \$2,700. To meet this cost, a simple navigation control system would need to be implemented as described in Section 3.5.4. While this cost may initially seem to preclude the use of this type of weapon system against targets currently mitigated with missiles, a simple comparison shows that this is still a cost effective means of mitigating targets. Using the lethality calculations given in Section 3.5.2.1 given a kinetic kill, 29 rounds would be required to mitigate a Su-35: totaling nearly \$80,000. By contrast, the same aircraft may be mitigated with a variety of missiles shown in Table 3.5, and the cost savings associated with the mitigation of a Su-35 with guided munitions is shown.

Table 3.5: Potential Savings Per Su-35 Mitigation^[86]

Missile	FY 2017 Total Cost Per Unit (\$ thousands)	Cost Savings Per Kill (\$ thousands)
<i>AIM-120 AMRAAM</i>	1,580	1,500
<i>AIM-9X</i>	743	660
<i>SM-6 Standard</i>	5,010	4,390

4 Results

Although non-trivial cost savings per kill were noted with the implementation of guided hard-launch munitions over conventional missiles, the overall value in this concept is the utility of the weapon system itself. These highly maneuverable rounds have the capability to negate threats posed to aircraft from hostile aerial vehicles (including both aircraft and missiles) while enabling offensive fire against both air and ground targets. The implementation of this technology will fundamentally alter the way aircraft are used in any engagement and allow the maintenance of complete combat superiority over virtually any existing system.

This conceptual study indicates that a family of guided hard-launch munitions may be a viable solution for aerial defensive and offensive engagements. General performance trends and the outline of the design requirements for a general engagement scenario were given. In order to further demonstrate the capability of these projectiles, example configurations were applied to two different aircraft: the F-35A and the AC-130U. Each of these aircraft, the updated F/A-35 and FAC-130, were then analyzed in order to project approximate performance in offensive and defensive engagements using the existing airframe gunnery system. The results of this study are provided in this section.

Using the methodology outlined in Section 3.5.3.1, the required Phase I acceleration was tabulated for the selected projectile configuration. With the acceleration known, assuming a circular arc trajectory, the normal force that must be exerted by the round may be tabulated. The angle of attack of the projectile relative to the freestream velocity is then known, and the control surface deflection may be calculated by moment equilibrium. For a given trajectory, a simple analysis involving two iterations is used. The first iteration assumes the muzzle velocity is the average velocity along the trajectory. The impact velocity is then estimated with a single time

step drag calculation over the total time of flight. The second iteration velocity is then taken as the average of these two values.

4.1 Defensive Capability

To demonstrate the defensive capability of each airframe with this guided munitions system, firing cones (similar to those demonstrated on the B-17 in Figure 1.19) based on a two second engagement time are shown. Note, these engagement cones are representative of an order of magnitude analysis only due to the approximation methods described in Section 4.

4.1.1 Application to the F-35

The existing gunnery system onboard the F-35A, the GAU-12/U that fires a 25mm projectile at approximately 1040m/s, was used for this defense engagement study in both a forward and aft mounted barrel configuration [87]. For this system, a 20mm guided sabot projectile was selected for aerial defense. A conventional, tail-guided, configuration system was used and is shown in Figure 4.1. The salient characteristics of this projectile used in both a forward and aft mounted barrel are noted in Table 4.1.

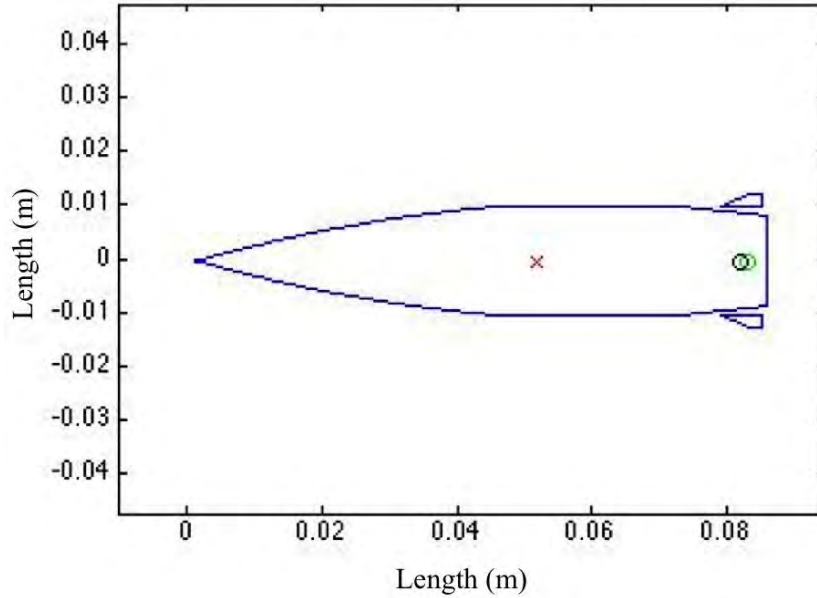


Figure 4.1: F-35 Sample Guided Projectile

Table 4.1: F-35 Guided Projectile Characteristics

Characteristic	Value Forward Value Aft	Units
S	314	mm ²
S _{t, exposed}	100.0	mm ²
Λ_{LE}	60.0	deg.
b _t	25.0	mm
n _{max} (estimated)	36.0 24	g's
SM _{supersonic}	-0.0694 0.0942	%
m	0.1123	kg
V _{muzzle} (including airspeed)	1,770 1160	m/s
h	2,130 2,130	m
d _F (absolute value)	3.63 2.73	deg.

The engagement cones generated for both a forward and aft mounted GAU-12/U gunnery system firing the projectile shown in Figure 4.1 are demonstrated in Figure 4.2. The distance traveled by the aircraft during the engagement scenario is also demonstrated. Note, the aircraft and distance traveled by the airframe are magnified by one order of magnitude relative to the cones for ease of viewing. As the aft mounted barrel does not take advantage of the forward velocity of the aircraft, the overall distance traveled is smaller, though this lower velocity equates

to equivalent maneuverability at lower required accelerations. For this reason, the surface deflection required for the aft-fired projectiles is significantly less than the forward. The same projectile geometry was used in each of these cases for both simplicity and commonality, though this difference merits the consideration of geometries tailored to the gun position on the aircraft.

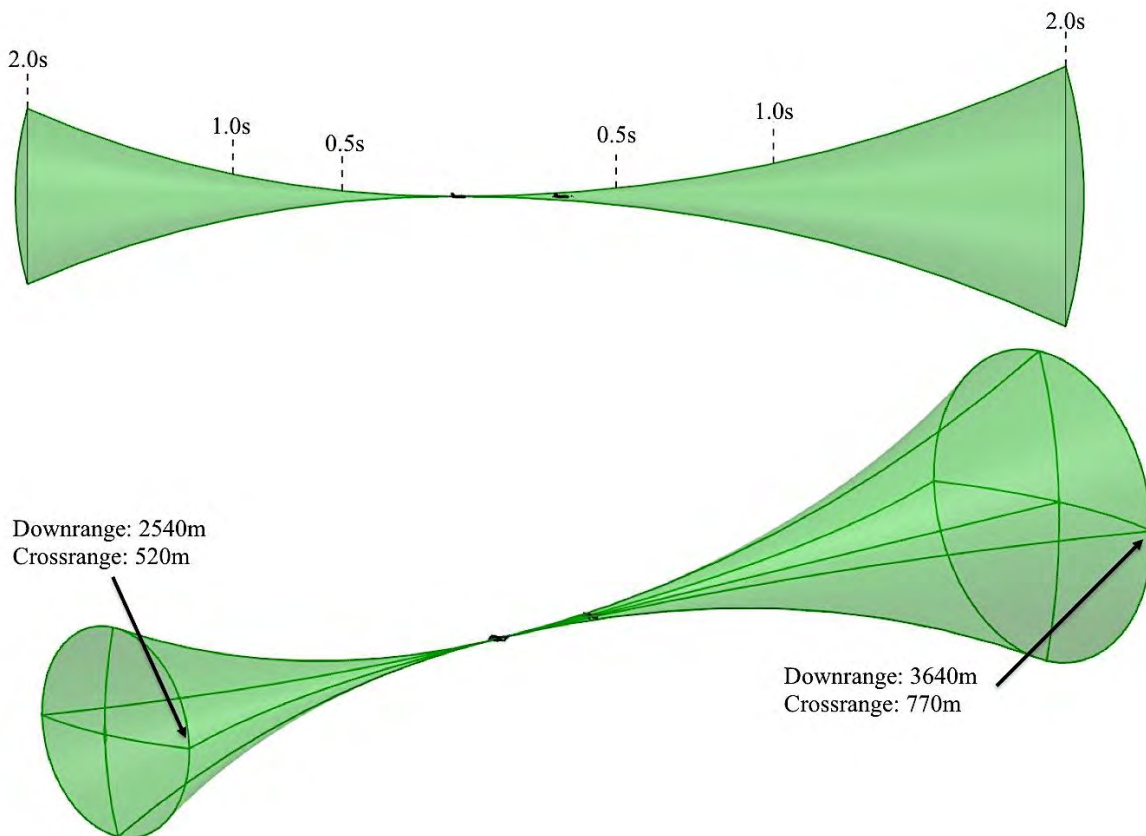


Figure 4.2: F-35 Defensive Engagement Cones 2.0s

4.1.2 Application to the AC-130

The procedure used for the defensive engagement scenario was applied to the AC-130U “Spooky” gunship. Of the three types of gunnery onboard, the 25mm GAU-12/U gatling gun (also used on the F-35A) and the 40mm L60 Bofors cannon were selected for this conceptual study with defensive guided munitions [88]. These gunnery systems are mounted on the side of

the fuselage. The defensive combat scenario presented assumes the aircraft is flying in a left-handed orbit (counter to standard operations) in order to orient the guns to engage at greater distances. The projectile used in the GAU-12/U is identical to that analyzed for the F-35 (Figure 4.1). The configuration used in the 40mm cannon is a 30mm tail guided projectile shown in Figure 4.3 where the muzzle velocity of 881m/s has been increased to reflect the sabot as described in Section 3.5.1 [89]. The salient characteristics for each of these projectiles are listed in Table 4.2.

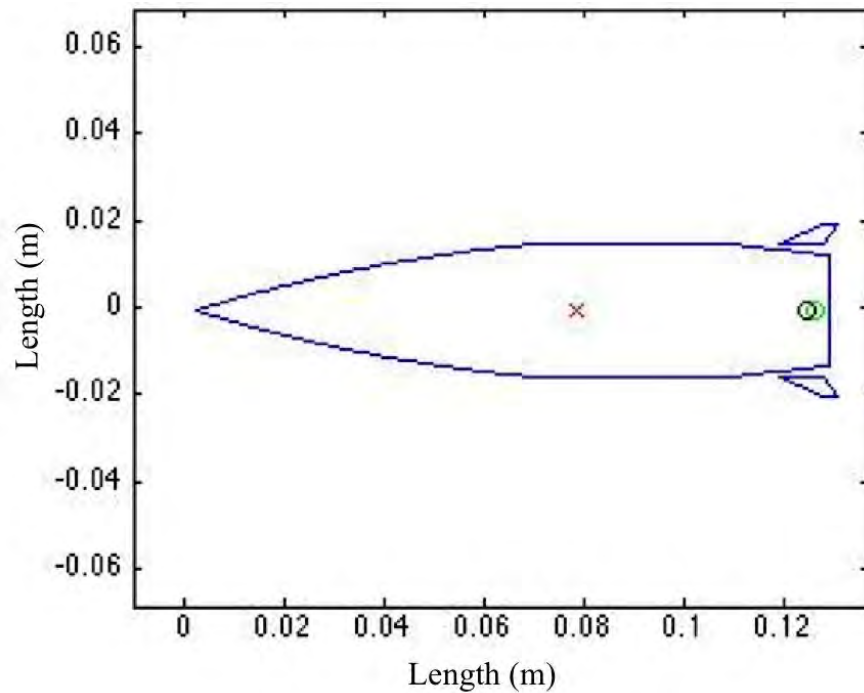


Figure 4.3: AC-130 30mm Sample Guided Projectile

Table 4.2: AC-130 Guided Projectile Characteristics

Characteristic	Value 20mm	Value 30mm	Units
S	314	707	mm ²
S _{t, exposed}	100.	240.	mm ²
Λ_{LE}	60.0	60.0	deg.
b _t	25.0	40.0	mm
n _{max} (estimated)	30	27	g's
SM _{supersonic}	0.0356	0.25	%
m	0.112	0.382	g
V _{muzzle} (including airspeed)	1460	1350	m/s
h	2,130	2,130	m
d _F (absolute value)	3.16	4.86	deg.

The engagement cones generated by firing guided projectiles after 2 seconds from the 25mm gatling gun and 40mm cannon are shown in Figure 4.4. As anticipated, the 20mm projectile traveled further during the two-second engagement time, but as it had higher velocity, it was not able to match the larger round in terms of turning radii. As such, it is recommended that the 40mm cannon be utilized for aerial defense. The GAU-12/U may also be used for defensive purposes, but it is apparent that the 40mm cannon should be able to mitigate all threats the 25mm gatling gun is capable of (with the noted exception that the time of engagement will be slightly longer).

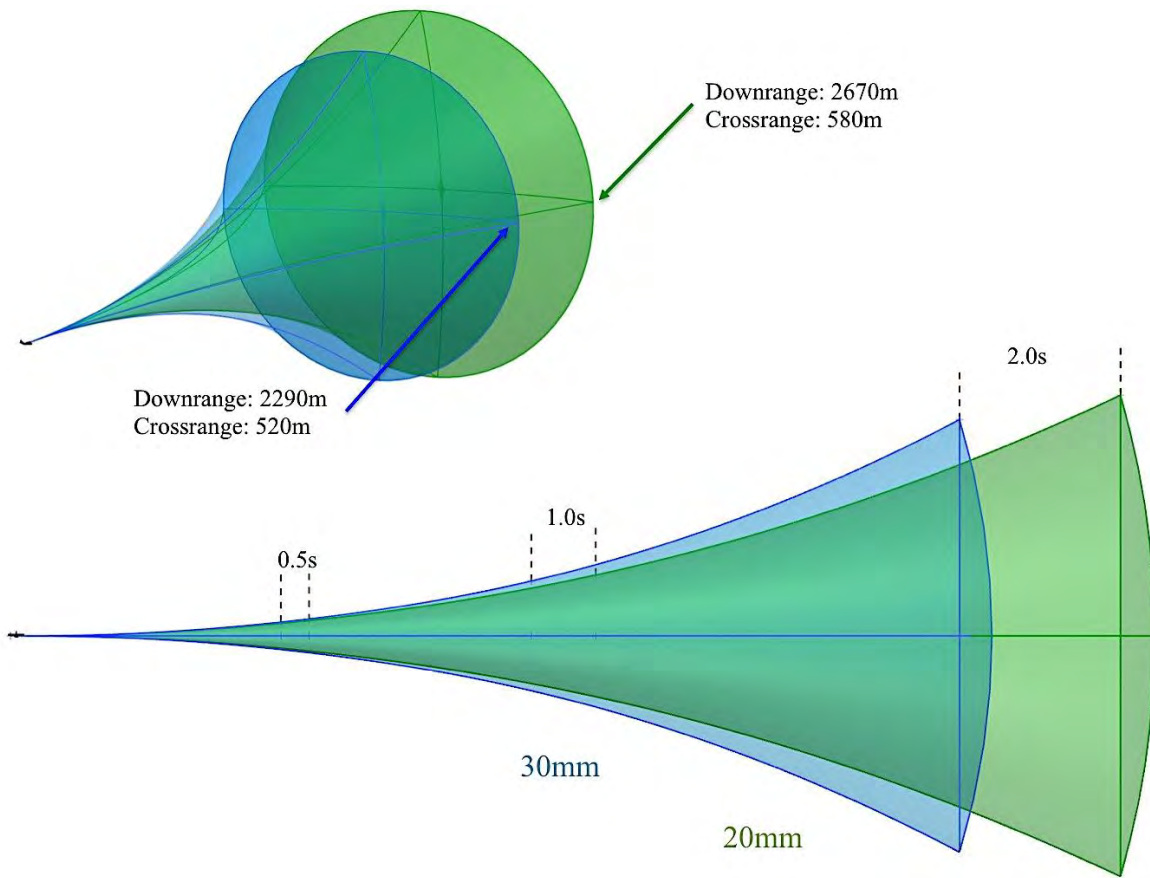


Figure 4.4: AC-130 Defensive Engagement Cones 2.0s

4.2 Offensive Capability

To determine the increased offensive capability with the implementation of guided hard-launch munitions on both the F-35A and AC-130U aerial platforms, the standard capability and loadout must be well defined. The weapons suite (shown in Figure 4.5) for the F-35 is designed to be carried on six external pylons in addition to four internal weapons bays.



Figure 4.5: F-35 Weapons Suite^[90]

The AC-130U as previously mentioned, is equipped with one of each of the following: 25mm GAU-12/U Equalizer gatling gun, 40mm L/60 Bofors cannon, and 105mm M102 Howitzer. Traditionally, these weapon systems have been used primarily for close air support missions.

4.2.1 Application to the F-35

To compare the weapons systems potential, an aerial combat scenario is used to demonstrate the range and lethality of the munitions compared.

4.2.1.1 Engagement Range

If it is assumed that the F-35A is fully fitted for an aerial engagement only, the weapons system loadout could include 8 AIM-120C AMRAAMs (6 external and 2 in the central weapons bays) and 2 AIM-9X Sidewinders (in the smaller weapons bays) [91]. The range of the AIM-120C is on the order of 45mi [92]. The AIM-9 on the other hand has a range on the order of 10 miles [53]. The 25mm conventional munition used by the F-35 was sabot down to a 20mm round shown in Figure 4.6 at 150% density; this projectile has a maximum engagement range of over 21 miles, solidly between the range of the two aerial missiles studied and well into the BVR engagement range. The projectile was fired at an elevation of 15,000m with assumed aircraft airspeed 306m/s. The addition of a tail greatly increases the drag on the projectile and results in decreased overall range when compared with the maximum scenario described in Section 3.5.1.

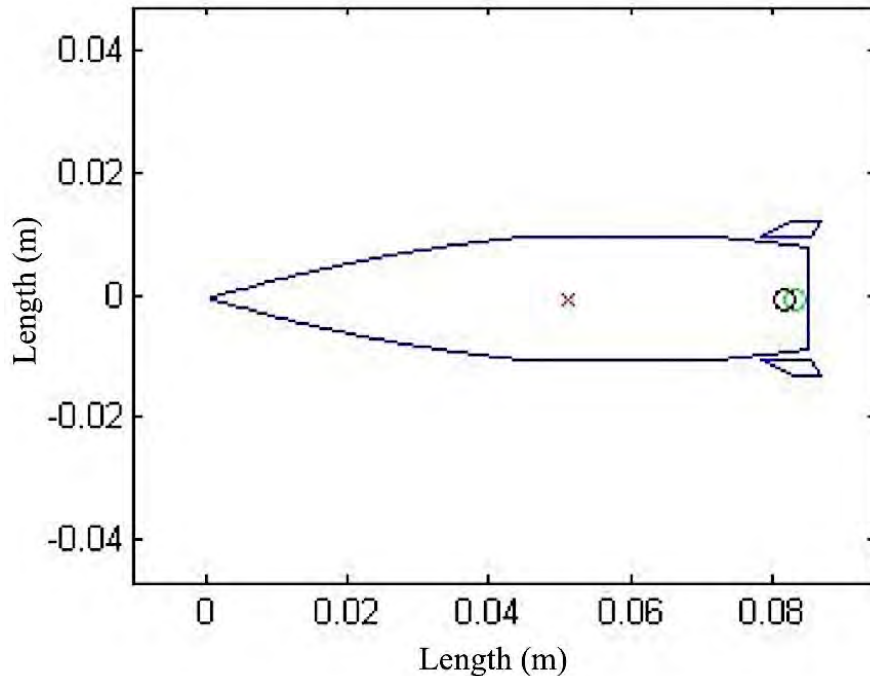


Figure 4.6: Sample F-35 Guided Projectile

4.2.1.2 Potential Targets Engaged

An aerial engagement scenario is again used in order to facilitate the quantification of the lethality of a given type of munition. It is assumed in this scenario that the munition shown in Figure 4.6 is guided in order to achieve a kinetic kill (direct impact against the target). The same kinetic kill is assumed for the missile engagement scenario.

From the maximum aerial engagement loadout of the F-35, it is obvious to the reader that the maximum number of aerial targets engaged is 10 (the total number of missiles). Assuming the cross section of the target is equivalent to that of a Su-35 (as analyzed in Section 3.5.2), 29 projectiles are required to impact to achieve a 95% kill against this target. As the F-35A has a standard loadout of 182 projectiles, an additional 6 targets may be engaged by implementing guided hard-launch munitions. The author would recommend that neither the missile systems nor the hard-launch projectiles be used exclusively. Rather, it is recommended that all external

missiles (6 AIM-120C) be removed in order to maintain VLO (Very Low Observables) by reducing the RCS (radar cross section), and all munitions in the GAU-12/U be used for offensive and defensive purposes. This would allow for the same 10 maximum targets to be engaged without compromising any low observables requirements.

4.2.1.3 Target Engagement Cost

For this comparison, the projected cost of the guided munitions is estimated using the trends discussed in Section 3.5.5 for a generalized 20mm projectile. The order of magnitude costs for the mitigation of the maximum number of targets engaged (10 total) using only missiles and a combination of 4 missiles (2 each of AIM-9X and AIM-120C) and hard-launch munitions are demonstrated in Figure 4.7.

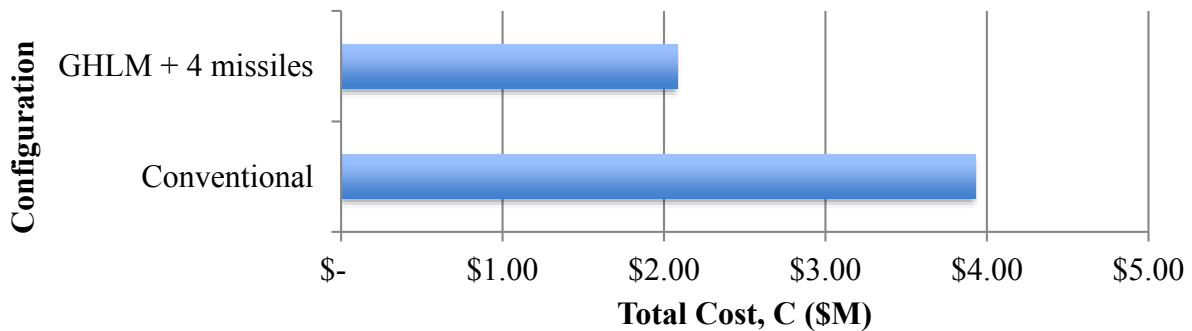


Figure 4.7: F-35 10 Target Mitigation Cost^{[93], [94]}

Note, this comparison does not take into effect the probability of a hit and instead assumes a 0 miss radius for each type of munition. This is also not normalized for engagement environment and assumes that 2 AIM-9X and 2 AIM-120 missiles are used in conjunction with the standard 182-bullet loadout on the F-35A. The order of magnitude analysis required assumes guided projectiles are fired out of the existing gun system, so there are no additional airframe modifications necessary to achieve potential cost savings of 47%. This excludes the tracking and

communications systems necessary to guide the projectiles. The author would also like to note that the quantification of aircraft or overall engagements lost was not included in this analysis. While the overall cost savings per kill do lend additional value to the guided-munition concept, the true value in the implementation of this system is overall aircraft survivability and engagement capability.

4.2.1.4 Target Type

The application of guided hard-launch munitions to the F-35A poses significant advantages when comparing the types of targets engaged in a typical sortie. Whereas a standard airframe is generally equipped for either a strike or fighter mission, guided projectiles may in fact be used in both engagement scenarios. Each of these munitions may be designed to contain a dynamically configured fragmentation warhead. In this scenario, based upon the type of target being engaged, a signal is sent to the munition that determines the timing and order of explosives detonation within the projectile. Based upon the detonation configuration, the projectile may serve as a HEI round, an API round, or even an area charge that would scatter debris into a targets path (for use against missiles). This solution may also be implemented on the AC-130 projectiles discussed in Section 4.2.2. Alternatively, a variable chambering mechanism may be designed to integrate with the gun system to chamber various types of rounds (HEI, API, etc.) based upon the target type while in the air. The simplification of the F-35A gatling gun to a single barrel, smooth bore system would greatly decrease the weight, volume, and complexity of the gunnery system. A chambering system may then be designed to occupy this vacant volume following the gun system modification. As previously noted, with the type of hard-launch aerial engagement envisioned for this family of projectiles, high rates of fire are no longer necessary to achieve a high probability of kill.

4.2.2 Application to the AC-130

The AC-130U is uniquely configured such that the application of guided projectiles for medium and long-range engagements will be more simplified when compared with other US armed forces aircraft. The advanced radar systems onboard fielded AC-130Us enable the aircraft to track 40mm and 105mm projectiles. This capability is currently used in order to provide feedback to the crew on impact locations, though this system may instead be used to track the flight path of the modified guided projectiles to provide controller inputs. [95]

4.2.2.1 Engagement Range

Assuming the 105mm M102 Howitzer is used for offensive engagements, the maximum engagement range for a given projectile may be tabulated. For this study, the 50mm sabot projectile shown in Figure 4.8 was selected for use in medium and long-range engagements. It is assumed that the aircraft is orbiting at its service ceiling of 9,100m. The airspeed of the aircraft does not contribute to the forward velocity of the projectile as it is fired perpendicular to the aircraft flight path. A 150% density was used in this analysis. The maximum range of this projectile is 29 miles.

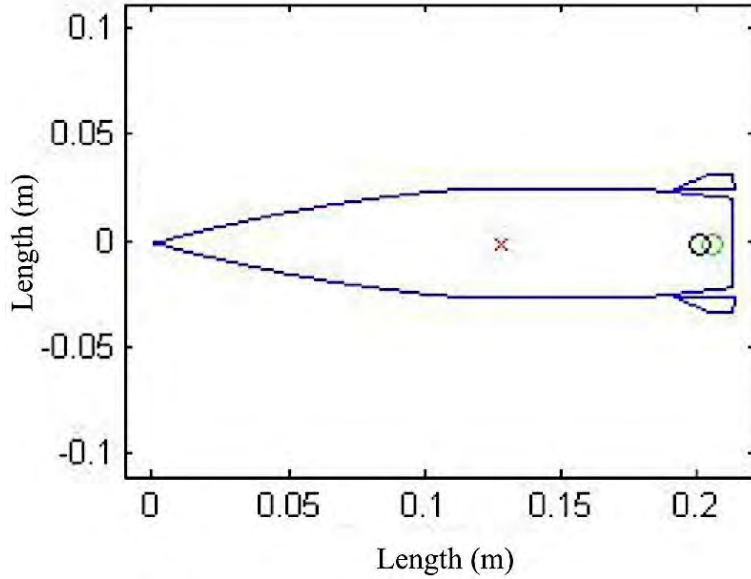


Figure 4.8: Sample AC-130 Guided Projectile

4.2.2.2 Potential Targets

The P_k of the projectile demonstrated in Figure 4.8 against a target aircraft (for example, a Su-35) may be approximated with the equations outlined in Section 3.5.2.1. From these relations, at either the standard density or 150% density, the probability of a kill is tabulated to be greater than one. Although this result is not physical, this demonstrates that given a hit, the munition will be able to mitigate the target threat with very high probability (>95%). In the case of a miss, the miss radius for this projectile against the Su-35 may be estimated using Section 3.5.2.2 with a known MR of ~ 9700 . However, as this mass ratio exceeds the limit discussed in that section, a single projectile will not achieve a 95% probability of kill at any miss radius.

Although the author was unable to determine the exact number of 105mm munitions onboard a conventional AC-130U, the lower limit is set to 40 rounds from descriptions of combat experience [97]. This would imply that a minimum of 40 single-shot targets may be engaged by the AC-130 in a single mission. If the other two gunnery systems (discussed in

Section 4.1.2) were used for offensive purposes as well, the AC-130 would also be able to engage at least two targets simultaneously (provided the targets are close together) [95].

4.2.2.3 Target Mitigation Cost

Using the trends found in Section 3.5.5, the cost of the projectile used in this example is approximately \$28,000. This per unit cost, while large, enables more freedom in design with navigation and controls. Should the AC-130 be unloaded and engage targets at a higher elevation, the range of these projectiles would increase dramatically. As such, a different navigational system, such as GPS, may be used instead of VHF link for long-range targets.

5 Conclusions and Recommendations

The results of this conceptual study are outlined in Section 5.1. The recommendations and planned future work are highlighted in Section 5.2.

5.1 Conclusions

In conclusion, the design requirements for a family of guided hard-launch munitions were outlined for applications on aerial platforms. Conceptual analysis outlined the following requirements:

- Range must be on the order of magnitude of AAM (greater than 10 miles);
 - Range may be increased with sabot rounds
 - Range is increased with increasing firing altitude
 - Increasing density (with the same muzzle energy) negatively impacts range, but increases impact velocity
- Lethality must be sufficient to remove missile and aircraft threats;
 - Kinetic kills are the primary driver with P_k based upon a PGU-28 20mm round
 - Allowable miss radii may be estimated with the mass ratio of projectile and target for a given P_k
- Control authority is broken into two phases;
 - Phase I control is a function of the projectile velocity, typically 30-50g's
 - Phase II control authority is governed by the short period (nutation) frequency with actuator corner frequencies required on the order of 40Hz
- Guidance and navigation stems from the airframe;

- A VHF communication link may be used to control the flight path of the projectiles
- Communication on the order of 250MHz is desired to reduce losses due to environmental effects and free space absorption
- Projectile costs per kill should be less than comparable missile costs per kill

With these requirements in mind, a sample guided projectile configuration was devised for application on the existing F-35A and AC-130U airframes. In offensive engagements, the ranges of these projectiles were comparable to that of standard air-to-air missiles while the overall cost per kill was greatly reduced. The application of these guided hard-launch munitions to any airframe is not only cost effective, but offers a new range of aerial defense capability that will fundamentally alter the way aerial engagements are carried out in the future. True “flying fortresses” may be designed with only a few gunnery systems onboard an airframe. These munitions will allow aircraft to further penetrate into hostile territory, negate aerial and land based threats, and increase the overall safety of our pilots while providing a lower cost aerial engagement solution to the taxpayers of this nation.

5.2 Recommendations and Future Work

The analysis performed in this thesis serves to act as a conceptual, order of magnitude analysis of both the capabilities of this family of guided hard-launch munition, and the overall design requirements. It is recommended that further analysis be performed in the following areas:

- Hypersonic aerodynamics if sabot rounds enter this flight regime;

- Aerodynamic drag model updates to include higher fidelity estimates in different flight regimes and for configurations dissimilar to the PGU-28 and G7 standard rounds;
- Engagement environment effects on the performance of the projectiles for conditions outside of the standard day conditions at various altitudes.

Future work will include the detailed design of a family of these guided munitions for applications on selected airframes. From this work, higher fidelity cost models and performance parameters will be devised in order to determine the viability of the concept for retrofit on existing aerial gunnery systems as well as new gunnery systems. A scale model of one of these guided hard-launch munitions must be constructed for wind tunnel testing and to serve as a demonstrator for component integration.

6 References

- [1] Reichhardt, T. "The First Aerial Combat Victory," *Air & Space Magazine*, 2014. [Online]. <http://www.airspacemag.com/daily-planet/first-aerial-combat-victory-180952933/?no-ist> [Accessed: Feb- 2016].
- [2] Anon., "The First Dogfight?" *Fly.historicwings.com*, 2012. [Online]. <http://fly.historicwings.com/2012/11/the-first-dogfight/> [Accessed: Feb- 2016].
- [3] Park, Edwards, "Jet Jockeys," *Fighters The World's Great Aces And Their Planes*, 1st ed. Thomasson-Grant Inc., 1990, pp. 155-161.
- [4] O'Dell, N., "Frank Whittle and the Race for the Jet," *HistoryNet*, 2012. [Online]. <http://www.historynet.com/frank-whittle-and-the-race-for-the-jet.htm> [Accessed: Mar- 2016].
- [5] Rathjen, W. "100 Jahre Hans von Ohain und die Entwicklung des ersten Strahltriebwerkes," *Deutsches Museum*, 2011. [Online]. <http://www.deutsches-museum.de/information/vortraege/fuer-jedermann-1112/021111-rathjen/> [Accessed: Mar- 2016].
- [6] Username: guardiann usaa, "Nazi Jets (Me262) shot down by Red Tails (Tuskegee Airmen)", *YouTube*, 2012. [Online]. <https://www.youtube.com/watch?v=q8AcGJNkkuc> [Accessed: Mar- 2016].
- [7] Jones, Lloyd S., "Lockheed F-80 Shooting Star," *U.S. Fighters Army - Air Force 1925-1980*, 1st ed. Aero Publishers Inc., 1975, pp. 202-204.
- [8] Anon., "Flying Heritage Collection - Messerschmitt 163 B Komet", *Flyingheritage.com*, [Online]. <http://www.flyingheritage.com/TemplatePlane.aspx?contentId=18> [Accessed: Mar- 2016].
- [9] Anon., "Striking by Night | Australian War Memorial", *Awm.gov.au*, [Online]. <https://www.awm.gov.au/exhibitions/striking/planes/german/me262/> [Accessed: Mar- 2016].
- [10] Futrell, Robert F. *The United States Air Force In Korea 1950-1953*, 3rd ed. Duell, Sloan and Pearce, 1991, pp. 27-686.

- [11] Username: FootageArchive - Videos From The Past, "1953 Korean War Dogfight - Mig 15 VS F86F2 Saber", *YouTube*, 2015. [Online].
<https://www.youtube.com/watch?v=wrVLNikBKho> [Accessed: 08- Aug- 2016].
- [12] Bridgman, Taylor, *Jane's All the World's Aircraft*, Volumes 1955-1956, 1969-1970, 1985-1986, 1989-1990, Sampson, Low, Mcgraw-Hill, Jane's Publishing.
- [13] Knaack, Marcelle, *Encyclopedia of US Air Force Aircraft and Missile Systems*, 1st ed. Washington, D.C.: U.S. Government Printing Office, 1978, pp. 52-81.
- [14] Anon., "Air Superiority: Controlling the Skies," Nationalmuseum.af.mil, 2015. [Online].
<http://www.nationalmuseum.af.mil/Visit/MuseumExhibits/FactSheets/Display/tabid/509/Article/196089/air-superiority-controlling-the-skies.aspx> [Accessed: Mar-2016].
- [15] Safarik, J., "Korean War Aerial Victory Credits: by date," Jan J. Safarik: Aces; United States of America - Wartime Aerial Victory Credits, *Aces.safarikovi.org*, 2014. [Online PDF]
<http://aces.safarikovi.org/usa.wartime.aerial.victory.credits.html> [Accessed: Dec-2015].
- [16] Safarik, J., "Navy and Marine Corps Shoot Downs Since 1950," Jan J. Safarik: Aces; United States of America - Wartime Aerial Victory Credits, *Aces.safarikovi.org*, 2014. [Online PDF]
<http://aces.safarikovi.org/usa.wartime.aerial.victory.credits.html> [Accessed: Dec-2015]
- [17] Futrell, Frank R., *The United States Air Force in Southeast Asia 1965-1973: Aces and Aerial Victories*, 2st ed. U.S. Government Printing Office, 1991.
- [18] Anon., "Royal Australian Air Force (RAAF)," Australia and the Vietnam War, *Vietnam-war.commemoration.gov.au*, 2016. [Online]. <http://vietnam-war.commemoration.gov.au/royal-australian-air-force/other-raaf-personnel.php> [Accessed: Mar- 2016].
- [19] Gillcrist, Paul T., *Crusader! Last of the Gunfighters*, 1st ed. Schiffer Publishing Ltd., 1995.

- [20] "24642 Air Strikes SE Asia Vietnam," *PeriscopeFilm - Stock Footage*. [Online]. <http://stock.periscopefilm.com/24642-air-strikes-se-asia-vietnam/> [Accessed: Apr-2016].
- [21] Anon., "Boeing: F-15 Strike Eagle," *Boeing.com*, 2016. [Online]. <http://www.boeing.com/defense/f-15-strike-eagle/> [Accessed: Mar-2016].
- [22] Juniper, A., "MiG-29 / MiG-29OVT, Mikoyan-Gurevich Fulcrum," *Fighter-planes.com*. [Online]. http://www.fighter-planes.com/info/mig29_fulcrum.htm [Accessed: Mar-2016].
- [23] Safarik, J., "Vietnam War Aerial Victory Credits: by date," Jan J. Safarik: Aces; United States of America - Wartime Aerial Victory Credits, *Aces.safarikovi.org*, 2014. [Online PDF] <http://aces.safarikovi.org/usa.wartime.aerial.victory.credits.html> [Accessed: Dec-2015].
- [24] Keaney, Thomas A., Cohen, Eliot A., "Gulf War Air Power Survey Summary Report," United States Dept. of the Air Force, *Summary Report*, 1993.
- [25] Brown, Craig, *Debrief: A Complete History of U.S. Aerial Engagements 1981 to the Present*, 1st ed. Schiffer Publishing Ltd., 2007.
- [26] Grant, Rebecca, "The Air Force led the way when Kuwait was freed from its Iraqi occupiers," *AIR FORCE Magazine*, pp. 40-45, 2011.
- [27] Username: swampfoot's channel, "Declassified dogfight footage: F-14 Tomcat vs. Libyan MiG-23," *YouTube*, 2015. [Online]. <https://www.youtube.com/watch?v=PIUowqD0uY8> [Accessed: Mar-2016].
- [28] Simmons, D., Gould, P., Vomastic, V., and Walsh, P., "Air Operations over Bosnia", *Naval Institute Proceedings Magazine*, [Online Access]. <http://www.usni.org/magazines/proceedings/1997-05/air-operations-over-bosnia> no. 131, pp. 58-63, 2016.
- [29] Ball, G., "Factsheets : Operation Allied Force," *Afhsa.af.mil*, 2016. [Online]. <http://www.afhsa.af.mil/topics/factsheets/factsheet.asp?id=18652> [Accessed: Mar-2016].
- [30] Lambeth, Benjamin *NATO's air war for Kosovo*. Santa Monica, CA: Rand, 2001, pp 17-66.

- [31] Smith, Jeffrey D., "The DIVAD Procurement: A Weapon System Case Study", Department of the Army, *The Army Lawyer*, The Judge Advocate General's School, August 1988, DA PAM 27-50-188.
- [32] Username: Ed McNichol, "SGT YORK", *YouTube*, 2007. [Online].
<https://www.youtube.com/watch?v=EvwCMd4q2AI> [Accessed: Mar- 2016].
- [33] Anon., "Goalkeeper", *thalesgroup.com*. [Online].
http://www.thales7seas.com/flash_2014/files/GOALKEEPER.pdf [Accessed: Mar- 2016].
- [34] Username: Wilhelm Ax, "Goalkeeper CIWS," *YouTube*, 2011. [Online].
https://www.youtube.com/watch?v=hn_dH19R-q4 [Accessed: Mar- 2016].
- [35] Anon., "The US Navy -- Fact File: MK 15 - Phalanx Close-In Weapons System (CIWS)," *Navy.mil*, 2016. [Online].
http://www.navy.mil/navydata/fact_display.asp?cid=2100&tid=487&ct=2
[Accessed: May- 2016].
- [36] Username: Ultimate Military Channel, "US Navy PHALANX CIWS gun in ACTION FIRING! (Best collection of LIVE FIRE PHALANX footage ever!)," *YouTube*, 2015. [Online]. <https://www.youtube.com/watch?v=V5DU-uoLwj4>
[Accessed: Mar- 2016].
- [37] Gunston, Bill, *The Illustrated Encyclopedia of Aircraft Armament*, Orion Books, 1988.
- [38] Wagner, J., "30mm cannon GAU-8 Avenger – en," *Military.cz*, 2012. [Online].
http://www.military.cz/usa/air/in_service/weapons/cannons/gau8/gau8_en.htm
[Accessed: May- 2016].
- [39] Goebel, G., "[1.0] B-52 Evolution", *Airvectors.net*, 2015. [Online].
http://www.airvectors.net/avb52_1.html [Accessed: May- 2016].
- [40] Anon., "GAU-22/A 25mm Gatling Gun", General Dynamics Ordnance and Tactical Systems. [Online]. http://www.gd-ots.com/armament_systems/mbw_GAU-22A.html [Accessed: May- 2016].
- [41] Anon., "Gryazev-Shipunov GSh-301 | Weaponsystems.net", *Weaponsystems.net*, 2014. [Online]. <http://weaponsystems.net/weaponssystem/ii04%20-%20GSh-301.html> [Accessed: May- 2016].

- [42] *Field Artillery Cannon Weapons System and Ammunition Handbook*, U.S. Army Field Artillery School Weapons Department, Fort Sill, Oklahoma, 1983.
- [43] Gunston, Bill, *The Illustrated Encyclopedia of the World's Rockets & Missiles*, Crescent Books, New York, 1979.
- [44] Anon., "ASTER 15 & 30 - MBDA", *MBDA*, 2016. [Online]. <http://www.mbda-systems.com/aster-solution-maritime-superiority/aster-15-30/> [Accessed: May-2016].
- [45] Anon., "ЗЕНИТНАЯ РАКЕТНАЯ СИСТЕМА С-75 (SA-2 Guideline)," *Pvo.guns.ru*, 2005. [Online]. <http://pvo.guns.ru/s75/s75.htm> [Accessed: Aug-2016].
- [46] Parsch, A., "Raytheon FIM-92 Stinger," *Designation-systems.net*, 2016. [Online]. <http://www.designation-systems.net/dusrm/m-92.html> [Accessed: Aug-2016].
- [47] Anon., "MISTRAL ALBI - MBDA", *MBDA*, 2016. [Online]. <http://www.mbda-systems.com/ground-based-air-defence/mistral-albi/> [Accessed: May-2016].
- [48] Anon., "US Hellfire Missile Orders, FY 2011-2016," *Defense Industry Daily*, 2016. [Online]. <http://www.defenseindustrydaily.com/us-hellfire-missile-orders-fy-2011-2014-07019/> [Accessed: Jul-2016].
- [49] Anon., "Molniya (AS-14 Kedge)," *Fas.org*, 1999. [Online]. <http://fas.org/man/dod-101/sys/missile/row/as-14.htm> [Accessed: Aug-2016].
- [50] Anon., "AIM-9 Sidewinder," *Fas.org*, 2000. [Online]. <http://fas.org/man/dod-101/sys/missile/aim-9.htm> [Accessed: May-2016].
- [51] World Heritage Encyclopedia, "RIM-174 Standard ERAM," *Worldlibrary.org*. [Online]. http://www.worldlibrary.org/articles/rim-174_standard_eram [Accessed: May-2016].
- [52] Anon., "Weapons - Mim-104 Patriot," *Pbs.org*, 2014. [Online]. <http://www.pbs.org/wgbh/pages/frontline/gulf/weapons/patriot.html> [Accessed: May-2016].
- [53] Gunston, Bill, *The Illustrated Encyclopedia of Aircraft Armament*, Orion Books, New York, 1988.
- [54] Anon., "METEOR," *MBDA*, 2016. [Online]. <http://www.mbda-systems.com/air-dominance/meteor/> [Accessed: May-2016].

- [55] Anon., "The world's most effective air-to-air missiles," *Airforce Technology*, 2014. [Online]. <http://www.airforce-technology.com/features/featurethe-worlds-most-effective-air-to-air-missiles-4167934/> [Accessed: Jun- 2016].
- [56] Anon., "R-77," *Deagel.com*, 2016. [Online]. http://www.deagel.com/Air-to-Air-Missiles/R-77_a001032001.aspx [Accessed: May- 2016].
- [57] Piehler, G. Kurt, and Johnson, M. Houston V, "Bombs, Gravity," "Bombs, Nuclear," and "Bombs, Smart," *Encyclopedia of Military Science*, SAGE Publications, Inc., 2013, pp 234-243.
- [58] Anon., "Manhattan Project Facts: US History for Kids," *American-historama.org*, 2016. [Online]. <http://www.american-historama.org/1929-1945-depression-ww2-era/manhattan-project.htm> [Accessed: May- 2016].
- [59] Anon., "PROJECTILE, 155mm, COPPERHEAD, HE, M712," *Uxoinfo.com*, 2016. [Online]. http://uxoinfo.com/blogcfc/client/includes/uxopages/Mulvaney_Details.cfm?OrdId=P015 [Accessed: May- 2016].
- [60] Username: Jaglavak Military, "M712 Copperhead," *YouTube*, 2009. [Online]. <https://www.youtube.com/watch?v=j4sMeo8wdzE> [Accessed: Jun- 2016].
- [61] Stutts, J. C., and Barrett, R. M., "Development and Experimental Validation of a Barrel-Launched Adaptive Munition," proceedings of the 39th Structures, Structural Dynamics and Materials Conference, April 1998, American Institute of Aeronautics and Astronautics, Washington D.C. 1998, AIAA-98-2037.
- [62] Barrett, Ron, and Lee, Gary, "Guided Bullets: A Decade of Enabling Adaptive Materials R&D," proceedings of the 24th Army Science Conference, December 2005, ADM001736, 2004.
- [63] Graham, Jeff, "Extended Range Guided Munition (ERGM) Program," Brief for the NDIA International Armaments technology Symposium and Exhibition, June 2004.
- [64] Anon., "EXACTO Guided Bullet Demonstrates Repeatable Performance against Moving Targets", *Darpa.mil*, 2015. [Online]. <http://www.darpa.mil/news-events/2015-04-27> [Accessed: May- 2016].

- [65] Carlucci, Donald E., Jacobson, Sidney S., *Ballistics: Theory and Design of Guns and Ammunition*, 2nd ed., CRC Press Taylor & Francis Group, Boca Raton, FL, 2014.
- [66] Anon., "Historical Background of Flechettes and Flechette Ammunition," *Antipersonnel.net*. [Online]. <http://www.antipersonnel.net/sdlc/001.html> [Accessed: Jul- 2016].
- [67] Hess, Derek, "PGU Series 20mm Ammunition for the F-15," *USAF Fighter Weapons Review*, Eglin AFB, 1992.
- [68] Clark, Brandon L., "Effect of Barrel Length on the Muzzle Velocity and Report from a *Mosin-Nagant* 7.62x54R Rifle," Thesis, Honors College University of South Florida, Tampa, FL, May 2011.
- [69] Schumacher, Lauren, *Rocket Munition Concept*, generated image, 2016.
- [70] Schumacher, Lauren, *RF Target Defense Concept*, generated image, 2016.
- [71] McCoy, Robert L., *Modern Exterior Ballistics: The Launch and Flight Dynamics of Symmetric Projectiles*, Schiffer Publishing Ltd., Atglen, PA, 1999.
- [72] Darling, J. A., *Handbook of Blunt-Body Aerodynamics*, Naval Ordnance Laboratory, Silver Spring, MD *VOL. 1*, December 1973, NOLTR 73-225.
- [73] Schumacher, Lauren, *Maximum Maneuver Capability*, 2016.
- [74] Bornubus, "The Russian Philosophy of Beyond Visual Range Air Combat," *Indian Defence Forum*, 2016. [Online]. <http://defenceforumindia.com/forum/threads/the-russian-philosophy-of-beyond-visual-range-air-combat.74965/> [Accessed: Aug- 2016].
- [75] Roskam, Jan, "Stability and Control During Perturbed State Flight," *Airplane Flight Dynamics and Automatic Flight Controls*, Part I, DARcorporation, Lawrence, KS, 1995.
- [76] Barrett, R., McMurtry, R., Vos, R., Tiso, P., and De Breuker, R., "Post-Buckled Precompressed Piezoelectric Flight Control Actuator Design, Development and Demonstration," *Journal of Smart Materials and Structures*, Vol. 15, No. 5, October 2006, pp. 1323 – 1331.
- [77] Barrett, R. M., "Missile & Munitions Applications," *AE 781: Adaptive Aerostructures*, KU Course notes, Ch 9, 2015.

- [78] Voss, R., Barrett, R. "Post-Buckled Precompressed Techniques In Adaptive Aerostructures: An Overview," MD-08-1306 *Journal of Mechanical Design*, Vol. 132, Issue 3, March 2010.
- [79] Singh, S., and Sachan, D., "Thermal Battery as a Power Source in Guided Missiles," *Defense Science Laboratory*, Delhi, May 1973.
- [80] Walker, W., and Ardebili, H., "New Techniques of Thermo-electrochemical Analysis of Lithium-ion Batteries for Space Applications," *Thermal & Fluids Analysis Workshop TFAWS 2013*, KSC, FL, Jul 29 - Aug 2.
- [81] Anon., "Electrolytic Capacitors," KEMET Charged® *The Capacitance Company*, [Online Product Catalog]
<http://www.kemet.com/Lists/ProductCatalog/Attachments/235/F3304.pdf>
 [Accessed Aug- 2016].
- [82] Anon., "The Capattery," *Evanscap.com*, 2007. [Online].
http://www.evanscap.com/the_capattery.htm [Accessed Aug- 2016].
- [83] Wolff, C., "Radargrundlagen – Freiraumdämpfung," *Radartutorial.eu*. [Online].
<http://www.radartutorial.eu/01.basics/Freiraumd%C3%A4mpfung.de.html>
 [Accessed Jul- 2016].
- [84] Wolff, C., "Radar Basics", *Radartutorial.eu*. [Online].
<http://www.radartutorial.eu/07.waves/wa13.en.html> [Accessed Jul- 2016].
- [85] Anon., "Antenna Basic Concepts," *Pulse Electronics/Larsen Antennas*, [Online PDF] www.pulseelectronics.com/download/.../antenna_basic_concepts/pdf
 [Accessed Jul- 2016].
- [86] Anon., "Program Acquisition Cost By Weapon System: United States Department of Defense Fiscal Year 2017 Budget Request," *Office of the Under Secretary of Defense (Comptroller)/Chief Financial Officer*, February 2016, RefID: 6-919FF76.
- [87] Anon., "GAU-12/U 25mm Gatling Gun," *General Dynamics Ordnance and Tactical Systems*. [Online]. http://www.gd-ots.com/armament_systems/mbw_GAU-12U.html [Accessed Jul- 2016].
- [88] Anon., "AC-130 Spectre Gunship - USAF Special Operations," *Americanspecialops.com*, 2016. [Online].

- <http://www.americanspecialops.com/usaf-special-operations/aircraft/ac-130/>
[Accessed Jul- 2016].
- [89] Anon., "USA Bofors 40 mm/60 Model 1936," *Navweaps.com*, 2016. [Online].
http://www.navweaps.com/Weapons/WNUS_4cm-56_mk12.php [Accessed Jul-
2016].
- [90] Short, M., "F-35 Weapons Suite | F-35 Lightning II," *Lockheed Martin*, 2016.
[Online Image]. <https://www.f35.com/media/photos-detail/f-35-weapons-suite/>
[Accessed Jul- 2016].
- [91] Anon., "Lightning Rod: F-35 Fighter Family Capabilities and Controversies,"
Defense Industry Daily, 2015. [Online].
[http://www.defenseindustrydaily.com/lightning-rod-f-35-fighter-family-
capabilities-and-controversies-021922/](http://www.defenseindustrydaily.com/lightning-rod-f-35-fighter-family-capabilities-and-controversies-021922/) [Accessed Jul- 2016].
- [92] Anon., " AIM-120 AMRAAM," *AeroWeb*. [Online]. [http://www.bga-
aeroweb.com/Defense/AMRAAM.html](http://www.bga-aeroweb.com/Defense/AMRAAM.html) [Accessed Jul- 2016].
- [93] Anon., "AIM-120 AMRAAM Slammer," *Fas.org*, [Online].
<http://fas.org/man/dod-101/sys/missile/aim-120.htm> [Accessed Jul- 2016].
- [94] Anon., "AAIM-9 Sidewinder", *AeroWeb*. [Online]. [http://www.bga-
aeroweb.com/Defense/Sidewinder.html](http://www.bga-aeroweb.com/Defense/Sidewinder.html) [Accessed Jul- 2016].
- [95] Anon., "Lockheed AC-130 'Spectre' and AC-130U 'Spooky II'",
Theaviationzone.com, 2016. [Online].
<http://www.theaviationzone.com/factsheets/ac130.asp> [Accessed Jul- 2016].
- [96] Anon., "Boeing: Historical Snapshot: AC-130U Gunship," *Boeing.com*, 2016.
[Online]. <http://www.boeing.com/history/products/ac-130u-gunship.page>
[Accessed Jul- 2016].
- [97] Anon., "First AC-130U Spooky Retires," *Air Force Special Operations
Command*, 2015. [Online].
[http://www.afsoc.af.mil/News/ArticleDisplay/tabid/5003/Article/620328/first-ac-
130u-spooky-retires.aspx](http://www.afsoc.af.mil/News/ArticleDisplay/tabid/5003/Article/620328/first-ac-130u-spooky-retires.aspx) [Accessed Jul- 2016].

Appendix A: Source Code

MATLAB CODE
(text files)

Appendix B: F/A-10 Capability

Using the methodology described in Section 4, a sample 20mm guided projectile was applied to the existing GAU-8/A system onboard the A-10 airframe to demonstrate potential in both offensive and defensive engagements. The projectile and salient characteristics when used in a defensive maximum maneuver combat scenario (as outlined in Section 3.5.3.1) are demonstrated in Figure B.1 and Table B.1.

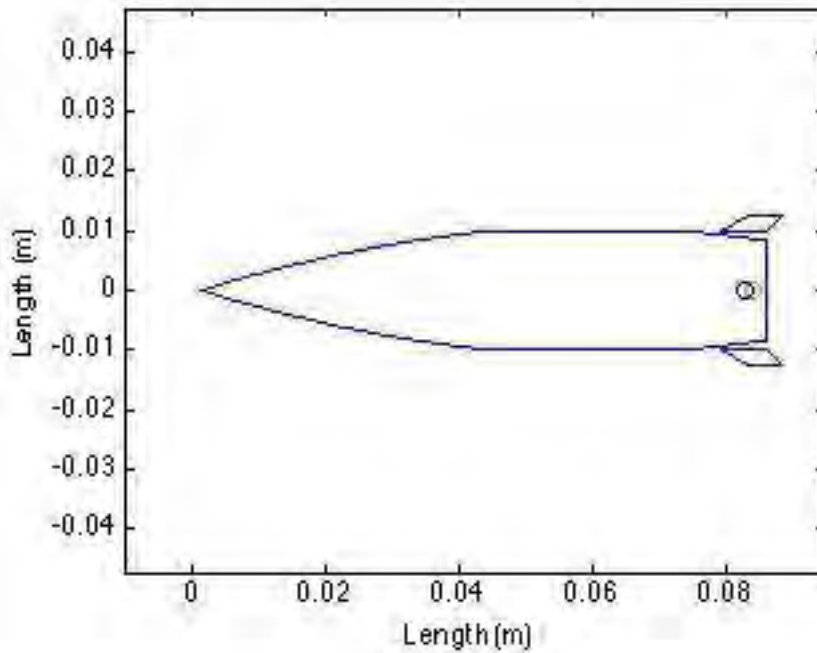


Figure B.1: Sample A-10 Guided Projectile

Table B.1: A-10 Guided Projectile Characteristics (Defensive Maneuver)

Characteristic	Value Forward	Units
S	314	mm ²
S _{t, exposed}	150	mm ²
Λ_{LE}	60.0	deg.
b _t	25	mm
n _{max} (estimated)	40.4	g's
SM _{supersonic}	0.66	%
m	0.112	kg
V _{muzzle} (including airspeed)	2010	m/s
h	2130	m
d _F (absolute value)	3.70	deg.

Figure B.2 demonstrates the maneuvering capability of this sample round in the form of engagement cones after a 1 second time of flight. This simulation was run as described in Section 4. When used offensively, the maximum range of this projectile (assuming the aircraft cruises at the service ceiling at 150m/s) is 20.5 miles. Additionally, with the standard loadout capacity of this airframe of over 1000 conventional rounds, if it is assumed that the same number of guided projectiles are loaded, this aircraft has the potential to engage up to 40 Su-35 type targets (see Section 3.5.2.1). As noted previously, the estimated cost of a 20mm guided projectile is \$2,700.

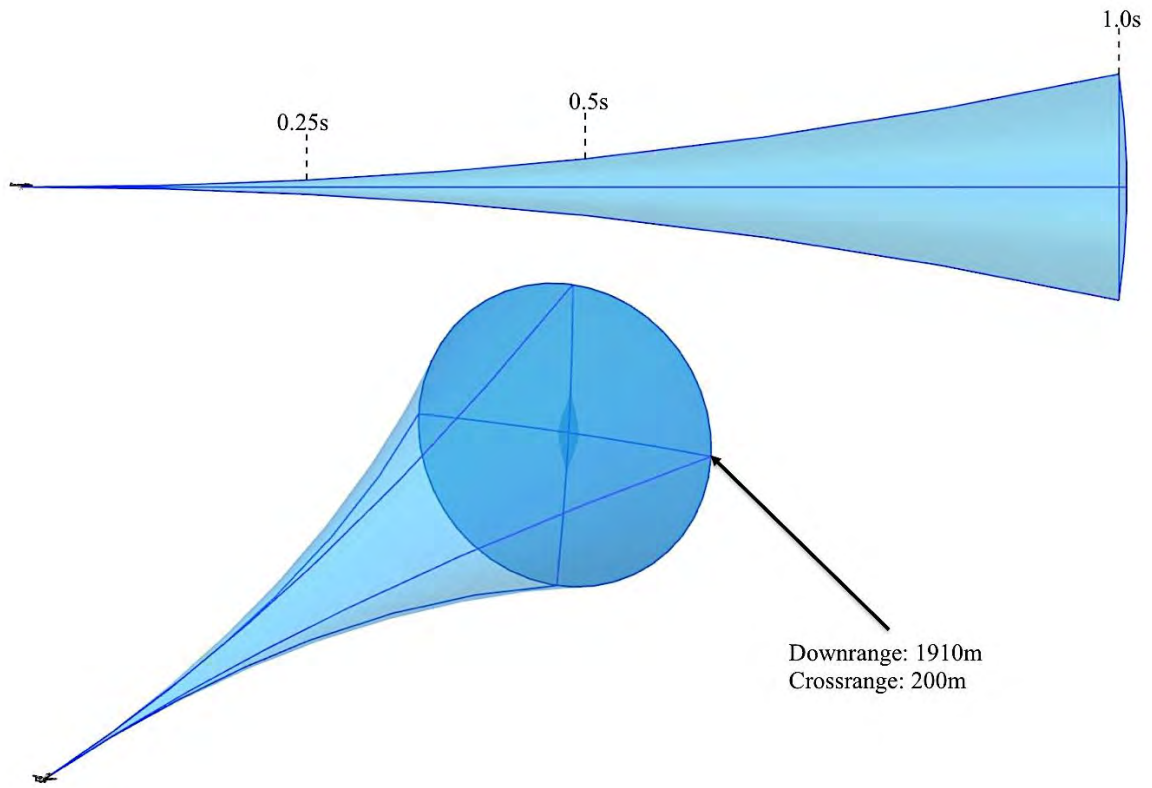


Figure B.2: A-10 Defensive Engagement Cones 1.0s